Universidade de Brasília
Instituto de Geociências
Programa de Pós-Graduação em Geologia

O Ambiente Geodinâmico do *Greenstone Belt* Crixás: Inferências Baseadas na Petrogênese das Rochas Metaígneas e Proveniência Sedimentar

Tese de Doutorado nº 178

Caio César Aguiar Borges

Brasília, 2021.

Universidade de Brasília
Instituto de Geociências
Programa de Pós-Graduação em Geologia

O Ambiente Geodinâmico do *Greenstone Belt* Crixás: Inferências Baseadas na Petrogênese das Rochas Metaígneas e Proveniência Sedimentar

Tese de Doutorado nº 178

Autor:

Caio César Aguiar Borges (IG/UnB)

Orientadora:

Dra. Catarina Labouré Bemfica Toledo (IG/UnB)

Coorientadora:

Dra. Adalene Moreira Silva (IG/UnB)

Banca Examinadora:

Dr. César Fonseca Ferreira Filho (IG/UnB)
Dr. Léo Afraneo Hartmann (IGEO/UFRGS)
Dr. Moacir José Buenano Macambira (IG/UFPA)
Dra. Natalia Hauser (IG/UnB – Suplente)

Aa

Aguiar Borges, Caio César
O ambiente geodinâmico do greenstone belt Crixás: Petrogênese das rochas metaígneas e proveniência sedimentar / Caio César Aguiar Borges; orientador Catarina Labouré Bemfica Toledo; co-orientador Adalene Moreira Silva. -- Brasília, 2021.
133 p.

Tese (Doutorado - Doutorado em Geologia) -- Universidade de Brasília, 2021.

1. Geologia Regional. 2. Geoquímica. 3. Geologia Isotópica. 4. Proveniência Sedimentar. 5. Petrologia. I. Labouré Bemfica Toledo, Catarina, orient. II. Moreira Silva, Adalene, co-orient. III. Título.

“Science knows no country, because knowledge belongs to humanity, and is the torch which illuminates the world. Science is the highest personification of the nation because that nation will remain the first which carries the furthest the works of thought and intelligence.”

Louis Pasteur.

“Geologists have a saying – Rocks remember.”

Neil Armstrong.

Agradecimentos

Agradeço primeiramente a Deus, sempre uma presença constante em minha vida. Aos meus pais, Divino e Luciene, à minha irmã, Suellen, e à minha avó, Maria, por me incentivarem. Sou grato a todos os professores e professoras do Instituto de Geociências e à Universidade de Brasília, por terem contribuído imensuravelmente com a minha formação. Meus agradecimentos especiais às minhas queridas orientadoras, Catarina e Adalene, que acreditaram e me deram apoio e oportunidades desde os meus primeiros passos na pesquisa, durante a Iniciação Científica, ainda na graduação em Geologia, até o Mestrado e Doutorado. Agradeço ao IG/UnB e à toda sua equipe de servidores pelas facilidades laboratoriais que contribuíram com esta pesquisa. Este trabalho não seria possível sem a parceria fundamental com a Mineração Serra Grande S.A. e todo o seu time que sempre esteve disposto a contribuir. Meus agradecimentos especiais aos geólogos Bruno, Renan, Carol, Glauber, Frederico e Marcelo, e à toda equipe do galpão, onde passei boa parte do meu tempo em Crixás (GO). Agradeço à Luana pela parceria durante os longos dias de trabalhos de campo e coleta de dados. Agradeço aos Profs. Hardy Jost e Farid C. Jr. pelas incansáveis e valiosas discussões a respeito da geologia do Bloco Arqueano-Paleoproterozoico de Goiás e do *greenstone* de Crixás. Meus profundos agradecimentos ao Prof. Jason Kirk e à Universidade do Arizona pelo aprendizado da metodologia Re-Os durante o período sanduíche em Tucson (EUA). O presente trabalho foi realizado com apoio da Coordenação de Aperfeiçoamento de Pessoal de Nível Superior – Brasil (CAPES) – Código de Financiamento 001, CAPES-PrInT (88881.312018/2018-01) e CNPq (MCTIC/CNPq 28/2018 – 420308/2018-0). Agradeço à CAPES pela bolsa de doutorado (PROEX – 88882.347184/2019-01).

Resumo

O *greenstone belt* Crixás é um dos principais componentes do Domínio Crixás-Goiás, porção central do Brasil, e compreende uma sequência metavulcânica ultramáfica-máfica sobreposta por uma sucessão metassedimentar associada a rochas magmáticas de composição intermediária. Neste trabalho, são apresentadas informações de campo e descrições de testemunhos de sondagem, integradas com dados petrográficos, geoquímicos e isotópicos (Sm-Nd, Re-Os e U-Pb) visando a caracterização das diferentes unidades tectonoestratigráficas, com foco nos processos petrogenéticos e na proveniência sedimentar do *greenstone belt* Crixás. As rochas metavulcânicas da base do *greenstone* englobam metakomatiitos que localmente preservam textura spinifex. Essas rochas apresentam composição química semelhante aos komatiitos depletados em Al, incluindo as baixas razões Al_2O_3/TiO_2, a depleção nos elementos terras raras pesados (ETRP) e as anomalias negativas em Zr-Hf. Os metabasaltos consistem de toleítos de alto Mg metamorfizados em fácies anfibolito e que apresentam padrões predominantemente planos de ETR e sistemática de elementos traço semelhante aos basaltos de platôs oceânicos fanerozóicos. Sugere-se que essas rochas foram formadas sob a ação de uma pluma mantélica heterogênea em um ambiente de platô oceânico, onde os komatiitos representam o magma gerado sob alta taxa de fusão parcial do manto em grandes profundidades, com retenção da granada como fase residual, e os basaltos representam o magma gerado em porções mais rasas do manto, associado a menores taxas de fusão parcial. A idade do vulcanismo ultramáfico-máfico ainda é imprecisa, porém estimada como sendo mesoarqueana (~3.0 – 2.8 Ga), com base em dados isotópicos publicados anteriormente. Dados Re-Os em rocha total em amostras de metakomatiito e metabasalto apresentados neste trabalho forneceram uma isócrona de 2609 ± 65 Ma, interpretada como reflexo de um evento neoarqueano que resetou a sistemática isotópica Re-Os original dessas rochas, possivelmente relacionado à fase final de cratonização do Domínio Crixás-Goiás, marcado pelo metamorfismo e intrusão dos granitos arqueanos mais jovens da região (~2.70 Ga). Os metakomatiitos e principalmente os metabasaltos estão comumente imbricados tectonicamente com metagrauvacas e filitos carbonosos, que predominam no topo da estratigrafia do *greenstone*. As rochas metassedimentares apresentam baixa maturidade mineralógica e textural. O baixo grau de selecionamento dos grãos e a ausência de transporte significativo dos sedimentos são denotados também pelas baixas razões Zr/Sc, indicando área-fonte proximal. A composição das metagrauvacas e dos filitos carbonosos se sobrepõe e sugere uma mistura de fontes félsicas e máficas, também coerente com o predomínio de fontes de composição intermediária relacionadas a arco magmático. Geocronologia U-Pb em zircão detrítico indica distribuição unimodal, com um pico em 2.2 – 2.1 Ga e proveniência apenas incipiente de fontes siderianas (~2.4 Ga) e arqueanas (~2.7 Ga). As rochas apresentam idades modelo Sm-Nd entre 2.44 e 2.34 Ga e valores aproximadamente condríticos a positivos de ε_{Nd} calculados em t = 2.1 Ga (ε_{Nd} = -0.27 a +1.25). Datação Re-Os em arsenopirita proveniente de sulfeto maciço hospedado em filitos carbonosos forneceu a idade de 2137 ± 11 Ma. Essa idade é considerada uma idade mínima para a sedimentação no *greenstone belt* Crixás e é relativamente próxima à idade máxima de sedimentação calculada a partir da população de cristais de zircão detrítico mais jovens (2149 ± 4 Ma). Propõe-se que os protólitos sedimentares foram depositados em uma bacia relacionada a um arco intraoceânico riaciano e derivaram da rápida erosão do próprio arco. Além disso, essas rochas são alóctones e foram transportadas tectonicamente sobre um embasamento arqueano (formado por terrenos granito-gnáissicos e vulcânicas ultramáficas e máficas) durante a colisão do arco magmático com um paleocontinente arqueano (referido como a proto-crosta do Domínio Crixás-Goiás). Registros desse arco magmático também estão localmente representados por meta-andesitos e metadioritos associados à sucessão metassedimentar do *greenstone belt* Crixás. A datação U-Pb em cristais de zircão provenientes de uma amostra de meta-andesito forneceu intercepto superior com idade de 2172.2 ± 12.7 Ma, interpretada como a idade do magmatismo intermediário. Os meta-andesitos e metadioritos apresentam idades modelo Sm-Nd em torno de 2.2 Ga e valores positivos de ε_{Nd} inicial (+2.34 a +2.69). A orogênese em questão está inserida no contexto da amalgamação do Maciço de Goiás durante o Paleoproterozoico e compreende o principal período da mineralização aurífera na região do *greenstone belt* Crixás.

Palavras-Chave: Maciço de Goiás; *Greenstone Belt*; Proveniência Sedimentar; Geoquímica; Geologia Isotópica.

Abstract

The Crixás greenstone belt is one of the most important components of the Crixás-Goiás Domain, Central Brazil, and comprises an ultramafic-mafic metavolcanic sequence overlaid by a metasedimentary succession associated with magmatic rocks of intermediate composition. In this work, field information and description of drill cores, integrated with petrographical, geochemical, and isotopic (Sm-Nd, Re-Os, and U-Pb) data, are present to characterize the different tectonostratigraphic units, with focus on the petrogenetic processes and sediment provenance of the Crixás greenstone belt. Lower metavolcanic rocks encompass metakomatiites that locally present spinifex texture. These rocks have a chemical composition similar to the Al-depleted komatiites, including the low ratios of Al_2O_3/TiO_2, depleted patterns of HREE, and the negative anomalies of Zr-Hf. Metabasalts consist of amphibolite facies high-Mg tholeiites with mostly flat REE patterns and trace element systematics that resemble the Phanerozoic oceanic plateau mafic lavas. It is suggested that these rocks were formed above a heterogeneous mantle plume in an oceanic plateau setting, where the komatiites represent the magma generated at high degrees of partial melting at great depths, with residual garnet in the mantle source, whereas the basalts represent the magma generated at shallower depths and lower degrees of mantle melting. The age of the ultramafic-mafic volcanism is imprecise, though estimated in the Mesoarchean (~3.0 – 2.8 Ga), on the basis of previously published isotopic data. Whole rock Re-Os data of samples of metakomatiite and metabasalt presented here yielded an isochron of 2609 ± 65 Ma, interpreted to reflect a Neoarchean resetting event that overprinted the original Re-Os isotopic systematics of the rocks, possibly related to the late stages of the cratonization of the Crixás-Goiás Domain, marked by metamorphism and emplacement of the youngest Archean granites of the region (~2.70 Ga). The metakomatiites and especially the metabasalts are commonly tectonically imbricated with metagraywackes and carbonaceous phyllites that prevail at the top of the greenstone stratigraphy. Metasedimentary rocks have low mineralogical and textural maturity. Absence of significative sorting and recycling are also denoted by the low ratios of Zr/Sc, indicating a proximal source area. Composition of the metagraywackes and carbonaceous phyllites overlap and suggests a mixture of felsic and mafic sources, also consistent with arc related intermediate rocks. Detrital zircon U-Pb geochronology indicates a unimodal age spectra, with a peak at 2.2 – 2.1 Ga and incipient provenance of Siderian (~2.4 Ga) and Archean (~2.7 Ga) sources. Rocks have Sm-Nd model ages of 2.44 to 2.34 Ga and near-chondritic to positive ε_{Nd} calculated at t = 2.1 Ga (ε_{Nd} = -0.27 a +1.25). Re-Os dating of arsenopyrite from a massive sulfide hosted in carbonaceous phyllites yielded an age of 2137 ± 11 Ma. This age is considered a minimum sedimentation age in the Crixás greenstone belt and is relatively close to the maximum depositional age calculated from the youngest cluster of the detrital zircon U-Pb data (2149 ± 4 Ma). It is proposed that the sedimentary protoliths were deposited in a Rhyacian intraoceanic arc-related basin and derived from rapid erosion of the rising arc. Furthermore, these rocks are allochthonous and were tectonically transported onto an older Archean basement (formed of granite-gneissic terranes and ultramafic-mafic greenstone volcanic flows) during the collision between the magmatic arc and an Archean paleocontinent (referred as a proto-crust of the Crixás-Goiás Domain). Records of this magmatic arc are also locally represented by meta-andesites and metadiorites associated with the upper metasedimentary succession of the Crixás greenstone belt. U-Pb zircon geochronology of a meta-andesite sample yielded an upper intercept Concordia age of 2172.2 ± 12.7 Ma, interpreted as the age of the intermediate magmatism. Meta-andesites and metadiorites present Sm-Nd model ages of ~2.2 Ga and positive values of initial ε_{Nd} (+2.34 to +2.69). The characterized orogenesis is inserted in the context of the Paleoproterozoic amalgamation of the Goiás Massif and encompasses the main period of gold mineralization in the region of the Crixás greenstone belt.

Keywords: *Goiás Massif; Greenstone Belt; Sediment Provenance; Geochemistry; Isotope Geology.*

Sumário

Capítulo IV – Conclusão

Índice de Figuras

Artigo 1: Unravelling a hidden Rhyacian magmatic arc through provenance of metasedimentary rocks of the Crixás greenstone belt, Central Brazil.

Artigo 2: Archean to Paleoproterozoic evolution of the Crixás greenstone belt, Central Brazil: Insights from two contrasting assemblies of metaigneous rocks.

Índice de Tabelas

Artigo 1: Unravelling a hidden Rhyacian magmatic arc through provenance of metasedimentary rocks of the Crixás greenstone belt, Central Brazil.

Artigo 2: Archean to Paleoproterozoic evolution of the Crixás greenstone belt, Central Brazil: Insights from two contrasting assemblies of metaigneous rocks.

Anexos

Artigo 1: Unravelling a hidden Rhyacian magmatic arc through provenance of metasedimentary rocks of the Crixás greenstone belt, Central Brazil.

Supplementary Material 1. Major and trace element data of metagraywackes and carbonaceous phyllites of the Crixás greenstone belt.

Supplementary Material 2. LA-ICP-MS U-Pb detrital zircon data of metagraywackes and carbonaceous phyllites of the Crixás greenstone belt.

Artigo 2: Archean to Paleoproterozoic evolution of the Crixás greenstone belt, Central Brazil: Insights from two contrasting assemblies of metaigneous rocks.

Supplementary Material 1. Sampling locations.

Supplementary Material 2. Major and trace element data of metaigneous rocks of the Crixás greenstone belt.

Outros:

Re-Os systematics of carbonaceous phyllites of the Crixás greenstone belt: Isotopic data and discussion.

Capítulo I - Introdução

1. Contextualização e Motivação do Trabalho

O termo "*greenstone belt*" é usualmente empregado para descrever sequências supracrustais metamorfizadas, principalmente de idade arqueana a paleoproterozóica, que ocorrem como faixas deformadas e englobadas por terrenos granito-gnáissicos (geralmente do tipo TTG; tonalito-trondhjemito-granodiorito). Os *greenstones* são encontrados em regiões cratônicas e apresentam elevado interesse científico e econômico por fornecerem informações a respeito da evolução da Terra primitiva e por hospedarem importantes depósitos de ouro e metais base. Os avanços no conhecimento dos *greenstone belts* têm revelado suas complexidades e variabilidades em termos litológicos, estratigráficos, estruturais, petrogenéticos e metalogenéticos (De Wit & Ashwall, 1995; Anhaeusser, 2014; Furnes et al., 2015).

Os estilos tectônicos atuantes durante os estágios primordiais da Terra levantam discussões historicamente polarizadas entre argumentos uniformitaristas (ex: Barley et al., 1984; Wyman, 2013; Kusky et al., 2018) e não-uniformitaristas (ex: Campbell & Hill, 1988; Bédard et al., 2013; Bédard, 2006, 2017). No entanto, a crescente integração de dados de campo, estruturais, geofísicos, geoquímicos, isotópicos e paleomagnéticos, associados a estudos experimentais e de modelamento, tem mostrado que processos de tectônica de placas semelhantes aos atuais operaram desde o Arqueano (Brenner et al., 2020; Kusky et al., 2021; Windley et al., 2021).

Neste sentido, o estudo sistemático do magmatismo registrado nos *greenstone belts* é potencialmente útil para decifrar as fontes mantélicas, os processos magmáticos e o ambiente tectônico de formação dessas sequências. Por exemplo, muitos estudos geoquímicos têm reconhecido em terrenos arqueanos assembleias de rochas típicas de arcos magmáticos, incluindo vulcânicas cálcio-alcalinas, boninitos, adakitos, andesitos magnesianos e basaltos enriquecidos em Nb (Kerrich et al., 1998; Hollings & Kerrich, 2000; Wyman et al., 2000; Polat & Kerrich, 2006; Manikyamba et al., 2009; Khanna et al., 2015; Borges et al., 2017). Associações de komatiitos e basaltos toleíticos com afinidade geoquímica de platôs oceânicos e continentais gerados sob a ação de plumas mantélicas (Campbell et al., 1989; Herzberg, 1992; Xie et al., 1993; Arndt, 1994; Puchtel et al., 1998; Polat, 2009), que podem inclusive estar associadas a uma interação pluma-arco (Dostal &

Mueller, 1997; Wyman, 1999; Polat et al., 2006; Wyman & Kerrich, 2009), também tem sido documentadas. Similarmente, os registros sedimentares dos *greenstone belts* são bastante variados e essenciais no provimento de informações sobre processos ocorridos durante e após a deposição em bacias sedimentares antigas. As rochas sedimentares detríticas possuem o potencial de preservar as assinaturas geoquímicas e isotópicas de suas áreas-fonte, sendo, portanto, fundamentais em estudos de proveniência e evolução crustal (Floyd & Leveridge, 1987; McLennan et al., 1990, 1993; Hartmann et al., 2006). Além disso, as rochas sedimentares muitas vezes são a única fonte de dados a respeito de crosta continental que não se encontra mais preservada no registro geológico (Feng & Kerrich, 1990; Cawood et al., 2012).

A porção centro-oeste do Estado de Goiás, região central do Brasil, contém uma área de aproximadamente 18.000 km^2 onde ocorrem rochas granito-gnáissicas arqueanas e *greenstone belts* arqueanos a paleoproterozoicos. Nas últimas décadas, a região foi designada de diferentes maneiras em diversas publicações, por exemplo, Bloco Arqueano de Goiás (Jost et al., 2005; Pimentel, 2016), Bloco Arqueano de Crixás-Goiás (Pimentel et al., 2003), Terreno Arqueano do Brasil Central (Queiroz et al., 2008), Terreno Arqueano-Paleoproterozoico do Brasil Central (Jost et al., 2013), Terreno Arqueano-Paleoproterozoico de Goiás (Jost et al., 2014; Borges et al, 2017; Campos et al., 2017), Terreno Crixás-Goiás (Jost et al., 2019; Ferreira et al., 2021), e Bloco Arqueano de Goiás (Bogossian et al., 2020; Bogossian, 2020). Com o intuito de favorecer uma padronização e facilitar as referências de trabalhos futuros, a nomenclatura "Domínio Crixás-Goiás", sugerida por Cordeiro & Oliveira (2017) em uma revisão do contexto geotectônico do Maciço de Goiás, será adotada na presente tese de doutorado.

O *greenstone belt* Crixás é a faixa supracrustal mais bem estudada e uma das mais bem expostas e preservadas do Domínio Crixás-Goiás, e hospeda o segundo maior depósito do tipo *gold-only* da Faixa Brasília (Jost et al., 2010, 2014). A estratigrafia dessa sequência foi definida como um típico *greenstone belt* constituído na base por lavas komatiíticas com textura spinifex localmente preservada, seguidas por derrames basálticos, por vezes almofadados, sobrepostos por rochas sedimentares ricas em matéria orgânica com lentes de dolomito e grauvacas que predominam no topo (Sabóia, 1979; Sabóia & Teixeira, 1983; Jost & Oliveira, 1991). Recentemente, rochas metavulcânicas e intrusivas de composição intermediária foram reconhecidas, evidenciando a variabilidade e complexidade litológica da faixa. O *greenstone belt* Crixás foi submetido a metamorfismo com pico em fácies anfibolito e eventos de deformação com geração de múltiplas falhas de empurrão em sistema duplex que resultaram na comum repetição estratigráfica e imbricamento das diferentes

unidades. A idade das rochas vulcânicas ultramáficas foi inicialmente definida em ~2.8 Ga, com base em isócronas Pb-Pb e Sm-Nd (Arndt et al., 1989), o que levou a interpretação de que toda a sequência do *greenstone belt* Crixás é do Mesoarqueano. Por outro lado, os primeiros dados isotópicos referentes a sucessão sedimentar, sobretudo a datação U-Pb em zircão detrítico, indicaram uma contribuição dominada por áreas-fonte do Paleoproterozoico (~2.2 – 2.1 Ga) (Tassinari et al., 2006; Jost et al., 2010), revelando que pelo menos parte da sequência *greenstone* não é arqueana como anteriormente imaginado.

Em síntese, apesar dos grandes avanços ocorridos nas últimas décadas, diversas questões ainda permanecem em aberto em relação ao *greenstone belt* Crixás, por exemplo: i) A determinação de idades para os diferentes episódios de magmatismo e da sedimentação; ii) A caracterização detalhada dos tipos de magmatismo, das fontes mantélicas, e dos processos petrogenéticos envolvidos; iii) A investigação das potenciais áreas-fontes das rochas metassedimentares; iv) A delineação do ambiente tectônico em que cada unidade foi formada; e v) A elaboração de um modelo evolutivo para o *greenstone belt* Crixás e suas implicações regionais no contexto geotectônico do Domínio Crixás-Goiás e do Maciço de Goiás. Portanto, o foco deste trabalho consiste na caracterização das rochas metaígneas e metassedimentares do *greenstone belt* Crixás por meio da integração de informações de campo, descrição de testemunhos de sondagem, e análises petrográficas, geoquímicas e isotópicas com o intuito de contribuir para a elucidação dessas questões.

2. Objetivos

O objetivo central desta pesquisa é a investigação do ambiente geodinâmico do *greenstone belt* Crixás por meio do estudo petrogenético das rochas metaígneas e de proveniência das rochas metassedimentares. De modo a alcançar o objetivo central proposto, este trabalho engloba os seguintes objetivos específicos:

i. Estabelecer as relações tectono-estratigráficas das seções metavulcânicas e metassedimentares e suas relações com as rochas intrusivas a partir da descrição de testemunhos de sondagem distribuídos em diferentes partes do *greenstone belt* Crixás;

ii. Identificação dos diferentes protólitos e estudo das assembleias metamórficas estabilizadas nos eventos tectônicos por meio do estudo petrográfico e de química mineral;

iii. Investigação das fontes mantélicas e das condições de geração dos magmas de diferentes composições por meio da caracterização geoquímica e isotópica (Sm-Nd) das rochas metavulcânicas e intrusivas;

iv. Obtenção da idade do magmatismo de composição intermediária por meio da datação U-Pb em zircão;

v. Caracterização das áreas-fonte e do ambiente de deposição das rochas sedimentares por meio da análise petrográfica, geoquímica e isotópica (datação U-Pb em grãos de zircão detrítico e análise Sm-Nd em rocha total) em metagrauvacas e filitos carbonosos;

vi. Caracterização da composição isotópica Re-Os dos diferentes tipos de rochas e minerais do *greenstone belt* Crixás visando obter informações geocronológicas para as idades de sedimentação (filitos carbonosos), vulcanismo (metakomatiitos e metabasaltos) e mineralização (arsenopirita/ouro).

3. Estruturação da Tese

Os principais resultados e discussões da presente tese de doutorado estão estruturados na forma de dois artigos científicos (Capítulos II e III). No Capítulo IV, é apresentada uma breve síntese das discussões realizadas na tese, assim como as considerações finais. Os assuntos tratados em cada artigo científico são resumidos abaixo:

i. O primeiro artigo (Capitulo II) é intitulado "*Unravelling a hidden Rhyacian magmatic arc through provenance of metasedimentary rocks of the Crixás greenstone belt, Central Brazil*", publicado no periódico internacional *Precambrian Research*. O foco desse artigo é o estudo de proveniência sedimentar do *greenstone belt* Crixás por meio da integração de dados geoquímicos e Sm-Nd em rocha total, e geocronologia U-Pb em zircão detrítico de metagrauvacas e filitos carbonosos. Além disso, são discutidas as implicações regionais dos resultados no contexto geotectônico do Maciço de Goiás;

ii. O segundo artigo (Capítulo III) é intitulado "*Archean to Paleoproterozoic evolution of the Crixás greenstone belt, Central Brazil: Insights from two contrasting assemblies of metaigneous rocks*", submetido para publicação no periódico internacional *Lithos*. Esse artigo aborda o estudo do vulcanismo ultramáfico-máfico e do magmatismo de composição intermediária do *greenstone belt* Crixás, com foco nas assinaturas geoquímicas e isotópicas (Sm-Nd) das rochas e suas implicações petrogenéticas e de ambiente tectônico. Nesse artigo é apresentada a primeira datação U-Pb em zircão do magmatismo intermediário do *greenstone belt* Crixás. Além disso, são apresentados dados Re-Os de amostras de metakomatiito, metabasalto e arsenopirita (hospedada nas rochas metassedimentares) e suas implicações geocronológicas.

4. Referências Bibliográficas

Almeida, F.F.M. de, Hasui, Y., Brito Neves, B.B., Fuck, R.A., 1981. Brazilian structural provinces: an introduction. Earth-Sci. Rev. 17, 1-29.

Anhaeusser, C.R., 2014. Archaean greenstone belts and associated granitic rocks – A review. J. Afr. Earth Sc. 100, 684–732.

Arndt N.T., Teixeira N.A., White W.M., 1989. Bizarre geochemistry of komatiites from the Crixás Greenstone belt, Brazil. Contr. Mineral. Petrol. 74, 549-564.

Arndt, N.T., 1994. Archaean komatiites. In: K.C. Condie (Ed.), Archaean Crustal Evolution. Elsevier, Amsterdam, pp. 11-44.

Barley, M.E., Sylvester, G.C., Groves, D.I., Borley, G.D., Rogers, N., 1984. Archaean calc-alkaline volcanism in the Pilbara Block, Western Australia. Precambrian Res. 24, 285–319.

Bédard, J.H., 2006. A catalytic delamination-driven model for coupled genesis of Archaean crust and subcontinental lithospheric mantle. Geochim. Cosmochim. Ac. 70, 1188–1214.

Bédard, J.H., 2017. Stagnant lids and mantle overturns: implications for Archaean tectonics, magmagenesis, crustal growth, mantle evolution, and the start of plate tectonics. Geosci. Front. 9 (1), 19-49.

Bédard, J.H., Harris, L.B., Thurston, P.C., 2013. The hunting of the snArc. Precambrian Res.229, 20–48.

Bogossian, J., 2020. Gold systems in the Faina greenstone belt and crustal evolution of the southern Goiás Archean Block, central Brazil. PhD thesis, School of Earth Sciences, The University of Western Australia, 246 pp.

Bogossian, J., Hagemann S.G., Rodrigues V.G., Lobato L.M., Roberts M., 2020. Hydrothermal Alteration and Mineralization in the Faina greenstone belt: evidence from the Cascavel and Sertão orogenic gold deposits. Ore Geol. Rev. 119, 10323.

Borges, C.C.A., Toledo, C.L.B., Silva, A.M., Chemale, F., Jost, H., Lana, C.C., 2017. Geochemistry and isotopic signatures of metavolcanic and metaplutonic rocks of the Faina and Serra de Santa Rita

greenstone belts, Central Brazil: evidences for a Mesoarchean intraoceanic arc. Precambrian Res. 292, 350-377.

Brenner, A.R., Fu, R.R., Evans, D.A.D., Smirnov, A.V., Trubko, R., Rose, I.R., 2020. Paleomagnetic evidence for modern-like plate motion velocities at 3.2 Ga. Science Advances 6, eaaz8670. https://doi.org/10.1126/sciadv.aaz8670.

Campbell, I.H., Griffiths, R.W., Hill, R.I., 1989. Melting in an Archaean mantle plume: heads it's basalts, tails it's komatiites. Nature 339, 697-698.

Campbell, I.H., Hill, R.I., 1988. A two-stage model for the formation of the granite-greenstone terrains of the Kalgoorlie–Noresman area. Earth Planet. Sci. Lett. 90, 11-25.

Campos, D.S. de, Silva, A.M., Toledo, C.L.B., Carvalho, M.J. de, Rodrigues, V.G., Araújo, K., 2017. Prospectivety analysis of gold and iron oxide copper-gold-(silver) mineralization from the Faina Greenstone Belt, Brazil, using multiple data sets. Braz. J. Geol. 47 (4), 561-590.

Cawood, P.A., Hawkesworth, C.J., Dhuime, B., 2012. Detrital zircon record and tectonic setting. Geology 40, 875-878.

Cordeiro P.F.O., Oliveira. C.G., 2017. The Goiás Massif: Implications for a pre-Columbia 2.2–2.0 Ga continent-wide amalgamation cycle in central Brazil. Precambrian Res. 288, 403-420.

De Wit, M.J., Ashwal, L.D., 1995. Greenstone belts; what are they? S. Afr. J. Geol. 98 (4), 505-520.

Dostal, J., Mueller, W.U., 1997. Komatiite flooding of rifted Archean rhyolite arc complex: geochemical signature and tectonic significance of Stoughton-Roquemaire Group, Abitibi greenstone belt, Canada. J. of Geol. 105, 545-563.

Feng, R., Kerrich, R., 1990. Geochemistry of fine-grained clastic sediments in the Archean Abitibi greenstone belt, Canada: Implications for provenance and tectonic setting. Geochim. Cosmochim. Acta 54, 1061-1081.

Ferreira, B.F., Marques, J.C., Frantz, J.C., de Souza, R.G., Campos, M.P., Figueiredo, F.L.A.R., Padilha, N.L., 2021. Stratigraphy and U–Pb detrital zircon provenance, Crixás Greenstone Belt, Goiás-Brasil: Gold-bearing vs barren siliciclastic rocks. J. S. Am. Earth Sci. 105, 102994. https://doi.org/10.1016/j.jsames.2020.102994.

Floyd, P.A., Leveridge, B.E., 1987. Tectonic environment of the Devonian Gramscatho basin, south Cornwall: framework mode and geochemical evidence from turbiditic sandstones. J. Geol. Soc. London 144, 531–542.

Fortes, P.T.F.O., Pimentel, M.M., Santos, R.V., Junges, S., 2003. Sm-Nd study of the Crixás greenstone belt, Brazil: implications for the age of deposition of the upper sedimentary rocks and associated Au mineralization. J. S. Am. Earth Sci. 16, 503–512.

Furnes, H., Dilek, Y., De Wit, M., 2015. Precambrian greenstone sequences represent different ophiolite types. Gondwana Res.27, 649–685.

Hartmann A., Endo I., Tadeu M., Suita F., Santos J.O.S., Frantz J.C., Carneiro M.A., McNaughton N.J., Barley M.E., 2006. Provenance and age delimitation of Quadrilátero Ferrífero sandstones based on zircon U-Pb isotopes. J. S. Am. Earth Sci. 20 (4), 273-285.

Herzberg, C., 1992. Depth and degree of melting of komatiites. J. Geophys. Res. 97, 4521-4540.

Hollings, P., Kerrich, R., 2000. An Archean arc basalt-Nb-enriched basalt-adakite association: the 2.7 Ga confederation assemblage of the Birch-Uchi greenstone belt, superior province. Contrib. Miner. Petrol. 139, 208–226.

Jost, H., Apollo, J.F.H., Weber, W., Salles, R.R., Marques, J.C.M., Massucatto, A.J., Costa, D.A., Santos, B.A., 2019. Stratigraphic update, paleotectonic, paleogeographic, and depositional environments of the Crixás Greenstone Belt, Central Brazil. J. S. Am. Earth Sci. 96, 102329.

Jost, H., Carvalho, M.J., Rodrigues, V.G., Martins, R., 2014. Metalogênese dos greenstone belts de Goiás. In: Silva, M.G., Neto, M.B.R., Jost, H., Kuyumjian, R.M. (Orgs.), Metalogênese das províncias tectônicas brasileiras, Belo Horizonte, CPRM, pp. 141-168.

Jost, H., Chemale Jr., F., Dussin, I.A., Tassinari, C.C.G., Martins, R., 2010. A U–Pb zircon paleoproterozoic age for the metasedimentary host rocks and gold mineralization of the Crixás greenstone belt, Goiás, Central Brazil. Ore Geol. Rev. 37, 127–139.

Jost, H., Chemale Jr., F., Fuck, R.A., Dussin, R.A., 2013. Uvá complex, the oldest orthogneisses of the Archean Paleoproterozoic terrane of central Brazil. J. S. Am. Earth Sci. 47, 201-212.

Jost, H., Fuck, R.A., Dantas, E.L., Rancan, C.C., Rezende, D.B., Santos, E., Portela, J.F., Mattos, L., Chiarini, M.F.N., Oliveira, R.C., Silva, S.E., 2005. Geologia e geocronologia do Complexo Uvá, Bloco Arqueano de Goiás. Rev. Brasil. Geocienc. 35, 559-572.

Jost, H., Oliveira, A.M., 1991. Stratigraphy of the greenstone belts, Crixás region, Goiás, Central Brazil. J. S. Am. Earth Sci. 4, 201 -214.

Kerrich, R., Wyman, D.A., Fan, J., Bleeker, W., 1998. Boninite series: low-Ti tholeiite associations from the 2.7 Ga Abitibi greenstone belt. Earth Planet. Sci. Lett. 164, 303–316.

Khanna, T.C., Sesha Sai, V.V., Bizimis, M., Krishna, A.K., 2015. Petrogenesis of basalthigh-Mg andesite-adakite in the Neoarchean Veligallu greenstone terrane: Geochemical evidence for a rifted back-arc crust in the eastern Dharwar craton, India. Precambr. Res. 258, 260–277.

Kusky, T.M., Windley, B.F., Polat, A., 2018. Geological evidence for the operation of plate tectonics throughout the Archean: Records from Archean Paleo-Plate Boundaries. J. Earth Sci. 29 (6), 1291–1303.

Kusky, T.M., Windley, B.F., Polat, A., Wang, L., Ning, W., Zhong, Y., 2021. Archean dome-and-basin style structures form during growth and death of intraoceanic and continental margin arcs in accretionary orogens. Earth-Sci. Rev. 103725.

Kuyumjian, R.M., Jost, H., 2006. Low- and high- alumina komatiites of Goiás, Central Brazil. J. S. Am. Earth Sci. 20, 315–326.

Manikyamba, C., Kerrich, R., Khanna, T.C., Satyanarayanan, M., Krishna, A.K., 2009. Enriched and depleted arc basalts, with high-Mg andesites and adakites: a potential paired arc-backarc of the 2.7 Ga Hutti greenstone terrane, India. Geochim. Cosmochim. Acta 73, 1711–1736.

McLennan, S.M., Hemming, S., McDanniel, D.K., Hanson, G.N., 1993. Geochemical approaches to sedimentation, provenance, and tectonics. In: In: Johnsson, M.J., Basu, A. (Eds.), Processes Controlling the Composition of Clastic Sediments. Geol. Soc. Am. Spec. Pap. 285, 21–40.

McLennan, S.M., Taylor, S.R., McCulloch, M.T., Maynard, J.B., 1990. Geochemical and Nd-Sr isotopic composition of deep-sea turbidites: crustal evolution and plate tectonic associations. Geochim. Cosmochim. Acta 54, 2015-2050.

Pimentel, M.M., 2016. The tectonic evolution of the Neoproterozoic Brasília Belt, central Brazil: a geochronological and isotopic approach. Braz. J. Geol. 46, 67-82.

Pimentel, M.M., Jost, H., Fuck, R.A., Armstrong, R.A., Dantas, E.L., Potrel, A., 2003. Neoproterozoic anatexis of 2.9 Ga old granitoids in the Goiás-Crixás block, Central Brazil: evidence from new SHRIMP U-Pb data and Sm-Nd isotopes. Geol. USP, Sér. Cient. 3, 1-12.

Polat, A., 2009. The geochemistry of Neoarchean (ca. 2700 Ma) tholeiitic basalts, transitional to alcaline basalts, and gabbros, Wawa Subprovince, Canada: Implications for petrogenetic and geodynamic processes. Precambrian Res. 168, 83–105.

Polat, A., Kerrich, R., 2006. Reading the geochemical fingerprints of Archean hot subduction volcanic rocks: evidence for accretion and crustal recycling in a mobile tectonic regime. In: Benn, K., Mareschal, J.C., Condie, K.C. (Eds.), Archean Geodynamics and Environments. AGU Geophysics Monograph Series 164, 189–213.

Polat, A., Li, J., Fryer, B., Kusky, T., Gagnon, J., Zhang, S., 2006. Geochemical characteristics of the Neoarchean (2800-2700 Ma) Taishan greenstone belt, North China Craton: Evidence for plume-craton interaction. Chem. Geol. 230, 60–87.

Puchtel, I.S., Hofmann, A.W., Mezger, K., Jochum, P.K., Scipansky, A.A., Samsanov, A.V., 1998. Oceanic plateau model for continental crustal growth in the Archean: a case study from the Kostomuksha greenstone belt, NW Baltic Shield. Earth Planet. Sci. Lett. 155, 57–74.

Queiroz, C.L., 2000. Evolução Tectono-Estrutural dos Terrenos Granito-Greenstone Belt de Crixás, Brasil Central. Tese de Doutorado, Instituto de Geociências, Universidade de Brasília, 209 pp.

Queiroz, C.L., Jost, H., Silva, L.C., McNaughton, N.J., 2008. U-Pb SHRIMP and Sm-Nd geochronology of granite-gneiss complexes and implications for the evolution of the central Brazil Archean terrain. J. S. Am. Earth Sci. 26, 100-124.

Sabóia, L.A., 1979. Os greenstone be1ts de Crixás e Goiás, GO. Sociedade Brasileira de Geologia. Núcl. Centro-Oeste, Goiâ., Boletim Inf. 9, 43–72.

Sabóia, L.A., Teixeira, N.A., 1983. Ultramaphic flows of the Crixás greenstone belt, Goiás. Precambrian Res. 22, 23–40.

Tassinari, C.C.G., Jost, H., Santos, J.C., Nutman, A.P., Bennell, M.R., 2006. Pb and Nd isotope signatures and SHRIMP U-Pb geochronological evidence of Paleoproterozoic age for Mina III gold mineralization. In: South American Symposium on Isotope Geology, 5, Pucon, Chile, Proceedings, pp. 615-617.

Windley, B.F., Kusky, T., Polat, A., 2021. Onset of plate tectonics by the Eoarchean. Precambrian Res. 352, 105980. https://doi.org/10.1016/j.precamres.2020.105980

Wyman, D. A., 2013. A critical assessment of Neoarchean 'plume only' geodynamics: evidence from the Superior Province. Precambrian Res. 229, 3–19.

Wyman, D.A., 1999. A 2.7 Ga depleted tholeiite suíte: evidence of plume-arc interaction in the Abitibi Greenstone Belt, Canada. Precambrian Res.97, 27–42.

Wyman, D.A., Ayer, J.A., Devaney, J.R., 2000. Niobium-enriched basalts from the Wabigoon subprovince, Canada: evidence for adakitic metasomatism above an Archean subduction zone. Earth Planet. Sci. Lett. 179, 21–30.

Wyman, D.A., Kerrich, R. 2009. Plume and arc magmatism in the Abitibi subprovince: implications for the origin of Archean continental lithospheric mantle. Precambrian Res. 168 (1– 2), 4–22.

Xie, Q., Kerrich, R. and Fan, J., 1993. HFSE/REE fractionations recorded in the three komatite-basalt sequence, Archean Abititi belt: implications for multiple plume sources and depth. Geochim. Cosmochim. Acta 57, 4111-4118.

Capítulo II – Artigo 1

Unraveling a hidden Rhyacian magmatic arc through provenance of metasedimentary rocks of the Crixás greenstone belt, Central Brazil.

Caio César Aguiar Borges [a,*], Catarina Labouré Bemfica Toledo [a], Adalene Moreira Silva [a], Farid Chemale Jr [b], Bruno Araújo dos Santos [c], Frederico Lana Figueiredo [c], Érico Natal Pedro Zacchi [a].

[a] Instituto de Geociências, Universidade de Brasília, 70910-900, Brasília, Brasil.

[b] Departamento de Geologia, Universidade do Vale do Rio dos Sinos, 93022-000, São Leopoldo, RS, Brasil.

[c] AngloGold Ashanti Ltd., Rodovia GO-336, 97000 Km 97, 76510-000, Crixás, GO, Brasil.

[*] Corresponding author. E-mail address: caioaguiar0@gmail.com. Phone: +55 61 98130-9136.

Published in Precambrian Research: https://doi.org/10.1016/j.precamres.2020.106022

Abstract

The Crixás-Goiás Domain, Central Brazil, comprises an association of Archean TTG (tonalite-trondhjemite-granodiorite) and Archean-Paleoproterozoic greenstone belts. The Crixás greenstone belt, located in the northern part of the domain, is constituted of Mesoarchean metakomatiites and metabasalts overlaid by Paleoproterozoic carbonaceous phyllites and metagraywackes that host important gold deposits. In this work, we present new integrated petrographical, geochemical, and isotopic data to investigate the provenance and tectonic setting of the metasedimentary rocks of the Crixás greenstone belt. Mineral and textural immaturities, particularly of the metagraywackes, are consistent with a proximal source area; which is also evidenced by the chemical aspects that denote the absence of significant sediment sorting and recycling. Geochemical data indicate provenance from mixed mafic and felsic sources. U-Pb detrital zircon geochronology shows unimodal age spectra, with a dominant peak at ca. 2.2 – 2.1 Ga and minor contribution of ca. 2.7 and 2.4 Ga grains. Concordia diagrams yielded upper intercepts between 2213.4 ± 5.6 and 2162.2 ± 9.2 Ma, interpreted as the age range of the main source area. The rocks present relatively homogeneous Sm-Nd model ages (2.44 to 2.34 Ga) and slightly negative to positive ε_{Nd}, ranging from -0.27 to +1.25. We argue that the original sedimentary protoliths were deposited in a trench or forearc basin related to a ca. 2.2 - 2.1 Ga island arc formed adjacent to an Archean paleocontinent constituted of TTG-greenstone terranes. Rapid erosion of the rising intraoceanic arc resulted in syn-orogenic sedimentation that started with deep ocean black shale deposition in an anoxic environment followed by episodic turbidite currents of poorly-sorted immature sands. Sedimentary rock layers were tectonically transported to the continent and preserved in the elongated keels of Mesoarchean mafic-ultramafic volcanic rocks. This orogeny can be correlated with the amalgamation of the Goiás Massif during the Siderian-Rhyacian crustal growth related to a successive collage of arc-related terranes in the formation of the western margin of the São Francisco paleocontinent. Sediment provenance of the Crixás greenstone belt proved to be crucial to the recognition and characterization of Paleoproterozoic crust that is apparently no longer preserved in outcrops.

Keywords: Tocantins Province, Goiás Massif, Sediment Provenance, Rhyacian Crustal Growth.

1. Introduction

Composition of siliciclastic sedimentary rocks is controlled by tectonism, weathering, transportation, sorting, diagenesis, and source rock assembly. Therefore, it is a powerful tool to explore the provenance and tectonic setting of ancient sedimentary basins, and constrain the evolution of continental crust through geological time, especially when associated with detrital zircon geochronology and other isotopic methods (Bhatia, 1983; Bhatia and Crook, 1986; Floyd and Leveridge, 1987; McLennan et al., 1990; Condie, 1993; McLennan et al., 1993; Duller and Floyd, 1995; Hartmann et al., 2006; Condie et al., 2009; Cawood et al., 2012; Grisolia and Oliveira, 2012; Spencer et al., 2012; Greber et al., 2017; Drabon et al., 2019; Greber and Dauphas, 2019). Oftentimes, sedimentary rocks are the only available source of information about sialic crust that is no longer preserved (Feng and Kerrich, 1990; Cawood et al., 2012).

The present work demonstrates how the sediment provenance of the Crixás greenstone belt, Central Brazil, proved to be an outstanding example in depicting Paleoproterozoic tectonic processes and crustal growth in a context where the main source area is apparently not exposed. The Crixás greenstone belt is a component of the TTG-greenstone terrane known as Crixás-Goiás Domain and consists of Archean metakomatiites and metabasalts overlaid by a low-grade Paleoproterozoic metasedimentary succession composed essentially of carbonaceous phyllites and metagraywackes. Geochemical aspects of the metasedimentary rocks were formerly addressed by Jost et al. (1996). Scarce geochronological data, however, limited the provenance inferences. For instance, those rocks were initially thought to be Archean and older than their surrounding TTG gneisses. Progressive advances in isotopic studies occurring in the last decades indicated a mixed contribution of Archean and Paleoproterozoic sediment sources (Fortes et al., 2003; Tassinari et al., 2006; Jost et al., 2010). Thereafter, the provenance of metasedimentary rocks of the Crixás greenstone belt turned to be potentially useful to investigate the crustal growth of the Archean-Paleoproterozoic Crixás-Goiás Domain, particularly regarding the uncertain nature of the main Rhyacian source area.

In this contribution, we provide integrated whole-rock major and trace element data, Sm-Nd isotopes, and LA-ICP-MS U-Pb detrital zircon geochronology of carbonaceous phyllites and metagraywackes of the Crixás greenstone belt. Our systematic sampling focused on drill cores from different regions and depths in the central-northern part of the greenstone, around the immediate vicinity of the Mineração Serra Grande S.A. – AngloGold Ashanti gold company. We aim to characterize the source areas of the clastic debris and

interpret the tectonic setting of the paleobasin. Our results give insights to a Rhyacian orogeny recorded in the Crixás-Goiás Domain. Finally, we discuss the implications of this orogeny to the Paleoproterozoic crustal growth of the Goiás Massif (i.e. the crystalline basement of the Neoproterozoic Brasília Belt), recently interpreted as the western pericratonic margin of the São Francisco paleocontinent (Cordeiro and Oliveira, 2017; Martins-Ferreira et al., 2020), that was latterly involved in the amalgamation of the Western Gondwana in the Neoproterozoic.

2. Geological Context

The Tocantins Province (Almeida et al., 1981), located in the central part of Brazil, is an extensive Brasiliano/Pan-African orogen of the South American Platform formed during the collision between the Amazonian, São Francisco/Congo, West African/São Luís, and Paranapanema cratons that resulted in the amalgamation of the Western Gondwana supercontinent in the Neoproterozoic. The province is composed of three Neoproterozoic Brasiliano fold belts: the Paraguay, Araguaia and Brasília belts (Pimentel et al., 2000). The Brasília Belt borders the western margin of the São Francisco Craton and is one of the most important and preserved Brasiliano orogens of the South American Platform. The main components of the belt include thick east-verging fold-and-thrust Neoproterozoic passive margin sedimentary sequences, an extensive Neoproterozoic juvenile magmatic arc, a high-grade metamorphic core, ophiolitic fragments, and Meso-Neoproterozoic layered mafic-ultramafic complexes (Fuck et al., 2014; Pimentel, 2016 and references therein).

In the central-northern part of the Brasília Belt, all pre-Brasiliano (pre-Neoproterozoic) crystalline basement is grouped in the Goiás Massif (Fig. 1), which can be divided into four distinct tectonic domains (Cordeiro and Oliveira, 2017): The Archean-Paleoproterozoic Crixás-Goiás Domain and the Paleoproterozoic Almas-Conceição do Tocantins, Cavalcante-Arraias and Campinorte domains.

The Crixás-Goiás Domain, where our study is focused, consists of a typical TTG-greenstone terrane (Fig. 2a). The Almas-Conceição do Tocantins Domain, located in the northernmost portion of the Goiás Massif (Fig. 1), constitutes a complex collage of different terranes, including ca. 2.45 Ga greenstones and ca. 2.45 - 2.10 Ga metaluminous and peraluminous granite-gneissic rocks (Cruz et al., 2003; Sousa et al., 2016; Fuck et al., 2014; Martins-Ferreira et al., 2020; Saboia et al., 2020). Accretion of the different blocks of the Almas-Conceição do Tocantins Domain during the Siderian and early Rhyacian resulted in progressively younger rocks toward the west (Martins-Ferreira et al., 2020). This domain is

partially covered by Mesoproterozoic metavolcanosedimentary rocks of the Natividade Group (Toscani et al., 2020).

The Cavalcante-Arraias Domain is mainly composed of ca. 2.18 - 2.14 Ga peraluminous granites of the Aurumina Suite intruded in graphitic schists and paragneisses of the Ticunzal Formation (Botelho et al., 2006; Fuck et al., 2014; Cuadros et al., 2017a, 2017b). A collisional setting has been proposed for the Aurumina Suite (Botelho et al., 2006; Sousa et al., 2016), whereas Cuadros et al. (2017a) suggested a cordilleran hinterland setting for the peraluminous magmatism. This domain is partially covered by ca. 1.77 Ga rift sequences of the Araí Group and intruded by A-type granites of the 1.77 Ga Pedra Branca and 1.58 Ga Serra da Mesa suites (Pimentel et al., 1991) (Fig. 1).

The Campinorte Domain is a poorly exposed Rhyacian terrane that is currently largely covered by the Mesoproterozoic Serra da Mesa Group (Fig. 1) and comprises juvenile metagranitic rocks of the Pau de Mel Suite and a metavolcanosedimentary sequence (Campinorte Sequence) (Giustina et al., 2009; Cordeiro et al., 2014). The Pau de Mel Suite consists of ca. 2.17 – 2.07 Ga NNE-trending arc-related metatonalites, metagranodiorites, and metamonzogranites (Cordeiro et al., 2014). The Campinorte Sequence consists of low-grade quartz-muscovite schists, quartzites, chert, and gondite lenses associated with rare felsic metatuff and metavolcanic rocks (Giustina et al., 2009). The age of this sequence is constrained by a maximum depositional age of ca. 2.2 Ga, obtained for a quartzite sample, and a direct age of 2179 ± 4 Ma for a felsic metatuff (Giustina et al., 2009). Paragranulites and mafic granulites associated with the Campinorte Sequence register the metamorphic peak at ~2.1 Ga, as indicated by U-Pb dating of metamorphic zircon (Cordeiro et al., 2014). Newly recognized metatonalites and metagranodiorites in tectonic contact with metavolcanic and metasedimentary rocks occurring in the Artulândia area, located southeast of the Rio Maranhão Thrust (Fig. 1), have been correlated with the Campinorte Arc (Filgueiras et al., 2020).

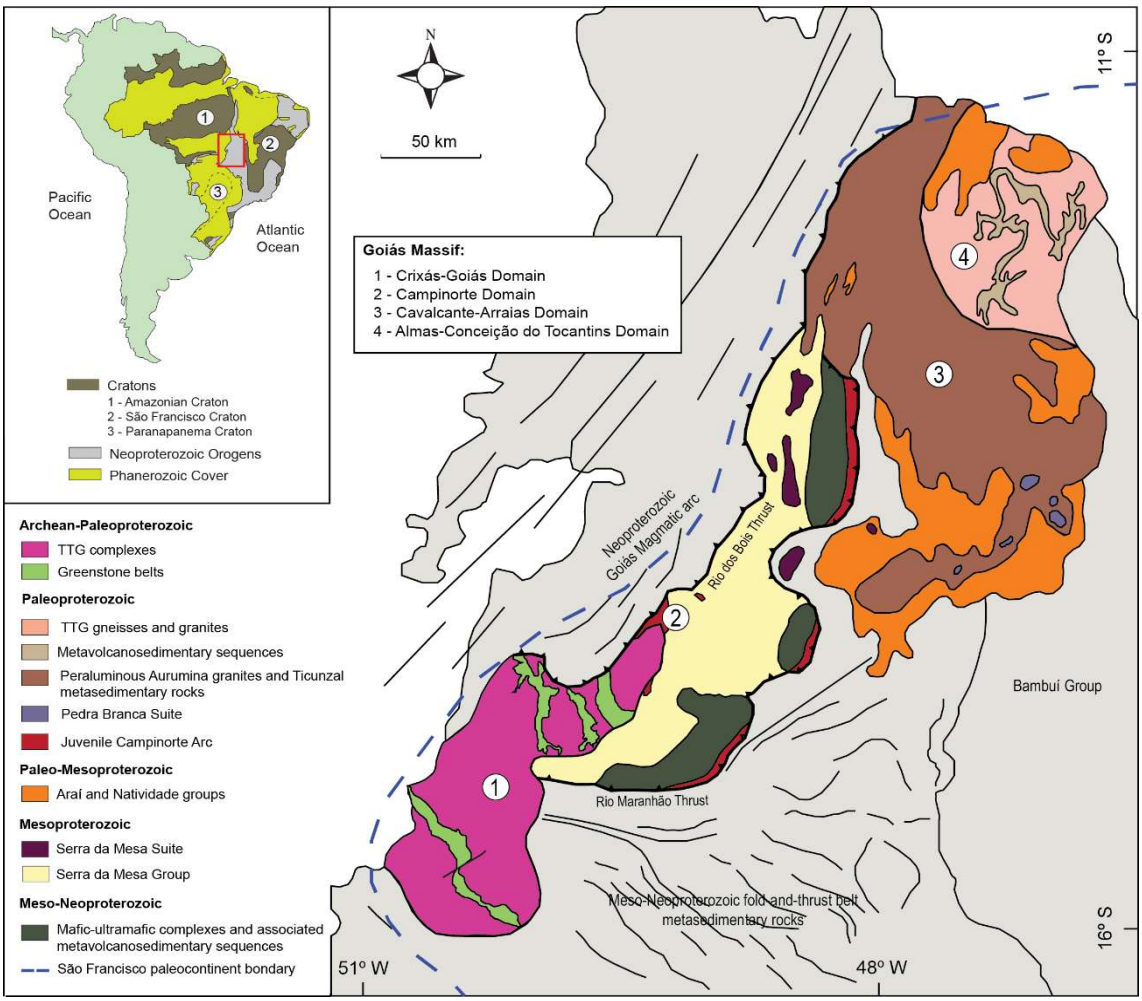

Fig. 1. The central-northern part of the Brasília Belt, highlighting the four tectonic domains of the Goiás Massif (modified after Cordeiro and Oliveira, 2017). The Crixás-Goiás domain is located in the southwesternmost part of the massif.

2.1. The Crixás-Goiás Domain

In the last decades, the region exposed in Central Brazil where Archean TTG and Archean-Paleoproterozoic greenstone belts occur in an approximately 18,000 km² area has been designated with different names in diverse publications, for example, Goiás Archean Block (Jost et al., 2005; Pimentel, 2016), Crixás-Goiás Archean Block (Pimentel et al., 2003), Archean Terrane of Central Brazil (Queiroz et al., 2008), Archean-Paleoproterozoic Terrane of Central Brazil (Jost et al., 2013), Archean-Paleoproterozoic Terrane of Goiás (Jost et al., 2014; Borges et al., 2017; Campos et al., 2017), Crixás-Goiás Terrane (Jost et al., 2019) and Goiás Archean Block (Bogossian et al., 2020; Bogossian, 2020). The region has been traditionally interpreted as an allochthonous microcontinent that was amalgamated to the western edge of the Brasília Belt during the Brasiliano Orogeny in the late Neoproterozoic (Pimentel et al., 2011; Jost et al., 2013, 2019). Otherwise, Cordeiro and Oliveira (2017), in

a broad regional review of the Goiás Massif, interpreted that this region and the other domains of the massif are a part of a continuous landmass of the São Francisco paleocontinent that was already amalgamated since the late Paleoproterozoic. Cordeiro and Oliveira (2017) also suggested the nomenclature "Crixás-Goiás Domain" to refer to the region comprising Archean TTG and Archean-Paleoproterozoic greenstone belts. In order to favor standardization and facilitate future references, we are adopting this nomenclature herein.

The Crixás-Goiás Domain consists of an association of six Archean TTG complexes (Uvá and Caiçara, to the south, and Anta, Caiamar, Moquém and Hidrolina, to the north) and five Archean-Paleoproterozoic greenstone belts (Faina and Serra de Santa Rita, to the south, and Crixás, Pilar de Goiás and Guarinos, to the north) (Fig. 2a). The TTG complexes of the northern part are divided into two stages of magmatism: The first comprises mainly ca. 2.8 Ga tonalitic and granodioritic gneisses of the Hidrolina, Caiamar, and Anta complexes, with mostly positive ε_{Nd} (t) values. Inherited zircon crystals of 3.3 Ga and Sm-Nd model ages of 3.0 Ga indicate that the magmas were contaminated with older sialic crust, of which there is no known exposure so far (Queiroz et al., 2008). The second stage is recorded in the Moquém Complex as ca. 2.7 Ga sheet-like granodiorites and granites with negative ε_{Nd} (t) values and inherited zircon from orthogneisses of the first stage (Queiroz et al., 2008).

The Caiçara Complex, located in the southern part of the Crixás-Goiás Domain, is composed predominantly of ca. 3.1 Ga tonalitic orthogneisses that were intruded by smaller bodies of ca. 2.8 Ga granodiorites, granites, and charnockites (Beghelli Junior, 2012). The Uvá complex, located in the southernmost part of the domain, is formed by two groups of orthogneisses (Jost et al., 2005, 2013). The dominant group is the oldest and comprise ca. 3.0 - 2.9 Ga polydeformed tonalitic to granodioritic gneisses (Jost et al., 2013) and a ca. 2.9 Ga diorite stock (Pimentel et al., 2003). The second group corresponds to sheet-like ca. 2.8 Ga tonalites and monzogranites (Jost et al., 2005, 2013).

The greenstone belts occur as narrow metavolcanosedimentary sequences situated between the TTG complexes. Stratigraphically, the five greenstones are composed of basal metakomatiites and metabasalts superimposed by varied gold-hosting metasedimentary successions (Jost et al., 2014). Lenses of Archean andesitic metavolcanic and metavolcaniclastic rocks are a particular feature of the Serra de Santa Rita greenstone belt (Resende et al., 1998; Borges et al., 2017). Intercalations of BIF and chert occur in different proportions among the volcanic flows (Saboia et al., 1981; Jost and Oliveira., 1991; Resende et al., 1998). Whole-rock Sm-Nd data of metakomatiites and metabasalts of the Crixás greenstone belt presented an isochron age of ca. 3.0 Ga (Fortes et al., 2003). Similar age of

2.96 Ga was obtained by robust zircon U-Pb dating of amphibolite and chloritite samples of the Faina and Serra de Santa Rita greenstone belts (Borges et al., 2017). Several isotopic data for metasedimentary rocks of the five greenstone belts have shown provenance from Archean and Paleoproterozoic sources (Resende et al., 1999; Fortes et al., 2003; Tassinari et al., 2006; Jost et al., 2010, 2012, 2014; Brant et al., 2015; this work).

The Crixás-Goiás Domain also registers local Siderian mafic magmatism related to crustal extension (Corrêa da Costa, 2003) and Rhyacian intermediate to felsic magmatism related to compression (Jost et al., 1992, 1993; Queiroz, 2000; Bogossian, 2020). Influences of the Brasiliano Orogeny are manifested as Neoproterozoic granitic intrusions, anatexis of Archean orthogneisses, and hydrothermal alteration related to ore deposits (Fortes, 1996; Fortes et al., 2003; Pimentel et al., 2003; Tassinari et al., 2006; Queiroz et al., 2008; Rodrigues, 2011; Jost et al., 2005, 2014).

2.2. The Crixás Greenstone Belt

The Crixás greenstone belt is a greenschist- to amphibolite- facies metavolcanosedimentary sequence located in the northern part of the Crixás-Goiás Domain. In the west, it is limited by the Anta Complex, in the east, by the Caiamar Complex, and in the northwest and north-northeast, it is overthrusted by the allochthonous Mina Inglesa Sequence and Neoproterozoic metasedimentary rocks of the Goiás Magmatic Arc, respectively (Fig. 2b).

The belt is divided from the base to the top in the Córrego Alagadinho, Rio Vermelho, Ribeirão das Antas and Córrego Geral formations (Jost and Oliveira, 1991; Jost et al., 2019) (Fig. 2c). The Córrego Alagadinho Formation is composed of a thick sequence of metaultramafic rocks, which protoliths are interpreted to be peridotitic and pyroxenitic komatiites. Primary igneous features comprise flux breccia, polyhedral joints, cumulates, and well-preserved spinifex textures (Kuyumjian and Teixeira, 1982; Saboia and Teixeira, 1983). The Rio Vermelho Formation is composed of metabasalts that locally preserve pillowed structures, vesicles, and amygdales. Some intercalations of BIF, manganese formation, and metachert occur along the metavolcanic rocks (Saboia et al, 1981; Jost and Oliveira, 1991). Sm-Nd and Pb-Pb isochrons from metakomatiites yielded inaccurate ages of ca. 2.82 and 2.72 Ga, respectively (Arndt et al., 1989). The Mesoarchean age of the metavolcanic sequence was later reinforced by Fortes et al. (2003) with a whole-rock Sm-Nd isochron obtained from metakomatiite and metabasalt samples that yielded a 2998 ± 70 Ma age.

The metasedimentary succession of the Crixás greenstone belt overrides the metavolcanic rocks above a nonconformity obliterated by thrust faults and stratigraphic overturning (Jost et al., 2019). Geochronological data show provenance from Archean to Paleoproterozoic source areas (Tassinari et al., 2006; Jost et al., 2010; this work), indicating that the deposition of the sedimentary rocks occurred a long time after the Mesoarchean volcanism. The Ribeirão das Antas Formation consists of carbonaceous phyllites and dolomite lenses with rare oolites (Jost et al., 2019). Metagraywackes of the Córrego Geral Formation predominate at the top of the stratigraphy. Preserved primary sedimentary structures include parallel lamination, sin-depositional faults, intraformational breccia, cross-lamination, flame, and fluid-escape structures (Jost et al., 2010, 2019). Deposition of black shales predominated during the early stages of the sedimentary basin and was coeval and laterally wedge-shaped with graywacke deposition that prevailed during the late stages (Jost et al., 2019).

Dolomite lenses present positive $\delta^{13}C$ values of +5.3 to +14‰ (PDB) (Dix et al., 1995; Fortes, 1996), which are comparable with the ca. 2.2 - 2.0 Ga positive $\delta^{13}C$ carbon isotope excursion (Lomagundi Event) that is reported in many Paleoproterozoic carbonates (Melezhik et al., 2007). This event took place after the 2.45 - 2.32 Ga Great Oxidation Event (Bekker et al., 2008) and the 2.45 - 2.22 Ga Huronian glaciation (Young et al., 2001). Jost et al. (2019) interpreted that the positive ^{13}C anomalies of dolomites of the Crixás greenstone belt can be correlated with the youngest population of detrital zircon grains of the metagraywackes (~ 2.1 Ga; Jost et al., 2010), indicating that the sediment deposition in the paleobasin took place in the Rhyacian.

Multiphase deformational events occurred in the Crixás greenstone belt and were responsible for the formation of tight to isoclinal regional folds and east-verging thin-skinned thrust faults that resulted in the stratigraphic overturning of the succession, as evidenced by the common overriding of the metakomatiites onto the metabasalts, which override the metasedimentary rocks (Jost et al., 2010, 2019 and references there in) (Fig. 3).

Gold mineralization occurs as stacked massive sulfide lenses, quartz veins, and several disseminated orebodies structurally controlled by low-angle thrust-faults within the metasedimentary succession (Jost et al., 2010, 2014). U-Pb data of zircon grains recovered from a silicified metagraywacke sample and interpreted to be of hydrothermal origin yielded a 2165 ± 47 Ma age, which was considered to reflect the timing of the gold mineralization in the Crixás greenstone belt (Tassinari et al., 2006). Re-Os dating of arsenopyrite from gold-bearing massive sulfide lenses yielded a 2126 ± 16 Ma age (Marques et al., 2013).

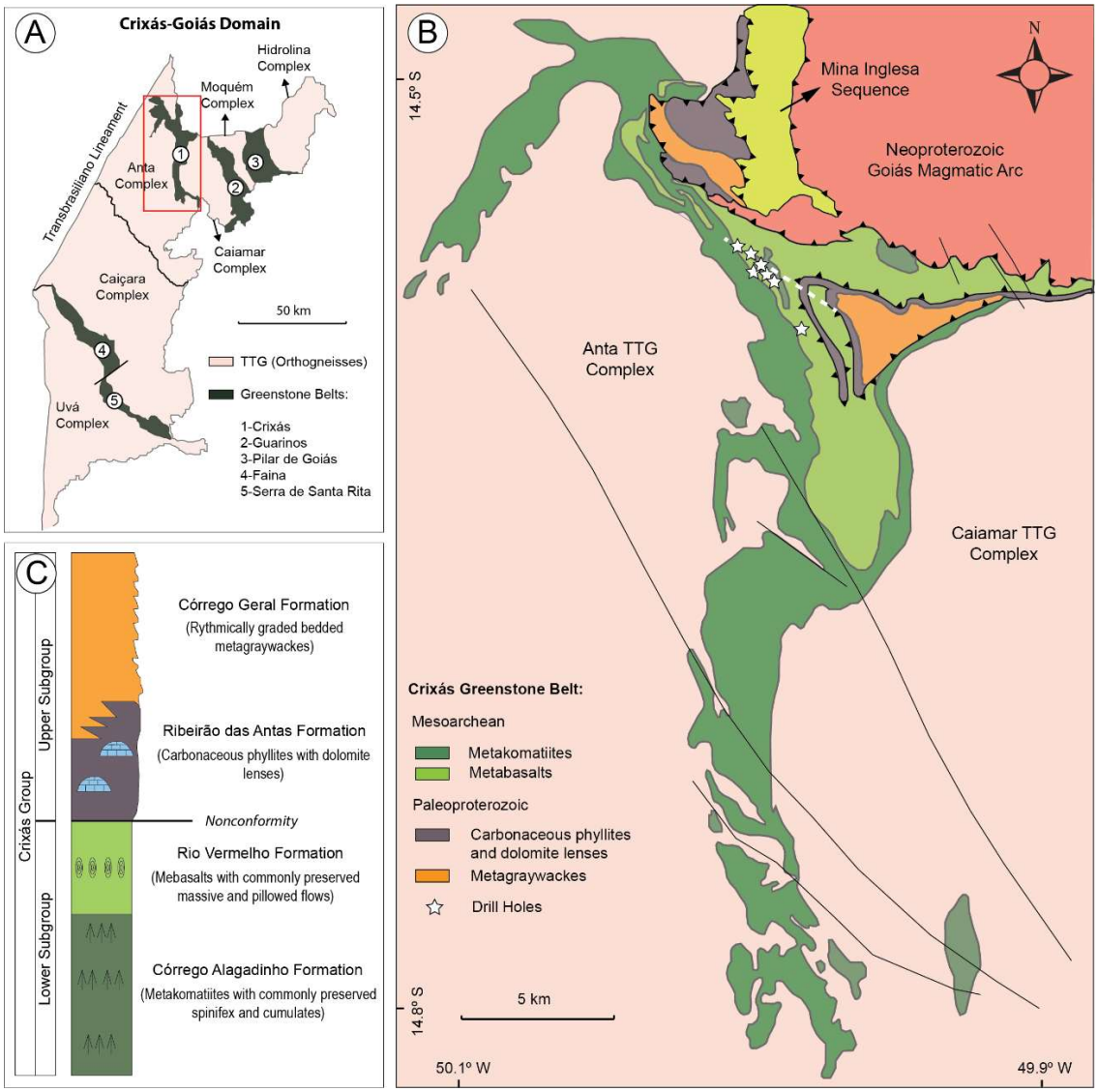

Fig. 2. The Crixás-Goiás Domain and the Crixás greenstone belt, located in the northern part of the domain. (A) The main components of the Crixás-Goiás Domain (modified after Jost et al. 2010). (B) Geological map of the Crixás greenstone belt (modified after Jost et al. 2010, 2019). Location of the drill hole cores sampled in this study is highlighted. (C) Stratigraphic column of the Crixás greenstone belt (modified after Jost et al., 2019). Schematic section of Fig. 3 is represented by the dotted line.

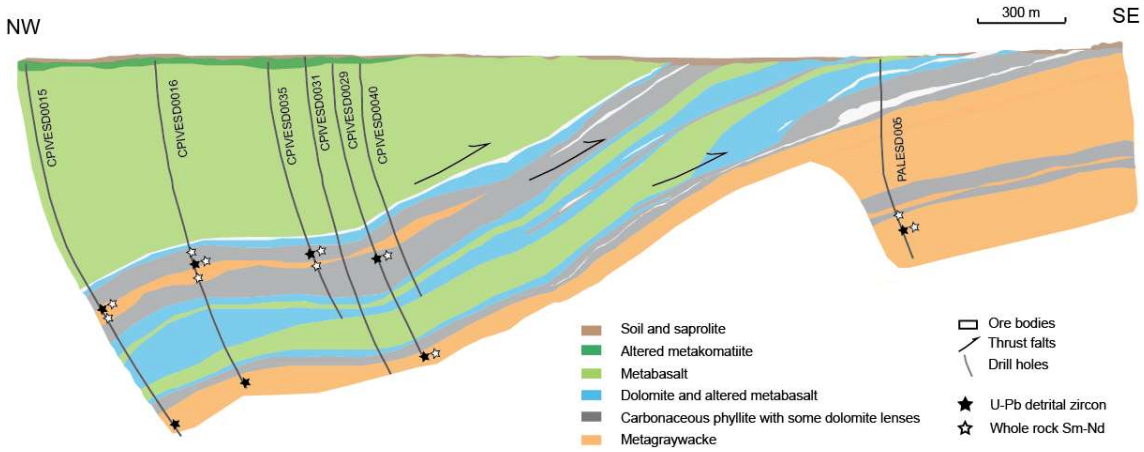

Fig. 3. NW-SE schematic section in the central-northern part of the Crixás greenstone belt. Note the stratigraphic overturning and tectonic repetition of layers due to detachment-thrusting. Location of samples collected for Sm-Nd and U-Pb isotopic studies is shown. Sampling for petrographic and geochemical analyses was systematically performed along different intervals of metasedimentary rocks.

3. Methods

3.1. Sampling

Core samples of metagraywackes and carbonaceous phyllites were collected in different intervals from seven drill holes located in the operation area of the Mineração Serra Grande S.A. - AngloGold Ashanti, a mining company that conducts the gold exploration in the region since 1980. The drill holes are roughly aligned in a NW-SE section in the central-northern part of the greenstone belt (Fig. 2b). Due to stratigraphic overturning, as a result of detachment faults and duplex structures, the shallow cores record saprolite and altered metakomatiites, mostly transformed into talc schists, followed by massive to foliated greenish metabasalts at deeper levels. Layers of metasedimentary rocks repeatedly appear in tectonic contact below the metabasalts. The section in Fig. 3 was constructed with detailed data from extensive drilling integrated with surface and underground information performed by Mineração Serra Grande S.A.

For the purpose of this work, drill cores were logged and described, and some specific intervals were selected for petrographical study. The most preserved samples were selected for whole-rock geochemical and Sm-Nd analyses. Core intervals of approximately 2 m of metagraywackes and carbonaceous phyllites without evidence of hydrothermal alteration were sampled for LA-ICP-MS U-Pb detrital zircon geochronology. In total, this work presents new whole-rock geochemical data of 50 samples, Sm-Nd isotopic data of 11 samples, and U-Pb geochronological data of 8 samples.

3.2. Whole-Rock Geochemistry

33 samples of metagraywacke and 17 samples of carbonaceous phyllite were pulverized and analyzed at the ALS Geochemistry Laboratory in Goiânia, Brazil. Major elements were determined by ICP-AES and are presented in weight oxides percentages. The rare earth elements (REE), high field strength elements (HFSE), and large ion lithophile elements (LILE) were analyzed by ICP-MS. The metals Cd, Co, Cu, Li, Mo, Ni, Pb, Sc, Tl, and Zn were determined by ICP-AES. A complete description of the laboratory procedures

and analytical methods is available on the Whole Rock Analysis catalog (package CCP-PKG01), accessible on the ALS Geochemistry homepage (www.alsglobal.com).

Major element analyses were recalculated to 100 wt.% anhydrous basis for inter-comparisons. Chondrite and Primitive Mantle compositions from Sun and McDonough (1989) and Post-Archean Australian Shale (PAAS) composition from Taylor and McLennan (1985) were used for normalizations. Europium (Eu/Eu*) and cerium (Ce/Ce*) anomalies were calculated concerning the neighboring elements on chondrite-normalized REE diagrams, following the method of Taylor and McLennan (1985). Major (wt.%) and trace elements (ppm) data are listed in Supplementary Material 1.

3.3. U-Pb Geochronology

Selected cores of 5 metagraywacke and 3 carbonaceous phyllite samples were prepared and analyzed at the Geochronology Laboratory of the University of Brasília. Samples were initially crushed, milled, and sieved. Non-magnetic grains were segregated from the heavy mineral concentrates using a Frantz isodynamic magnetic separator. Individual grains were manually separated using a binocular microscope and mounted in epoxy resin for further polishing. A FEI Quanta™ 450 Field Emission Scanning Electron Microscope provided cathodoluminescence and back-scatter electron images that were used to investigate the texture and internal structure of the zircon crystals.

All analyses were performed using a MC-ICP-MS Finnigan Neptune coupled to a New Wave 213 µm Nd-YAG laser. Methods and the equipment details are described by Bühn et al. (2009). In this work, we analyzed ^{238}U in a H4 Faraday cup, ^{232}Th in a H2 Faraday cup, ^{208}Pb in a L3 Faraday cup, and ^{206}Pb in a L4 Faraday cup. Ion counters (ICs) fixed in the L4 Faraday cup were used to measure ^{207}Pb, $^{204}Hg/^{204}Pb$, and ^{202}Hg. Due to He contamination, an isobaric interference correction between ^{204}Hg and ^{204}Pb was applied. Laser ablation was performed in 25 µm spots (simple spot mode) with a 10 Hz frequency and a 2.71 – 3.99 J/cm² intensity. Pulverized material was carried with a He (~0.40 L/min) and Ar (~1.00 L/min) flux. For the analyses, signals were collected in a single block with 40 cycles of 1.049 s time integration. ^{202}Hg, $^{204}(Pb + Hg)$, ^{206}Pb, and ^{207}Pb were measured in counts per second (CPS), while ^{232}Th and ^{235}U were measured in millivolts (mV). A standard-sample intercalation technique (Standard Bracketing) was used to correct the fractionation and the spectrometer induced instrumental deviation. Correction factor was calculated based on the intervals of analyses.

The GJ-1 zircon was used as the primary standard. This standard has an ID-TIMS age of 608.5 ± 0.4 Ma and isotopic ratios of $^{206}Pb/^{238}U$ = 0.09761 ± 0.00011, $^{207}Pb/^{235}U$ = 0.8093 ± 0.0009 and $^{207}Pb/^{206}Pb$ = 0.06014 ± 0.00001 (Jackson et al, 2004). As secondary standard, the 91500 zircon was used. This standard has an ID-TIMS age of 1065.4 ± 0.3 Ma and certified isotopic ratios of $^{206}Pb/^{238}U$ = 0.17917 ± 0.00008, $^{207}Pb/^{235}U$ = 1.8502 ± 0.0008 and $^{207}Pb/^{206}Pb$= 0.07488 ± 0.00001 (Wiedenbeck et al.1995). LA-MC-ICP-MS U-Pb data reduction was performed using the Chronus Add-in for Excel (Oliveira, 2015), following the protocols of the Geochronology Laboratory of the University of Brasília. Chronus adopts the decay constant values recommended by Steiger and Jäger (1977).

The data set of the GJ-1 standard presented average isotopic ratios of $^{206}Pb/^{238}U$ = 0.0944 ± 0.0015 (1.6%; 2σ; 95% conf.; n = 94) and $^{207}Pb/^{206}Pb$ = 0.05675 ± 0.00027 (0.48%; 2σ; 95% conf.; n = 94). The 91500 secondary standard presented a 1061.7 ± 6.1 Ma age (MSWD = 0.63; 2σ; n = 99). Age calculations and frequency histograms were carried using the Isoplot 4.15 software (Ludwig, 2012). LA-MC-ICP-MS U-Pb isotopic analytical data are listed in Supplementary Material 2.

3.4. Whole-Rock Sm-Nd

Sm-Nd analyses were performed in 7 samples of metagraywacke and 4 samples of carbonaceous phyllites. Samples were pulverized using a tungsten carbide grinding container and analyzed at the Geochronology Laboratory of the University of Brasília. Whole-rock powders (~100 mg) were spiked with a ^{150}Nd-^{149}Sm tracer and dissolved with a 5:1 HF - HNO_3 solution in Savillex® vials. After cooling and evaporation of the HF-HNO_3 solution, samples were redissolved in Savillex® vials with 7 ml of 6 N HCl. After evaporation, samples were taken up in 3 ml of 2.5 N HCl. Sm and Nd were extracted following the procedures described by Gioia and Pimentel (2000). Each sample was then loaded with 0.25 N H_3PO_4 on a Ta filament for Sm and a Re filament for Nd.

Samples were analyzed using a Thermo Scientific TRITON™ Plus Thermal Ionization Mass Spectrometer (TIMS) operation in static multi-collector mode. 100–120 ratios were collected with a 0.5 to 1-V 144 Nd beam. Nd ratios were normalized to $^{146}Nd/^{144}Nd$ = 0.7219. The analyses were adjusted for variations in instrumental bias due to periodic adjustment of collector positions as monitored by measurements of the internal standards. Repeated measurements on the USGS BHVO-1 standard gave $^{143}Nd/^{144}Nd$ = 0.512996 ± 0.000006 (2SD; n = 7). Average blank values were < 100 pg for Sm, and < 500 pg for Nd. Correction for blank was insignificant for Nd isotopic compositions and generally insignificant for Sm/Nd ratios. T_{DM} model ages were calculated according to DePaolo (1981, 1988). Sm-Nd isotopic data are listed in Table 1.

4. Results

4.1. Macroscopic Aspects and Petrography

On drill core records, the metasedimentary rocks occur below the metabasalts in sharp tectonic contacts marked by sheared zones with intense silicification and dolomitization. The highly deformed rocks gradually give place to well-preserved black-colored carbonaceous phyllites with some intercalations of light brown metagraywackes that progressively become predominant (Fig. 4). Some sheets of metabasalts occur along the metasedimentary rocks and evidence the duplication of stratigraphic layers due to multiple imbricate thrust faulting at depth (Fig. 3).

Metagraywackes are formed by a fine-grained matrix composed of quartz (40 - 45%), plagioclase (20 - 25%), muscovite (5 - 20%), biotite (5 - 10%), and chlorite (1 - 3%). Ilmenite and zircon are common accessory minerals. Foliation is well marked by the preferential orientation of muscovite, biotite, and chlorite in a lepidoblastic texture, while the recrystallized grains of quartz and plagioclase in the matrix form the main granoblastic domains. Medium- to coarse-grained, often rotated and associated with pressure shadows, clasts of quartz and plagioclase occur imbedded in the matrix (Fig. 5c). These grains are frequently angular to subangular, indicating a textural immaturity (Fig. 5a and 5b). These features imply a protolith formed by impure and poorly sorted clasts surrounded by a muddy matrix that was subsequently recrystallized due to later metamorphic processes. Garnet (1 - 3%) can occur either as syn- and post-tectonic porphyroblasts. The syn-tectonic porphyroblasts are associated with foliation bending and pressure shadows (Fig. 5d), originated during the prograde metamorphism, while the post-tectonic porphyroblasts are euhedral and crosscut the metamorphic foliation (Fig. 5e), with a likely hydrothermal origin. Along strongly fluid-altered zones in metagraywackes, post-tectonic garnet porphyroblasts occur in a very high concentration, sometimes forming garnetites.

Carbonaceous phyllites are highly friable foliated fine-grained rocks composed of quartz (40 - 45%), non-crystalline carbonaceous matter (30 - 35%), muscovite (5 - 10%), plagioclase (3%), and biotite (3%). Ilmenite and zircon occur as accessory minerals. Foliation in one or more direction is well marked by the preferential orientation of muscovite and biotite, characterizing a prominent lepidoblastic texture (Fig. 5f) that usually form crenulations. Stretched granoblastic domains are formed by recrystallized quartz and plagioclase (Fig. 5f). Presence of non-crystalline form of organic matter and absence of graphite indicate that the rocks were metamorphosed under low-grade conditions, differently

from the metabasalts, in which mineralogical paragenesis (hornblende and plagioclase) is diagnostic of amphibolite-facies metamorphism. Metagraywackes and carbonaceous phyllites are commonly associated with quartz and carbonate veinlets. Sulfide dissemination, mainly pyrrhotite and arsenopyrite, is also common in both rock types and may be related to gold mineralization.

Fig. 4. Drill core aspects of metasedimentary rocks of the Crixás greenstone belt. (A) Transition from black-colored carbonaceous phyllites to light brown-colored metagraywackes (increasing depth from left to right). (B) Highly foliated carbonaceous phyllite. (C) Metagraywacke with white angular clasts of quartz and feldspar.

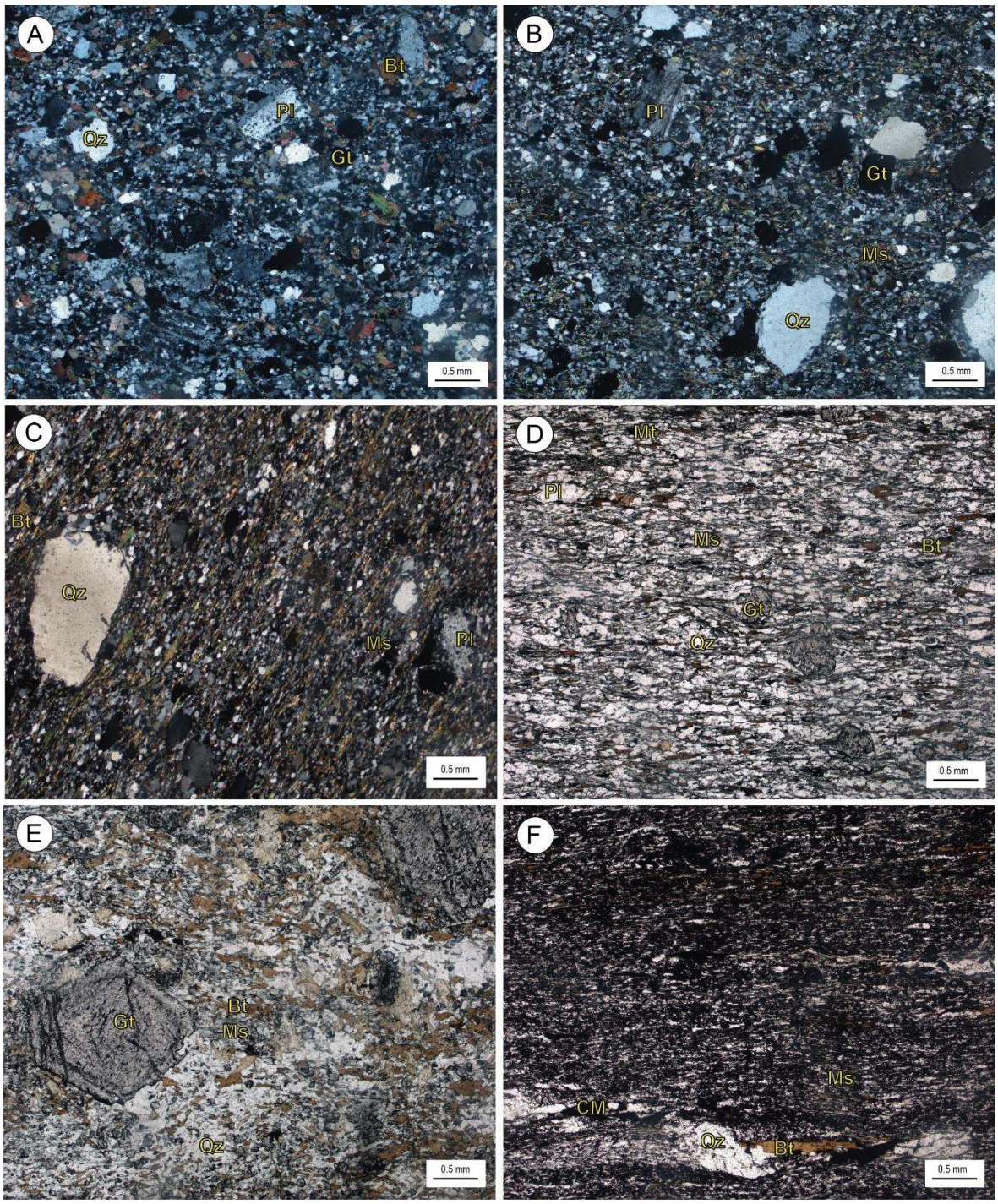

Fig. 5. Photomicrographs of metasedimentary rocks of the Crixás greenstone belt. (A-B) Metagraywacke composed of medium- to coarse-grained angular to subangular quartz and plagioclase clasts embedded in a fine-grained recrystallized matrix. (C) Coarse-grained quartz clast embedded in a foliated fine-grained matrix. (D) Syn-tectonic garnet porphyroblasts in metagraywacke. (E) Coarse-grained post-tectonic euhedral garnet porphyroblasts in metagraywacke. (F) Carbonaceous phyllite composed of quartz, non-crystalline carbonaceous matter, muscovite, and biotite. Crossed polarized lights (A, B, and C); Planar polarized lights (D, E, and F). Abbreviations: Qz (quartz), Pl (plagioclase), Ms (muscovite), Bt (biotite), Grt (garnet) Mt (magnetite) and CM (carbonaceous matter).

4.2. Major and Trace Elements

Metagraywackes and carbonaceous phyllites of the Crixás greenstone belt present most of the major and trace element composition in the same broad range and cannot be distinguished exclusively by their chemical composition, suggesting that both types of rocks received contribution from similar source areas. Samples are characterized by SiO_2 = 54 – 73 wt.%, Al_2O_3 = 12 - 22 wt.%, Fe_2O_3 = 5 - 17 wt.%, MgO = 2 - 7 wt.%, CaO = 0.3 - 7.0 wt.%, Na_2O = 0.2 - 4.6 wt.%, K_2O = 0.4 – 5.5 wt.%, TiO_2 = 0.5 - 1.4 wt.%, P_2O_5 = 0.1 - 0.4 wt.%, Cr = 60 - 400 ppm and Ni = 22 - 158 ppm (Supplementary Material 1).

On chondrite-normalized REE diagram, both metagraywackes and carbonaceous phyllites show enriched LREE patterns (La/Sm_{cn} = 2.05 - 4.20; La/Yb_{cn} = 3.01 - 20.42) and near-flat to variably depleted HREE patterns (Gd/Yb_{cn} = 1.19 - 3.58) (Fig. 6a and 6b). Negative Eu anomalies are present in most samples, while some show no anomalies (Eu/Eu* = 0.38 - 1.01). A positive Ce anomaly is observed only in one sample of carbonaceous phyllite (Ce/Ce* = 1.33) (Fig. 6a and 6b). On primitive mantle-normalized diagram, samples show strong Nb - Ta and Ti negative anomalies (Nb/Th_{pm} = 0.07 - 0.41; Ti/Sm_{pm} = 0.10 - 0.86), and less prominent negative to positive Zr - Hf anomalies (Zr/Sm_{pm} = 0.67 - 1.90) (Fig. 6c and 6d). On PAAS-normalized diagram, metagraywackes and carbonaceous phyllites present similar patterns. The most distinguished aspects are the depletion in Ti and Zr – Hf (Ti/Sm_{paas} 0.27 – 0.88; Zr/Sm_{paas} = 0.45 - 0.89) observed in most samples and some negative to positive Nb – Ta anomalies in some samples (Nb/Th_{paas} = 0.48 - 2.62) (Fig. 6e and 6f).

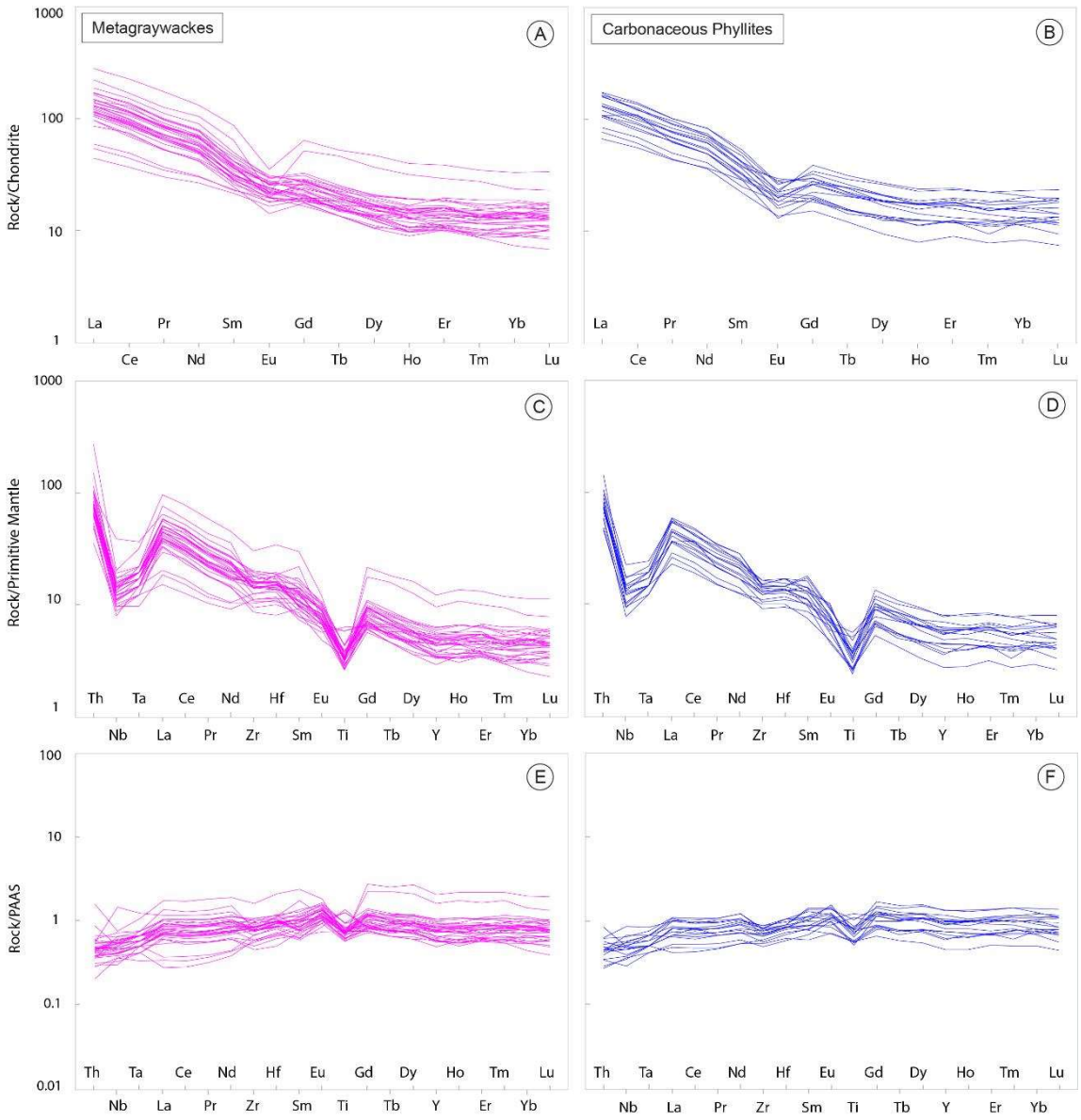

Fig. 6. Chondrite- (A and B), primitive mantle- (C and D), and PAAS-normalized (E and F) diagrams for metagraywackes and carbonaceous phyllites of the Crixás greenstone belt. Normalization values are those of Sun and McDonough (1989) for chondrite and primitive mantle, and Taylor and McLennan (1985) for PAAS.

4.3. Detrital Zircon U-Pb Geochronology

Detrital zircon populations of all analyzed samples are heterogeneous and include euhedral prismatic, rounded, and sub-rounded shapes with internal growth zoning. U-Pb ages of the vast majority of grains from either metagraywackes and carbonaceous phyllites overlap and are concentrated in a relatively uniform interval in the Rhyacian (ca. 2.2 - 2.1 Ga), despite some minor Neoarchean and Siderian grains. U-Pb data of each sample are presented in Concordia diagrams and probability density plots in Figs. 7 and 8, and listed in Supplementary Material 2.

Sample CPIEVESD0015-1 (metagraywacke; 1049 m) provided 95 detrital zircon grains in which 73 within 10% discordance were used in a probability density plot showing a peak at 2158 Ma. Upper and lower intercepts in the Concordia diagram yielded ages of 2168.1 ± 4.1 and 228 ± 55 Ma (MSWD = 0.90), respectively (Fig. 7a). A total of 87 grains were recovered from sample CPIVESD0015-2 (metagraywacke; 1450 m) in which 44 within 10% discordance were plotted in a probability density histogram evidencing a peak at 2197 Ma. Upper and lower intercepts in the Concordia diagram yielded ages of 2213.4 ± 5.6 and 437 ± 36 Ma (MSWD = 1.6), respectively (Fig. 7b).

Sample CPIVESD0016-1 (carbonaceous phyllite; 768 m) provided 68 grains in which a group of 39 grains within 10% discordance resulted in a peak at 2168 Ma in the probability density plot. A single older grain with a $^{207}Pb/^{206}Pb$ age of 2343 Ma was also recognized. Upper and lower intercepts in the Concordia diagram yielded ages of 2172.1 ± 8.8 and 385 ± 86 Ma (MSWD = 1.6), respectively (Fig. 7c). Sample CPIVESD0016-3 (metagraywacke; 1235 m) provided 87 grains in which 47 within 10% discordance were used in a probability density plot showing a main peak at 2182 Ma. Two grains presented Siderian $^{207}Pb/^{206}Pb$ ages (2350 and 2315 Ma) and one Archean grain presented a $^{207}Pb/^{206}Pb$ age of 2561 Ma. Upper and lower intercepts in the Concordia diagram yielded ages of 2206.4 ± 6.2 and 323 ± 44 Ma (MSWD = 1.5), respectively (Fig. 7d).

Sample CPIVESD0029-1 (carbonaceous phyllite; 784 m) provided 63 grains in which 29 within 10% discordance resulted in a peak at 2182 Ma. A single Archean grain with a $^{207}Pb/^{206}Pb$ age of 2719 Ma was also recognized. Upper and lower intercepts in the Concordia diagram yielded ages of 2184.5 ± 8.3 and 167 ± 84 Ma (MSWD = 2.0), respectively (Fig. 8a). Sample CPIVESD0029-2 (metagraywacke; 1154 m) provided 60 grains in which 28 were used in a probability density plot resulting in a peak at 2194 Ma. Upper and lower intercepts in the Concordia diagram yielded ages of 2204.3 ± 6.6 and 491 ± 31 Ma (MSWD = 1.1), respectively (Fig. 8b).

Sample CPIEVESD0035-2 (carbonaceous phyllite; 998 m) provided 35 detrital zircon grains in which 18 grains within 10% discordance were used in a probability density plot showing a peak at 2162 Ma. The same age was obtained in the upper intercept of the Concordia diagram (2162.2 ± 9.2 Ma; MSWD = 1.7) (Fig. 8c). Sample PALESD005-2 (metagraywacke; 647 m) provided 70 grains in which 45 within 10% discordance were used in a probability density plot evidencing a main peak at 2191 Ma. A single grain with a $^{207}Pb/^{206}Pb$ age of 2406 Ma and two grains of 2762 and 2734 Ma were also recognized. Upper and lower intercepts in the Concordia diagram yielded ages of 2194.7 ± 7.1 and 183 ± 90 Ma (MSWD = 2.0), respectively (Fig. 8d).

The totality of detrital zircon grains (at least 90% concordant) of our study was compiled with data from Jost et al. (2010) and plotted in a probability density histogram (n = 351) that highlight a main peak in the Rhyacian (~2.1 Ga) and subordinated Archean (ca. 3.3 Ga, 2.9 Ga, and 2.7 Ga) and Siderian (ca. 2.4 Ga) contribution in the age spectra of the metasedimentary rocks of the Crixás greenstone belt (Fig. 9a). The maximum deposition ages (MDA) for each sample of our study were determined following the method of the youngest statistical population. As suggested by Coutts et al. (2019) and Sharman and Malkowski (2020), this conservative method produces accurate MDAs and is less susceptible to contamination and Pb-loss issues, thus yielding ages that are less likely to be younger than the true depositional age. Our eight samples provided individual MDAs between 2156 ± 4 and 2148 ± 4 Ma. Considering the relatively short interval of these ages, we calculated an estimate of the MDA from the weighted mean of the youngest population of detrital zircon grains (at least 90% concordant) from all samples taken together and obtained a more robust MDA of 2149 ± 4 Ma (35/36 grains; MSWD = 0.809; $p(\chi^2) = 0.79$) (Fig. 9b).

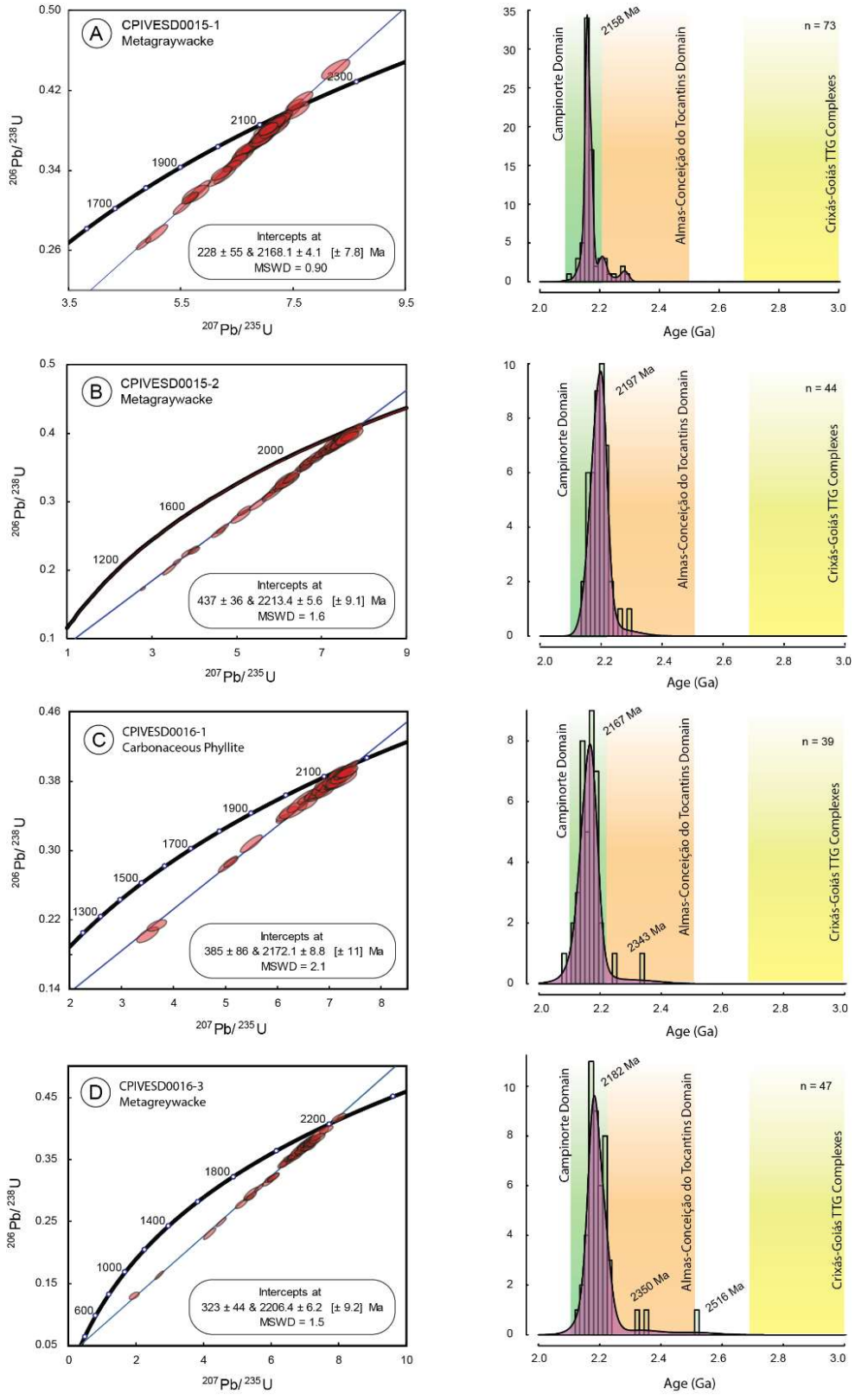

Fig. 7. Concordia diagrams and distribution frequency histograms for detrital zircon grains of metasedimentary rocks of the Crixás greenstone belt: (A) Sample CPIVESD0015-1. (B) Sample CPIVESD0015-2. (C) Sample CPIEVESD0016-1. (D) Sample CPIVESD0016-3. All zircon data presented in the histograms are at least 90% concordant. $^{207}Pb/Pb^{206}$ ages were used for histogram plots. The age range of potential source areas is represented by colored bars.

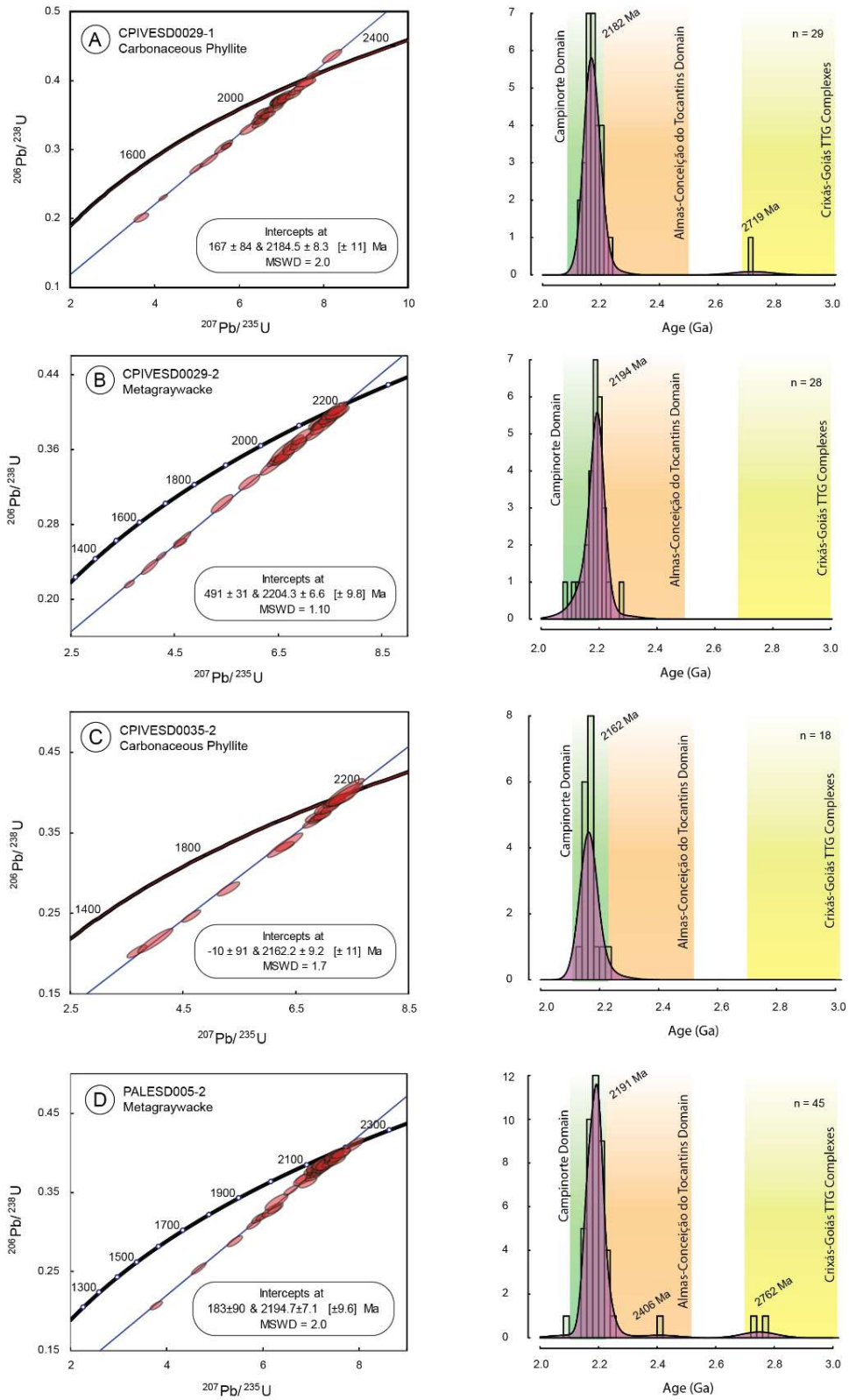

Fig. 8. Concordia diagrams and distribution frequency histograms for detrital zircon grains of metasedimentary rocks of the Crixás greenstone belt: (A) Sample CPIVESD0029-1. (B) Sample CPIVESD0029-2. (C) Sample CPIEVESD0035-2. (D) Sample PALESD0005-2. All zircon data presented in the histograms are at least 90% concordant. $^{207}Pb/Pb^{206}$ ages were used for histogram plots. The age range of potential source areas is represented by the colored bars.

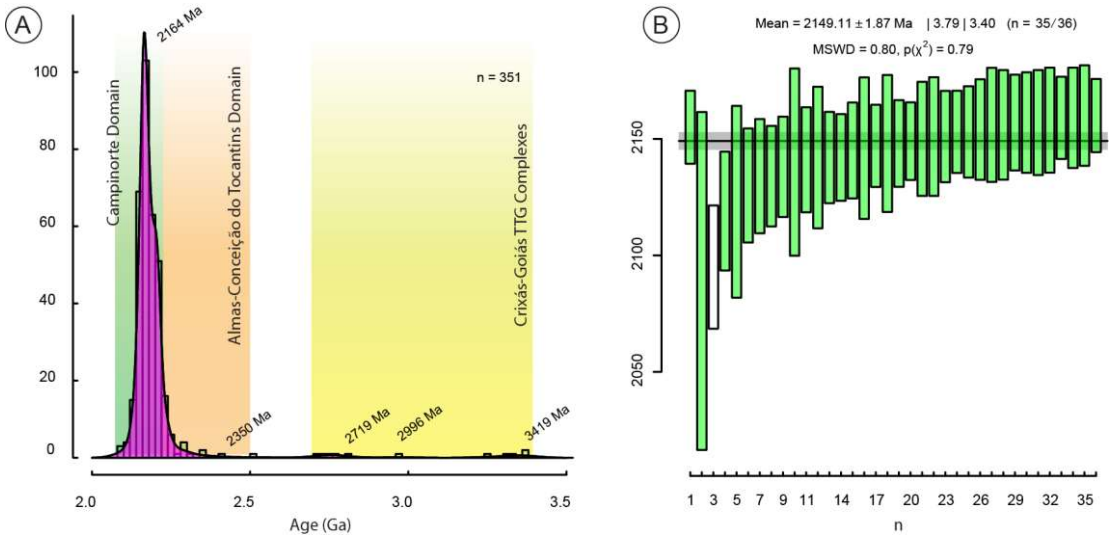

Fig. 9. Distribution frequency histogram and maximum deposition age estimate for the metasedimentary rocks of the Crixás greenstone belt. (A) Distribution frequency histogram for detrital zircon grains from all samples of this study compiled with data from Jost et al. (2010). (B) Maximum deposition age calculated from the weighted mean of the youngest population of detrital zircon grains from the samples of our study (MDA = 2149 ± 4 Ma; MSWD = 0.809; $p(\chi^2) = 0.79$). All zircon data presented are at least 90% concordant. $^{207}Pb/Pb^{206}$ ages were used for histogram plots. The age range of potential source areas is represented by the colored bars.

4.4. Sm-Nd Isotopes

Metagraywackes and carbonaceous phyllites of the Crixás greenstone belt present relatively homogeneous T_{DM} ages between 2.44 and 2.34 Ga. ε_{Nd} values were calculated at the maximum depositional age estimate (t = 2149 Ma) and range from -0.27 to +1.25 (Fig. 10). Sm-Nd data are listed in Table 1.

Table 1. Sm-Nd isotopic data of metagraywackes and carbonaceous phyllites of the Crixás greenstone belt.

Sample	Type	Sm (ppm)	Nd (ppm)	$^{147}Sm/^{144}Nd$	$^{143}Nd/^{144}Nd \pm 2\sigma$	ε_{Nd} (t = 2149 Ma)	T_{DM} (Ga)
CPIVESD0015A	Metagraywacke	4.813	26.816	0.1085	0.511376 ± 8	-0.27	2.43
CPIVESD0015B	Metagraywacke	4.719	26.049	0.1095	0.511398 ± 7	-0.11	2.42
CPIVESD0016A	Metagraywacke	4.175	21.885	0.1153	0.511496 ± 5	0.20	2.41
CPIVESD0016C	Metagraywacke	4.822	26.780	0.1088	0.511401 ± 6	0.14	2.40
CPIVESD0029D	Metagraywacke	5.676	30.292	0.1133	0.511490 ± 5	0.64	2.37
CPIVESD0035B	Metagraywacke	4.785	26.233	0.1103	0.511441 ± 9	0.51	2.37
PALESD005C	Carb. Phyllite	4.427	23.833	0.1120	0.511439 ± 8	0.00	2.42
CPIVESD0016B	Carb. Phyllite	4.864	25.067	0.1173	0.511523 ± 6	0.17	2.42
CPIVESD0029A	Carb. Phyllite	4.954	24.957	0.1200	0.511568 ± 8	0.31	2.41
CPIVESD0035A	Carb. Phyllite	8.843	46.811	0.1142	0.511534 ± 5	1.25	2.32
PALESD005A	Carb. Phyllite	8.454	44.653	0.1140	0.511497 ± 3	0.58	2.37

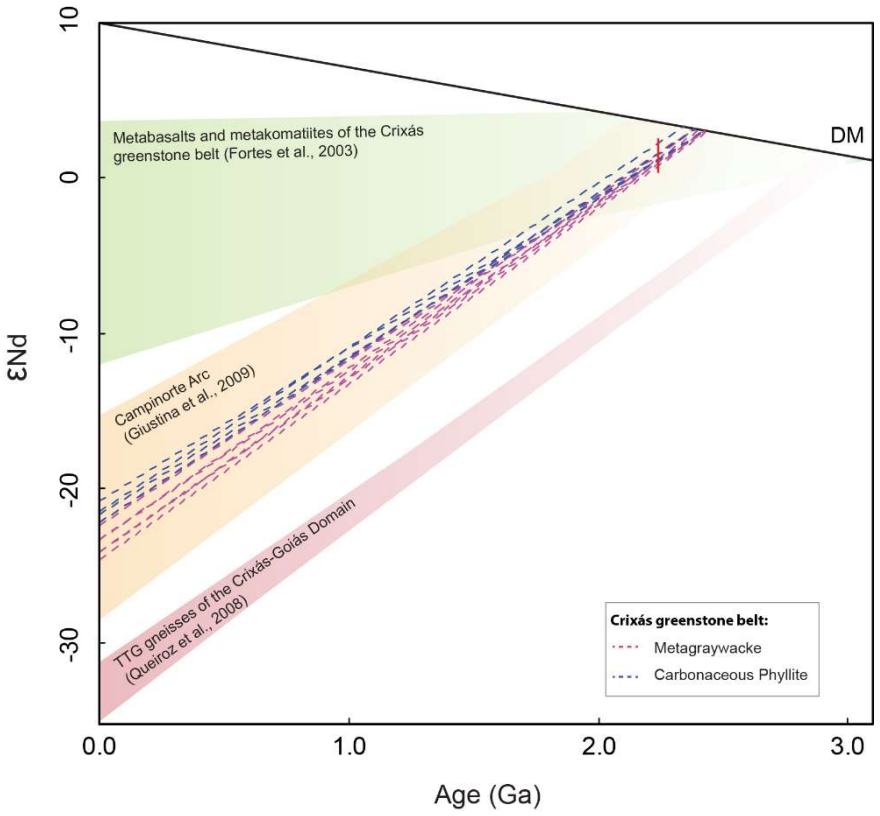

Fig. 10. Nd isotopic evolution of metagraywackes and carbonaceous phyllites of the Crixás greenstone belt. For comparison, the Nd growth curves of potential source areas are also shown.

5. Discussion

5.1. Depositional Ages

Despite the minor contribution of Archean and Siderian sources in the age spectra of detrital zircon grains of the metasedimentary rocks of the Crixás greenstone belt, the Concordia diagrams of the eight analyzed samples have upper intercepts between 2213.4 ± 5.6 and 2162.2 ± 9.2 Ma, which we interpret as the age range of the main Rhyacian source area (Figs. 7 and 8). This age differs only by about 13 Ma from the maximum depositional age of 2149 ± 4 Ma (Fig. 9). The lower intercepts range from 491 ± 31 to 167 ± 84 Ma. The former may be related to the late stages of the Brasiliano Orogeny that affected the region of the Crixás-Goiás Domain.

Previous U-Pb data of zircon grains interpreted to be of hydrothermal origin recovered from a silicified metagraywacke sample analyzed by Tassinari et al. (2006) yielded an upper intercept age of 2165 ± 47 Ma. This age was interpreted to reflect the timing of the gold mineralization in the Crixás greenstone belt and considered as a minimum depositional age for the paleobasin (Tassinari et al., 2006; Jost et al., 2010, 2019). Another attempt to constrain a minimum depositional age was conducted by Jost et al. (2010). The authors performed U-Pb zircon dating of a mafic dike that crosscut the metasedimentary rocks of the Crixás greenstone belt and obtained the 2170 ± 17 Ma age, initially interpreted to be the crystallization age of the dike and correlated with the hydrothermal zircon age obtained by Tassinari et al. (2006). However, the data was later reinterpreted by Jost et al. (2019), who observed that the zircon grains of the mafic dike is actually inherited xenocrysts and thus may reflect the source area age of the hosting metagraywacke.

Considering the associated error, the 2165 ± 47 Ma age of hydrothermal zircon obtained by Tassinari et al. (2006) overlaps either the age range of the main Rhyacian source area (2213.4 ± 5.6 and 2162.2 ± 9.2 Ma) and the maximum depositional age (2149 ± 4 Ma) defined by our data. Thus, the former should not be considered a minimum limit for the sediment deposition. Alternatively, a good estimate for the minimum depositional age in the Crixás greenstone belt is the Re-Os dating of arsenopyrite from gold-bearing massive sulfide lenses hosted in metasedimentary rocks that yielded the 2126 ± 16 Ma age (Marques et al., 2013). In summary, the current geochronological data for the Crixás greenstone belt constrain a robust interval of maximum and minimum depositional ages of 2149 ± 4 Ma and 2126 ± 16, respectively. This indicates that the deposition of the black shales and graywackes

took place in a relatively short time span since the formation of the main source area in the Rhyacian.

5.2. Post-Depositional Alteration

The greenstone belts of the Crixás-Goiás Domain have been submitted to metamorphism under greenschist- to amphibolite-facies conditions and multiple stages of deformational events in the Paleoproterozoic and Neoproterozoic (Fortes et al., 2003; Jost et al., 2010; Borges et al., 2017). Metasedimentary rocks of the Crixás greenstone belt commonly show evidence of hydrothermal alteration (e.g. silicification and carbonate alteration) and formation of secondary mineral phases (e.g. euhedral garnet, arsenopyrite, and pyrrhotite), especially in the gold-mineralized zones (Jost et al., 2010, 2019). Chemical changes during diagenesis and metasomatic processes can compromise the inferences about the source area composition and sedimentary processes. Indeed, even the most preserved samples of metagraywacke and carbonaceous phyllite of the Crixás greenstone belt show evidence of major elements (SiO_2, Na_2O, CaO, and K_2O) and LILE mobility, as noted by the large scatter in the distribution of those elements in bivariant diagrams, resulting in weak or no correlation. For this reason, the usage of weathering index (e.g. Chemical Index of Alteration; CIA; Nesbit and Young, 1982), commonly applied for sedimentary rocks in order to measure the chemical weathering intensity in the source area, does not seems to raise reliable information since those elements may have been remobilized by post-depositional processes, for instance.

On the other hand, relatively immobile elements like REE, HFSE (Th, Zr, Hf, and Y), Sc, V, Co, Cr, and Ni are particularly useful in provenance studies due to their short residence times in sea water, being readily incorporated into sediments, and low mobility during sedimentary and low-grade metamorphic processes (Taylor and McLennan, 1985; McLennan and Taylor, 1991). In the greenstone belts of the southern Crixás-Goiás Domain, Borges et al. (2017) discussed that many of the trace elements, such as the REE and HFSE, were still useful for petrogenetic interpretations of the amphibolite-facies metavolcanic rocks of the Faina and Serra de Santa Rita greenstone belts. Moreover, the amphibolite-facies metakomatiites and metabasalts of the Crixás greenstone belt still preserve a Mesoarchean Sm-Nd isochron (Fortes et al., 2003), suggesting that the REE systematics were not substantially altered after subsequent metamorphic and deformational events. The greenschist-facies metagraywackes and carbonaceous phyllites of the Crixás greenstone belt show fairly coherent and uniform patterns on the trace element diagrams (Fig. 6) and in the

whole-rock Sm-Nd isotopic systematics (Fig. 10), which seems unlikely that those elements were disturbed during metasomatic processes and may give important clues about the source area composition and sedimentary processes. In this work, we focus exclusively on the relative immobile trace elements for the following discussions about sedimentary sorting, provenance, and tectonic setting of the metasedimentary rocks.

5.3. Sediment Recycling

Effects of sediment sorting and recycling can be evaluated using Th/Sc and Zr/Sc ratios that strongly correlate in clastic sedimentary rocks and are an index of zircon enrichment. High mineral selection and sediment recycling result in increasing Zr/Sc ratios, reflecting zircon and other heavy accessory minerals concentration, whereas Th/Sc ratios reflect compositional differentiation processes since Th is an incompatible element and Sc is typically compatible in magmatic systems (McLennan et al., 1993). On a Zr/Sc vs. Th/Sc diagram (McLennan et al., 1993), metagraywackes and carbonaceous phyllites of the Crixás greenstone belt define a trend consistent with compositional variation in the source area, but no trend reflecting significative sediment sorting and recycling is evidenced (Fig. 11). This is consonant with the textural and mineralogical immaturity of the metasedimentary rocks of the Crixás greenstone belt, especially the metagraywackes, which one of its main features is the presence of angular to subangular fresh plagioclase clasts.

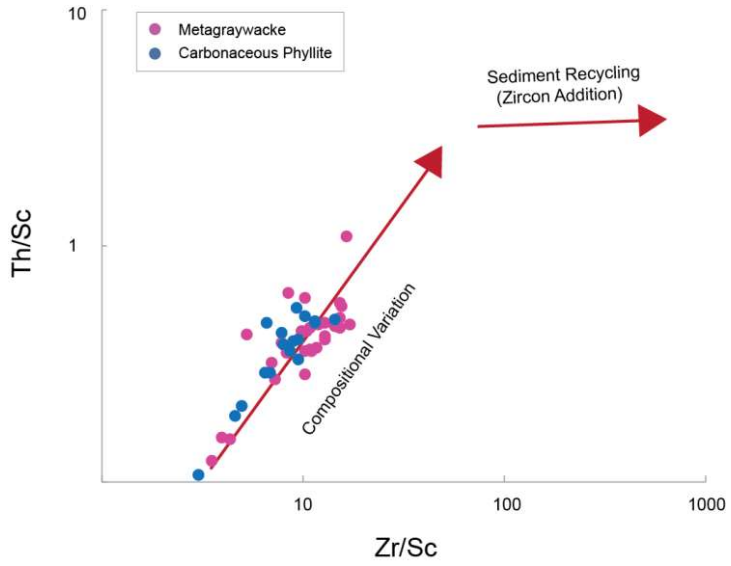

Fig. 11. Zr/Sc vs. Th/Sc diagram (McLennan et al., 1993) showing no significant recycling trend for metagraywackes and carbonaceous phyllites of the Crixás greenstone belt.

5.4. Source Area Composition

The metagraywackes and carbonaceous phyllites of the Crixás greenstone belts have chemical, mineralogical, and textural characteristics that indicate that the clastic sediments were not intensely weathered and re-worked. Thus, the geochemical properties of these rocks can provide valuable information about the characteristics and provenance of their sources. The elements Cr, Ni, Sc, and Co preferably partition into mafic minerals, whereas Th, Zr, Hf, and La are enriched in felsic sources, which usually have a higher abundance of heavy accessory minerals (e.g. zircon, monazite, and allanite). Therefore, ratios of these elements can be used to distinguish between mafic and felsic sources.

High ratios of Th/Co and La/Sc are characteristic of felsic sources while low ratios are consistent with mafic sources. The metagraywackes and carbonaceous phyllites of the Crixás greenstone belt plot in a trend close to the felsic component and toward the mafic component on a Th/Co vs. La/Sc diagram (Cullers, 2002), suggesting a mixture of the two endmembers (Fig. 12a). Cr/V ratio is a parameter of Cr enrichment over the other ferromagnesian trace elements, whereas the Y/Ni ratio monitors the behavior of ferromagnesian trace elements compared to a proxy of HREE (Y), discriminating between felsic and ophiolitic (ultramafic) sources (Hiscott, 1984; McLennan et al., 1993). As evidenced by the Y/Ni vs. Cr/V diagram (Fig 12b), the metagraywackes and carbonaceous phyllites show low Y/Ni ratios, mostly lower than 1, and varied Cr/V ratios, ranging from 0.46 to 2.88. Some samples present Cr/V ratios extensively higher than the average UCC (0.78; McLennan, 2001), which reflect an important contribution of ultramafic and/or mafic sources.

Composition of different sources can also be discriminated in a Hf vs. La/Th diagram (Floyd and Leveridge, 1987). In this diagram, increasing La/Th ratios with associated low Hf contents reflect compositional variation in magmatic arc systems, whereas high Hf contents are related to passive margin sources, in response to increasing old sediment input and zircon (and other heavy minerals) accumulation. The metagraywackes and carbonaceous phyllites plot close to the felsic sources related to a magmatic arc, but in a trend toward mixing of acidic and basic components (Fig. 13), that is also consistent with sources of intermediate composition, such as andesites and diorites.

Trace element distribution in sedimentary rocks on normalized diagrams also has a great potential to reflect many aspects of their provenance (Taylor and McLennan, 1985). The metagraywackes and carbonaceous phyllites of the Crixás greenstone belt display a prominent trough in Nb and Ti on the primitive mantle-normalized diagram (Fig. 6c and 6d),

which is one of the most diagnostic features of subduction-related rocks. Negative anomalies of Zr are evidenced on the PAAS-normalized diagram (Fig. 6e and 6f) and likely reflect a significantly less concentration of heavy minerals (zircon) than PAAS in response to the absence of significative sediment sorting and recycling. On the chondrite-normalized diagram (Fig. 6a and 6b), the samples show patterns of LREE that suggest a different range of magmatic differentiation processes and enrichment of incompatible elements in the source areas (La/Sm_{cn} = 2.05 – 4.20). Depletion of HREE is a peculiar feature observed only in a small number of samples. Steep patterns of HREE have been attributed to reflect igneous sources with garnet as a fractionating phase during petrogenetic processes. This compositional characteristic is noticeably more common in Archean sedimentary rocks when compared to Proterozoic and Phanerozoic counterparts (McLennan and Taylor, 1991; McLennan et al., 1993). Various extent of negative anomalies of Eu (Eu/Eu* = 0.38 – 0.90) are present and may reflect intracrustal processes that include partial melting and fractional crystallization with associated fractionation of plagioclase. The magnitude of the Eu anomalies, enrichment in incompatible elements, and textural/mineral immaturities of the metasedimentary rocks of the Crixás greenstone belt are characteristics of sedimentary rocks derived from young differentiated (intracrustal) magmatic arcs (McLennan et al., 1993).

A mixed mafic-ultramafic and felsic provenance for the metasedimentary rocks of the Crixás greenstone belt can be intuitively assigned to the underneath Mesoarchean metakomatiite/metabasalts and to the surrounding Meso-Neoarchean TTG orthogneisses, respectively. Nevertheless, as reflected by U-Pb detrital zircon ages, Archean source areas are only a minor part of the provenance, which is actually largely dominated by ca. 2.2 – 2.1 Ga rocks. Thus, arc-related Rhyacian sources must correspond to a major part of the mixed arc-related mafic and felsic contribution, which is also in agreement with sources of intermediate composition.

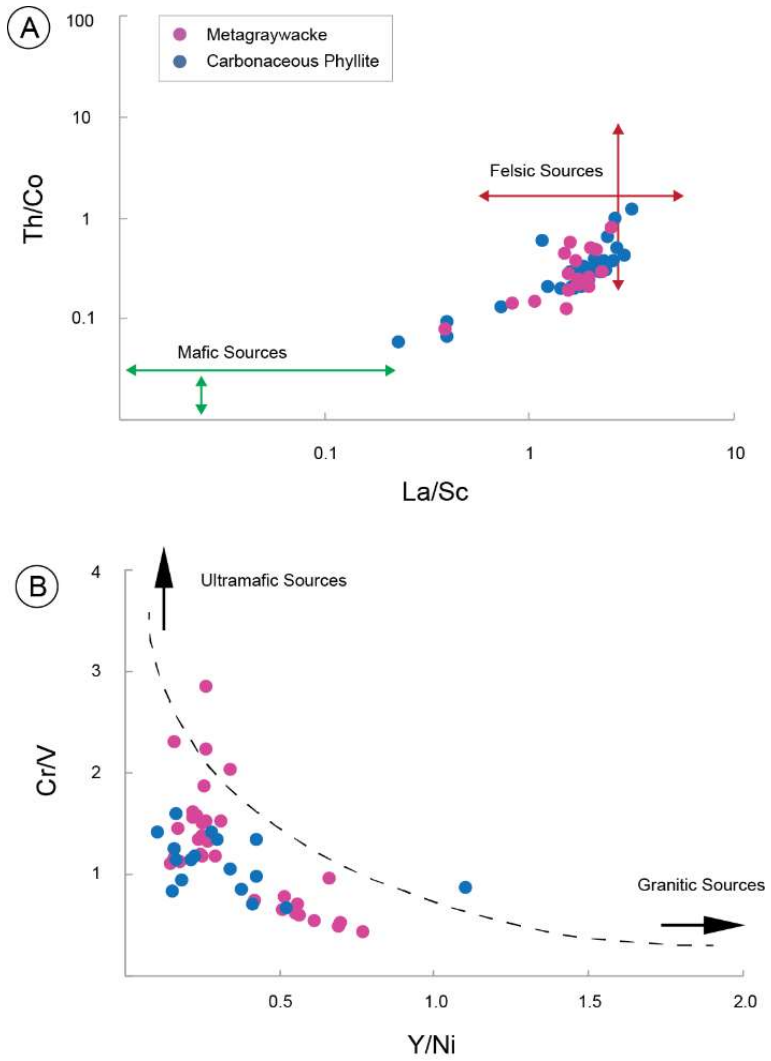

Fig. 12. Discrimination between mafic and felsic sources for the metagraywackes and carbonaceous phyllites of the Crixás greenstone belt. (A) Th/Co vs. La/Sc diagram (Cullers, 2002). (B) Y/Ni vs. Cr/V diagram (Hiscott, 1984).

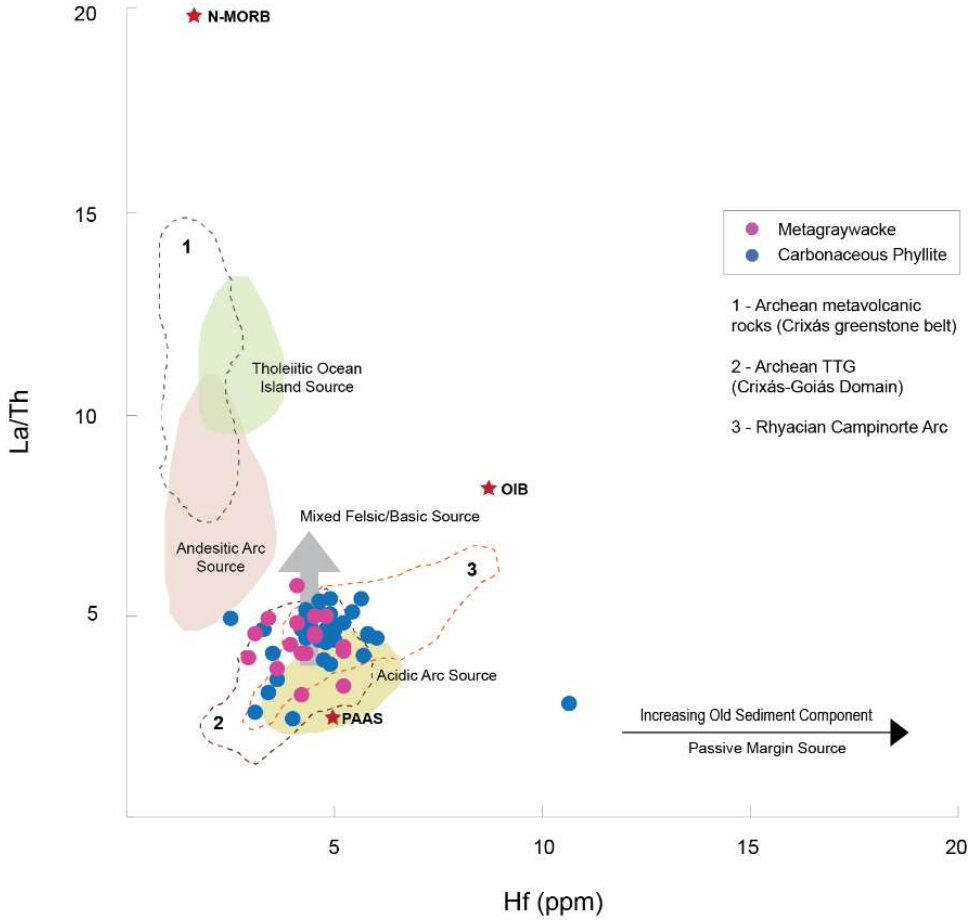

Fig. 13. Hf vs. La/Th discrimination diagram to access the composition of the source areas of the metagraywackes and carbonaceous phyllites of the Crixás greenstone belt (Modified after Floyd and Leveridge, 1987). Dotted lines represent the compositional range of potential source areas: 1) Mesoarchean mafic metavolcanic rocks of the Crixás greenstone belt (unpublished data from the authors); 2) Meso-Neoarchean TTG gneisses of the Crixás-Goiás Domain (data from Beghelli, 2012); 3) Granitic rocks of the Rhyacian Campinorte Arc (data from Cordeiro et al., 2014). N-MORB and OIB compositions are from Sun and McDonough (1989). PAAS composition is from Taylor and McLennan (1985).

5.5. Tectonic Setting

Chemical composition of sedimentary rocks can provide information about the tectonic environment in which the clastic sediments were deposited. Bhatia and Crook (1986) recognized that immobile trace elements (e.g. La, Ce, Nd, Th, Zr, Nb, Y, Sc, and Co) of graywackes are especially useful in tectonic setting discrimination of sedimentary basins. Ternary diagrams of Fig. 14 use La-Th-Sc and Th-Sc-Zr/10 relations to distinguish between oceanic island arc, continental island arc, active continental margin, and passive margin settings. On both diagrams, some samples of metagraywacke and carbonaceous phyllite of the Crixás greenstone belt plot in the “island arc” field while most samples plot in the

"continental island arc". The latter corresponds to sedimentary basins close to island arcs formed on a well-developed continental crust (e.g. Lau Basin; Japan Sea) or thin continental margins (e.g. Cascades-Western, USA). Sediments of these environments derive mainly from the volcanic arc and are deposited in intra-arc, back-arc, and forearc basins (Bhatia, 1983; Bhatia and Crook, 1986). These basins are distinct from those of the "active continental margin" type that corresponds to sedimentary basins related to thick continental margins (e.g. Andes) composed of varied rocks of older fold belts where the siliceous uplifted basement is an important sediment source (Bhatia, 1983).

Detrital zircon spectra also reflect the tectonic setting in which they were deposited. This approach is especially sensitive when the depositional age of the investigated sediments is well constrained (Cawood, 2012), which seems to be the case of the Crixás greenstone belt. Basins related to convergent margins typically contain igneous zircon with ages close to the time of sediment deposition (e.g. forearc, trench, and back-arc basins). A different situation occurs in basins related to continental collision settings (e.g. foreland basins), where zircon grains older than the sediment deposition occur in a significant proportion. Whereas in zones of extension (e.g. rift basins), the detrital zircon record is dominated by grains that are much older than the time of sediment deposition (Cawood, 2012).

Detrital zircon geochronology of the metagraywackes and carbonaceous phyllites of the Crixás greenstone belt evidence a dominant Rhyacian peak (2.2 - 2.1 Ga) (Figs. 7, 8, and 9). Minor contributions of Neoarchean and Siderian grains comprise only about 2% of the provenance, according to our data. This unimodal detrital zircon age spectra clearly resemble those of convergent setting basins, more specifically forearc and trench basins, with the source age close to the depositional age. Continental back-arc basins, on the other hand, are expected to contain an increased input of older sediments from the adjoining craton (Cawood et al., 2012). The apparent absence of Paleoproterozoic basalts with MORB geochemical signature in the Crixás greenstone belt is also not consistent with a back-arc setting. Positive to slightly negative values of ε_{Nd} (t) (Table 1) of the metagraywackes and carbonaceous phyllites suggest that the arc-source is dominated by juvenile material with a minor contribution of reworked crust.

Information provided by the ternary tectonic discriminant diagrams (Fig. 14) and the age spectra of the detrital zircon record (Figs. 7, 8, and 9) led us to suggest that the sedimentary rocks of the Crixás greenstone belts were derived from the erosion of a Rhyacian island arc formed adjacent to an Archean paleocontinent constituted of TTG-greenstone terranes. Rapid uplift, erosion of the Rhyacian arc edifice, and accumulation of syn-orogenic sediments in a trench or forearc basin resulted in unimodal age spectra of clasts.

The pieces of evidence show that the original sedimentary protoliths were not deposited directly on an erosive discordance above the Archean TTG and mafic-ultramafic volcanic rocks, but rather were tectonically emplaced on the TTG-greenstone crust during an arc-continent collision (Fig. 15).

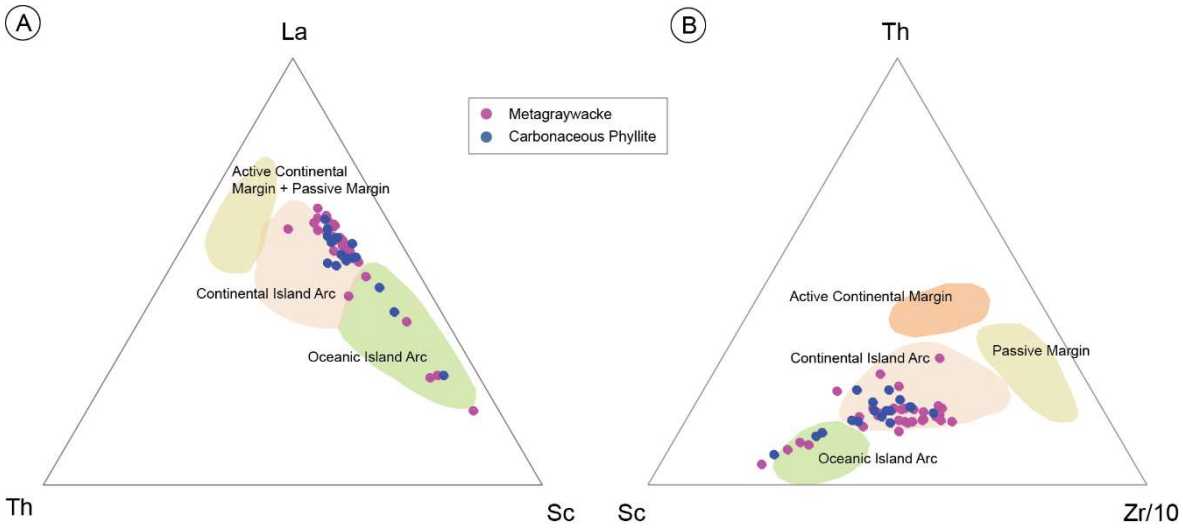

Fig. 14. Tectonic setting discrimination diagrams (Bhatia and Crook, 1986) for the metagraywackes and carbonaceous phyllites of the Crixás greenstone belt. (A) La-Th-Sc ternary plot. (B) Th-Sc-Zr/10 ternary plot.

5.6. Potential Source Areas and Implications to the Goiás Massif

5.6.1. Investigation of Potential Source Areas

Archean and Siderian detrital zircon grains comprise a minor part of the provenance of the metasedimentary rocks of the Crixás greenstone belt. Archean sources are likely related to the Meso-Neoarchean TTG complexes of the Crixás-Goiás Domain. Two zircon grains of 2762 and 2719 Ma were probably derived from the youngest Neoarchean granodioritic and granitic gneisses (Queiroz et al., 2008) (Figs. 7, 8, and 9). Metagraywacke samples investigated by Jost et al. (2010) presented an older population of ca. 3.3 Ga detrital zircon that is comparable with inherited Paleoarchean zircon xenocrysts recognized in Mesoarchean orthogneisses of the northern TTG complexes (Queiroz et al., 2008) (Fig. 9). Moreover, the depleted HREE patterns observed in some samples (Figs. 6a and 6b) can be linked to the ca. 3.1 – 2.8 Ga orthogneisses, which geochemical characteristics were interpreted to indicate the effects of garnet as a residual phase during mantle melting (Beghelli Jr, 2012; Borges et al., 2017).

Siderian grains range from 2405 - 2343 Ma and could be derived from ca. 2.4 Ga diabase dike swarms intruded in the TTG complexes of the Crixás-Goiás Domain (Corrêa da Costa, 2003) However, zircon grains crystallized in mafic dikes are often scarce, too small and irregular, being difficult to source. Alternatively, Siderian granite-gneissic rocks of the Almas-Conceição do Tocantins Domain (Martins-Ferreira et al., 2020; Saboia et al., 2020), located at northeast of the Crixás-Goiás Domain, could have sourced the ca. 2.4 Ga zircon grains (Figs. 7, 8, and 9).

The nature of the dominant Rhyacian provenance is dubious, as pointed out by Jost et al. (2010, 2019), since there is no extensive crust of that age exposed in the Crixás-Goiás Domain. Jost et al. (2019) suggested that the Rhyacian source area would occur to the west of the Crixás-Goiás Domain and raised the possibility that the domain could represent a headland of the border of a craton during the opening of the Goiás-Pharusian Ocean (Cordani et al., 2013). In this context, the domain is thought to be an allochthonous terrane that was separated from the original craton during its collision against the Brasília Belt in the Neoproterozoic. Another alternative considers that the Crixás-Goiás Domain decoupled from an early craton that is actually the basement of the Neoproterozoic Araguaia or Paraguay belts, that occur west of the Transbrasiliano Lineament (Jost et al., 2019). However, the allochthonous and "exotic" nature of the Crixás-Goiás Domain in the context of the Brasília Belt (and its basement) has been challenged by some authors. Cordeiro and Oliveira (2017), based on fieldwork and reassessment of geophysical data, interpreted that the tectonic domains that constitute the Goiás Massif were amalgamated in the Paleoproterozoic. This assumption has been further reinforced by other authors through different approaches (e.g. Martins-Ferreira et al., 2018; Reis et al., 2020; Filgueiras et al., 2020).

Provenance from the Paleoproterozoic terranes that comprise the other tectonic domains of the Goiás Massif, located northeast of the Crixás-Goiás Domain (see Fig. 1), gives a possible explanation for the origin of the main Rhyacian source area. Orthogneisses and granites of ca. 2.2 – 2.1 Ga are present in different proportions in the Almas-Conceição do Tocantins, Cavalcante-Arraias and Campinorte domains (Botelho et al., 2006; Giustina et al., 2009; Cordeiro et al., 2014; Fuck et al., 2014; Cuadros et al., 2017a; Martins-Ferreira et al., 2020). In this context, a highlight has been given to the neighboring Campinorte Domain (Cordeiro et al., 2014; Cordeiro and Oliveira, 2017). We following discuss this possibility and suggest an alternative scenario to account for the origin of the Rhyacian source area of the metasedimentary rocks of the Crixás greenstone belt.

5.6.1.1. Campinorte Arc: The Main Rhyacian Source Area?

Cordeiro et al. (2014) proposed that the Rhyacian provenance of the metasedimentary successions of the Crixás-Goiás Domain's northern greenstone belts may be related to the ca. 2.2 - 2.0 juvenile Campinorte Arc (Campinorte Domain). This interpretation was mainly based on the current relative geographical proximity of the two domains and the synchronicity of their sedimentary basins. The Campinorte Domain contains a Rhyacian metavolcanosedimentary sequence (Campinorte Sequence) that consists of chemical metasedimentary rocks, rhyolitic metatuffs, metapelites, and quartzites (Giustina et al., 2009). The provenance of the clastic sediments of this sequence is attributed to the adjacent orthogneisses and granitic rocks of the coeval Campinorte Arc (Giustina et al., 2009; Cordeiro et al., 2014). It was suggested by Cordeiro et al. (2014) that the Campinorte Arc was a proximal source area for the Campinorte Sequence and a distal source for the greenstone belts of the northern Crixás-Goiás Domain (Crixás, Pilar de Goiás and Guarinos greenstones).

As visualized in the distribution frequency histograms (Figs. 7, 8, and 9), Nd isotopic evolution curves (Fig. 10), and Hf vs. La/Th compositional diagram (Fig. 13), the metasedimentary rocks of the Crixás greenstone belt share similarities with granitic rocks of the Campinorte Arc, favoring arguments for the latter being the main source area for the former. However, although we state that this interpretation should not be totally discarded, we believe that there are a few issues to directly connect the metagraywackes and carbonaceous phyllites of the Crixás greenstone belt (and other greenstones of the Crixás-Goiás Domain) to the Campinorte Domain: 1) There is a lack of information between the Campinorte and our study area since this region is covered by Mesoproterozoic sedimentary rocks (see Fig. 1); 2) The structural orientation of the Crixás-Goiás Domain is marked by N70W-S70E trending structures, while the Campinorte structures are oriented at N10E-S10W; and 3) The clastic sedimentary protoliths of the Campinorte Sequence is characterized by mature sediments (now transformed into quartzites and metapelites), while the sedimentary rocks the Crixás greenstone belt are rather exclusively immature. Indeed, the different tectonic domains of the Goiás Massif record important accretion of juvenile terranes that might correspond to several different arcs, as suggested by different authors (e.g. Sousa et al., 2016; Cordeiro and Oliveira, 2017, Martins-Ferreira et al., 2020).

5.6.1.2. A Rhyacian Magmatic Arc in the Crixás-Goiás Domain

Although scarce, Rhyacian magmatic rocks occurring inside the Crixás-Goiás Domain have been locally described and include: i) 2146 Ma diorites intruded in a northwest-trending shear zone that crosscut the Hidrolina TTG Complex (Jost et al., 1993); ii) 2145 Ma trondhjemite stocks related to a gold-bearing shear zone located in the Pilar de Goiás greenstone belt (Jost et al., 1992; Queiroz, 2000); and iii) 2061 Ma syenite intrusion in the Faina greenstone belt, southern Crixás-Goiás Domain (Bogossian, 2020). It has been previously recognized that the Rhyacian was a period of crustal compression and the most important metallogenetic epoch in the Crixás-Goiás Domain (Jost et al., 2014); although a model that accounts for the Rhyacian magmatism and formation of ore deposits in a regional scale still lacks for the region.

The arc-related sedimentary basin occurring in the upper Crixás greenstone belt is an important piece to this puzzle insofar it can provide further information that cannot be reached directly from igneous rocks. We interpret that a Rhyacian island arc, denominated here as Crixás Arc, has formed adjacent to the Archean paleocontinent of which the Crixás-Goiás Domain derived (Fig. 15). Concordia diagrams provided by the metagraywacke and carbonaceous phyllite samples yielded upper intercepts between 2213.4 ± 5.6 and 2162.2 ± 9.2 Ma (Figs. 7 and 8), giving a good estimate of the arc magmatism age. Syn-orogenic sedimentation started with deposition of deep-water back shales and subsequent poorly sorted immature debris related to episodic turbidite currents in a trench or forearc basin.

Docking of the Rhyacian island arc to the Archean paleocontinent led to the formation of further magmatism, thrust systems, and tectonic transport of volcaniclastic graywackes and black shales that were originally deposited in the trench or forearc basin. Preservation of the Rhyacian sedimentary rock layers on the Mesoarchean metakomatiites and metabasalts might reflect a preservation bias, as they were more likely to be preserved in the greenstone belt (keels) rather than on Meso-Neoarchean felsic TTG domes.

Progressive advances in geochronological studies in the Crixás-Goiás Domain can provide further evidence of this Rhyacian orogeny. For instance, some deep drill cores in the central-northern region of the Crixás greenstone belt record foliated to massive gabbro and diorites just below the detachment zone of the lowest level of metagraywackes. Also, thin layers of quartz-feldspar-muscovite schists that have recently been interpreted as either porphyritic metarhyolite or felsic metatuff occur associated with some structures along the metasedimentary sequence. These rocks have geochemical arc-signatures but unknown ages. Their meaning is still under investigation, but we speculate that they can constitute more

examples of Rhyacian arc magmatism occurring in the region. The massive gabbro and diorites, only recognized in the deepest drill cores, might represent remnants of the roots of this island arc. Since no extensive Rhyacian magmatic rocks outcrop in the Crixás-Goiás Domain, the provenance study of metasedimentary rocks of the Crixás greenstone belt proved to be crucial for the characterization of a proximal magmatic arc that was mostly eroded, buried, or obliterated.

5.6.2. Implications to the Goiás Massif Crustal Evolution

The domains of the Goiás Massif differ in lithological association, stages of magmatism, and structural patterns, and encompass all pre-Brasiliano (pre-Neoproterozoic) basement of the Northern Brasília Belt in Central Brazil (Cordeiro and Oliveira, 2017). Moreover, it was suggested that the Goiás Massif is a pericratonic area of the São Francisco Craton that was affected by deformation and metamorphism during the Neoproterozoic Brasiliano/Pan-African orogeny, a result of the collision between the São Francisco/Congo, Amazonian, West African/ São Luís and Paranapanema cratons during Western Gondwana amalgamation (Cordeiro and Oliveira., 2017; Martins-Ferreira et al., 2018; Reis et al., 2020).

At northeast of the Crixás-Goiás Domain, extensive areas of Paleoproterozoic crust are widely exposed in the other domains of the Goiás Massif. The Almas-Conceição do Tocantins Domain consists of a Paleoproterozoic granite-greenstone terrane that comprise complex Siderian to late Rhyacian magmatic events (Cruz et al., 2003; Sousa et al., 2016; Fuck et al., 2014; Martins-Ferreira et al., 2020; Saboia et al., 2020). The Cavalcante-Arraias Domain is dominantly composed of ca. 2.18 - 2.14 Ga peraluminous granites of the Aurumina Suite intruded in graphite-bearing schists and paragneisses of the Ticunzal Formation (Botelho et al., 2006; Cuadros et al., 2017a, 2017b). Parts of a ca. 2.18 - 2.07 Ga juvenile magmatic arc occur in the Campinorte Domain and comprise a metavolcanosedimentary sequence associated with granites, orthogneisses, and granulites (Giustina et al., 2009; Cordeiro et al., 2014; Filgueiras et al., 2020).

The domains were amalgamated during successive Siderian to Rhyacian orogenic episodes that involved the collage of multiple island and continental arcs in the western border of the São Francisco paleocontinent (see Cordeiro and Oliveira, 2017, Martins-Ferreira et al., 2020 and Saboia et al., 2020 for a review). In this model, the role and position of the Crixás-Goiás Domain remained outshined due to its apparent lacking of Paleoproterozoic rocks that could match with the amalgamation of the Goiás Massif. Nevertheless, our work gives insights into the Paleoproterozoic crustal growth in the Crixás-

Goiás Domain and the existence of a Rhyacian island arc adjacent to the Archean paleocontinent in which the terrane derived, as pointed out by the provenance of syn-orogenic sedimentary rocks of the Crixás greenstone belt. We correlate this orogeny with the amalgamation of the Goiás Massif and insert it in the same context of the Paleoproterozoic crustal growth of the São Francisco paleocontinent, corroborating with the model proposed by Cordeiro and Oliveira (2017), with adaptations, as synthetized in Fig. 15.

At ca. 2.2 - 2.1 Ga, widespread arc formation occurred in different settings. Continental arc was stablished along the older Siderian crust (TTG and greenstone belts) of the Almas-Conceição do Tocantins domains (Cuadros et al., 2017a; Martins-Ferreira et al., 2020). This accretionary orogen was coeval with the juvenile arc of the Campinorte Domain. Mature clastic sediments of the Campinorte Sequence formed from the erosion of the Campinorte Arc (Giustina et al., 2009; Cordeiro et al., 2014). An island arc (Crixás Arc) formed adjacent to an Archean paleocontinent. Syn-orogenic immature sediments were deposited in the trench or forearc basin and were later tectonically transported towards the TTG-greenstone terranes, being preserved in elongated keels of Mesoarchean mafic-ultramafic volcanic rocks. During the collision, this arc was buried or obliterated. Erosion of the magmatic arc might have provided sediments to the distal Paleoproterozoic basins of the Faina and Serra de Santa Rita greenstone belts, located in the southern portion of the Crixás-Goiás Domain. The final collage of the different terranes in the Rhyacian formed the crystalline basement of the Goiás Massif as a part of the western border of the São Francisco-Congo paleocontinent. The region was latter subject to regional ca. 1.7 - 1.5 Ga rifting events and formation of intracontinental basins (Martins-Ferreira et al., 2018), and involved in the Neoproterozoic Brasiliano Orogeny during the amalgamation of Western Gondwana.

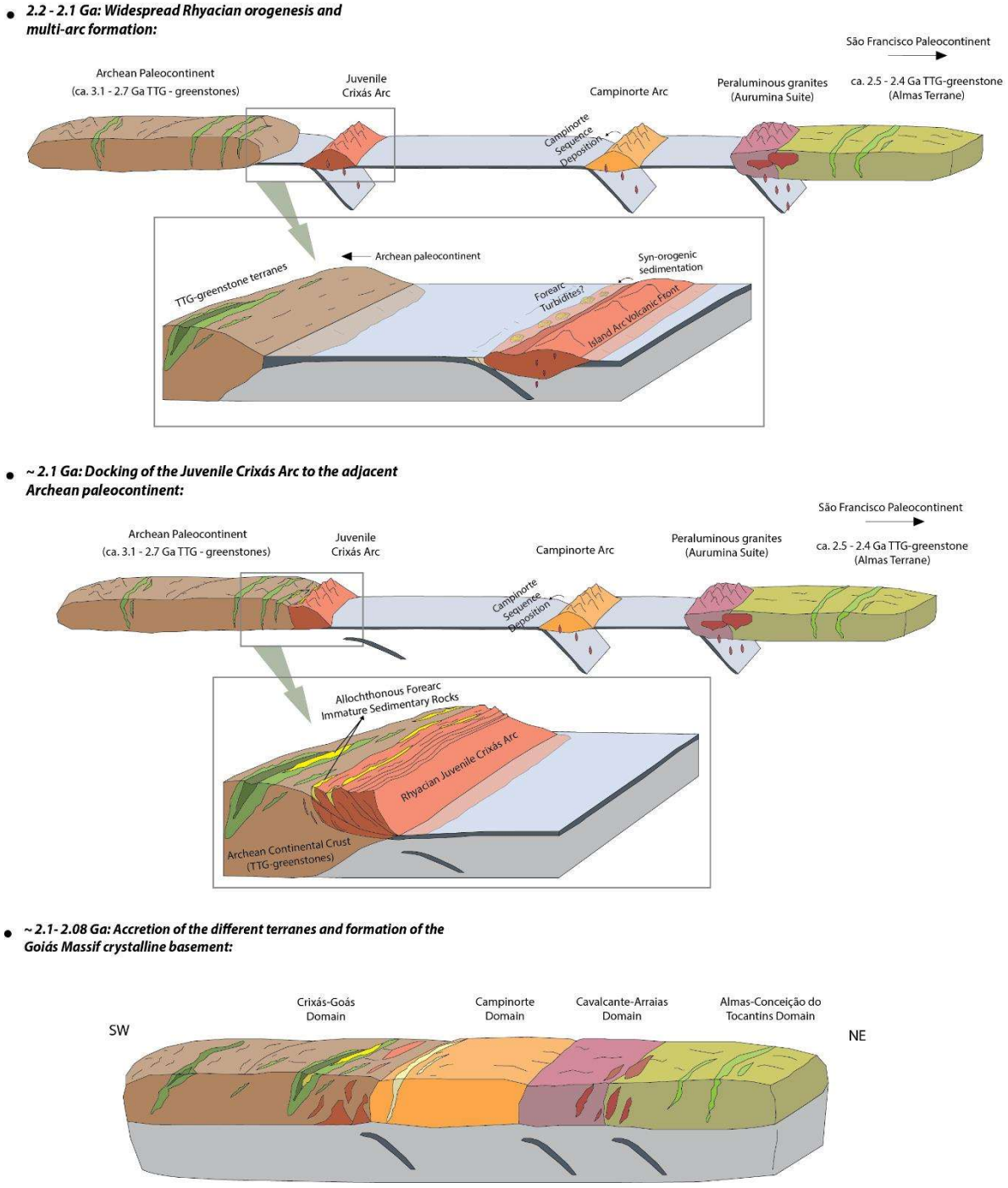

Fig. 15. Paleoproterozoic amalgamation of the Goiás Massif (modified after Cordeiro and Oliveira, 2017). During ca. 2.2 - 2.1 Ga, arc formation occurred in different settings: Continental arcs were established along the older Siderian crust (TTG and greenstone belts) of the Almas-Conceição do Tocantins domain (Cuadros et al., 2017a; Martins-Ferreira et al., 2020). This accretionary orogen was coeval with the juvenile Campinorte island arc and its associated mature clastic sedimentary rocks of the Campinorte Sequence (Giustina et al., 2009; Cordeiro et al., 2014). A Rhyacian island arc (Crixás Arc) formed adjacent to an older Archean paleocontinent. Syn-orogenic sedimentation in a trench or forearc basin started with deep-ocean back shale deposition in an anoxic environment followed by episodic turbidite currents of poorly sorted immature sands. Sedimentary rock layers were tectonically transported to the continent and preserved in the elongated keels of Mesoarchean mafic-ultramafic volcanic rocks. The Goiás Massif was established as a single block after the

final collage of the different arc terranes, belonging to the western São Francisco-Congo paleocontinent (see Fig. 1). The deposition and tectonic emplacement of the sedimentary rocks of the Crixás greenstone belt are highlighted in the squares.

6. Conclusions

The Crixás greenstone belt comprises Mesoarchean metakomatiites and metabasalts overlaid by allochthonous Paleoproterozoic metasedimentary rocks. Our integrated petrographical, geochemical, and geochronological data of the upper metagraywackes and carbonaceous phyllites indicate that the original protoliths were deposited in a basin related to a proximal magmatic arc and received a mixed mafic and felsic contribution. Syn-orogenic sedimentation started with deep-ocean back shale deposition in an anoxic environment followed by episodic turbidite currents of poorly sorted immature sands. Sediments were deposited in a trench or forearc basin filled by rapid erosion of a rising ca. 2.2 - 2.1 Ga island arc (Crixás Arc) formed adjacent to an older Archean crust constituted of TTG-greenstone terranes, of which the current Crixás-Goiás Domain may represent a detached fragment. Although the exact geographical position and extension of that early Archean crust are still uncertain. Sedimentary rock layers were tectonically transported to the continent and preserved in elongated keels of Mesoarchean mafic-ultramafic volcanic rocks. Furthermore, the Rhyacian magmatic arc was probably the main distal source area for the provenance of the sedimentary rocks of the greenstones located in the southern Crixás-Goiás Domain; where the variety of rocks may reflect different types of basins, sedimentation conditions, and distance to the arc source area.

No extensive occurrences of Rhyacian magmatic rocks outcropping within the Crixás-Goiás Domain suggest that most of this island arc was buried, obliterated, or eroded during the Paleoproterozoic. Massive gabbro and diorite intrusions that occur below the detachment zone of the lowest level of metagraywackes recorded by deep drill cores can evidence remnants of the Rhyacian magmatic arc roots. Future works can provide further evidence of records of this orogeny and its relations with the neighboring Rhyacian terranes, such as the Campinorte Arc. We correlate our tectonic model with the amalgamation of the Goiás Massif throughout the Siderian-Rhyacian crustal growth related to a successive collage of arc-related terranes in the formation of the São Francisco paleocontinent, that was latterly involved in the Western Gondwana assembly during the Brasiliano/Pan-African Orogeny. This is the first work specifically addressing Rhyacian rocks of the Crixás-Goiás Domain in the same broad geological evolution context of the pre-Brasiliano crystalline

basement of the Brasília Belt. Moreover, the sediment provenance study of metasedimentary rocks of the Crixás greenstone belt proved to be crucial for the recognition and characterization of Paleoproterozoic crust that is apparently no longer preserved in outcrops.

7. Acknowledgements

We would like to thank the Mineração Serra Grande S.A. and their staff for providing the drill cores and supporting the field works and analytical data acquisition. A.M. Silva, C.L.B. Toledo, and F. Chemale Jr. thank the Conselho Nacional de Desenvolvimento Científico e Tecnológico (CNPq) for their respective research grants. We are grateful to Dr. Fabrício A. Caxito and an anonymous reviewer for their comments that extensively improved the manuscript, and to Dr. Wilson Teixeira for the great editorial handling. This study was financed in part by the Coordenação de Aperfeiçoamento de Pessoal de Nível Superior - Brasil (CAPES) - Finance Code 001, CAPES-PrInt (Grant Number: 88881.312018/2018-01), and CNPq (MCTIC/CNPq 28/2018 – Grant Number: 420308/2018-0). The first author thanks CAPES for the PhD scholarship (PROEX – Grant Number: 88882.347184/2019-01).

8. References

Almeida, F.F.M. de, Hasui, Y., Brito Neves, B.B., Fuck, R.A., 1981. Brazilian structural provinces: an introduction. Earth-Sci. Rev. 17, 1-29.

Arndt N.T., Teixeira N.A., White W.M., 1989. Bizarre geochemistry of komatiites from the Crixás Greenstone belt, Brazil. Contr. Mineral. Petrol. 74, 549-564.

Beghelli Junior, L.P., 2012. Charnockitos e ortognaisses da porção centro-oeste do Bloco Arqueano de Goiás: Dados geoquímicos e isotópicos. Dissertação de Mestrado, Instituto de Geociências, Universidade de Brasília, 87 pp.

Bekker, A., Holmden, C., Beukes, N.J., Kenig, F., Eglington, B., Patterson, W.P., 2008. Fractionation between inorganic and organic carbon during the Lomagundi (2.22-2.1Ga) carbon isotope excursion. Earth Planet. Sci. Lett. 271, 278–291.

Bhatia, M.R., 1983. Plate tectonics and geochemical composition of sandstones. J. Geol. 91, 611-627.

Bhatia, M.R., Crook, K.A.W., 1986. Trace element characteristics of graywackes and tectonic setting discrimination of sedimentary basins. Contr. Mineral. Petrol. 92, 181-193.

Bogossian, J., 2020. Gold systems in the Faina greenstone belt and crustal evolution of the southern Goiás Archean Block, central Brazil. PhD thesis, School of Earth Sciences, The University of Western Australia, 246 pp.

Bogossian, J., Hagemann S.G., Rodrigues V.G., Lobato L.M., Roberts M., 2020. Hydrothermal Alteration and Mineralization in the Faina greenstone belt: evidence from the Cascavel and Sertão orogenic gold deposits. Ore Geol. Rev. 119, 10323.

Borges, C.C.A., Toledo, C.L.B., Silva, A.M., Chemale, F., Jost, H., Lana, C.C., 2017. Geochemistry and isotopic signatures of metavolcanic and metaplutonic rocks of the Faina and Serra de Santa Rita greenstone belts, Central Brazil: evidences for a Mesoarchean intraoceanic arc. Precambrian Res. 292, 350-377.

Botelho, N.F., Fuck, R.A., Dantas, E.L., Laux, J.L., Junges, S.L., 2006. The Paleoproterozoic peraluminous Aurumina granite suite, Goiás and Tocantins: whole-rock geochemistry and Sm–Nd isotopic constraints. In: The Paleoproterozoic Record of the São Francisco Craton, Brazil, IGCP 509, Brazil, September 9–21.

Brant, R.A.P., Souza, V.S., Dantas, E.L., Jost, H., Rodrigues, V.G., Carvalho, M.J., Araújo, K.C., 2015. Contribuição ao estudo de proveniência sedimentar com base em dados U-Pb para o greenstone belt de Faina, Goiás. In: SBG, XIV Simpósio de Geologia do Centro-Oeste, Brasília, Anais, pp. 30-33.

Bühn, B., Pimentel, M.M., Matteini, M., Dantas, E.L., 2009. High spatial resolution analysis of Pb and U isotopes for geochronology by laser ablation multi-collector inductively coupled plasma mass spectrometry (LA-MC-ICP-MS). An. Acad. Bras. Cienc. 81, 1–16.

Campos, D.S. de, Silva, A.M., Toledo, C.L.B., Carvalho, M.J. de, Rodrigues, V.G., Araújo, K., 2017. Prospectivety analysis of gold and iron oxide copper-gold-(silver) mineralization from the Faina Greenstone Belt, Brazil, using multiple data sets. Braz. J. Geol. 47 (4), 561-590.

Cawood, P.A., Hawkesworth, C.J., Dhuime, B., 2012. Detrital zircon record and tectonic setting. Geology 40, 875-878.

Condie, K.C., 1993. Chemical composition and evolution of the upper continental crust: Contrasting results from surface samples and shales. Chem. Geol. 103, 1-37.

Condie, K.C., Belousova, E., Griffin, W.L., Sircombe, K.N., 2009. Granitoid events in space and time: Constraints from igneous and detrital zircon age spectra. Gondwana Res. 15, 228-242.

Cordani U.G., Pimentel M.M., Araújo C.E.G., Fuck R.A., 2013. The significance of the Transbrasiliano-Kandi tectonic corridor for the amalgamation of West Gondwana. Bras. J. Geol. 43 (3), 583-597.

Cordeiro P.F.O., Oliveira. C.G., 2017. The Goiás Massif: Implications for a pre-Columbia 2.2–2.0 Ga continent-wide amalgamation cycle in central Brazil. Precambrian Res. 288, 403-420.

Cordeiro, P.F.O., Oliveira, C.G., Giustina, M.E.S.D., Dantas, E.L., dos Santos, R.V., 2014. The Paleoproterozoic Campinorte Arc: Tectonic evolution of a Central Brazil pre-Columbia orogeny. Precambrian Res. 251, 49–61.

Corrêa da Costa, P.C., 2003. Petrologia, geoquímica e geocronologia dos diques máficos da região de Crixás-Goiás, porção centro-oeste do Estado de Goiás. Tese de Doutorado, Instituto de Geociências, Universidade de São Paulo, 151 pp.

Coutts, D. S., Mattews, W. A., Hubbard, S. M., 2019. Assessment of widely used methods to derive depositional ages from detrital zircon populations. Geosci. Front. 10, 1421-1435.

Cruz, E.L.C.C., Kuyumjian, R.M., Boaventura, G.R., 2003. Low-K calc-alkaline granitic series of southeastern Tocantins state: chemical evidence for two sources for the granite-gneissic complexes in the Paleoproterozoic Almas-Dianópolis terrane. Rev. Brasil. Geocienc. 33, 125–136.

Cuadros, F.A., Botelho, N.F., Fuck, R.A., Dantas, E.L., 2017a. The peraluminous Aurumina granite suite in central Brazil: an example of mantle-continental crust interaction in a Paleoproterozoic cordilleran hinterland setting? Precambrian Res. 299, 75–100.

Cuadros, F.A., Botelho, N.F., Fuck, R.A., Dantas, E.L., 2017b. The Ticunzal Formation in central Brazil: record of Rhyacian sedimentation and metamorphism in the western border of the São Francisco Craton. J. S. Am. Earth Sci. 79, 307–325.

Cullers, R., 2002. Implications of elemental concentrations for provenance, redox conditions, and metamorphic studies of shales and limestones near Pueblo, CO, USA. Chem. Geol. 191, 305-327.

DePaolo D., 1981. Neodymiun isotopes in the Colorado Front Range and crust-mantle evolution in the Proterozoic. Nature 291, 193-196.

DePaolo, D.J., 1988. Neodymium Isotope Geochemistry: An Introduction. Springer Verlag, New York.

Dix, G.R., Thomson, M.L., Longstaffe, F.J., McNutt, R.H., 1995. Systematic decrease of high 13C values with burial in late Archean (2.8 Ga) diagenetic dolomite: evidence for methanogenesis from the Crixás Greenstone Belt, Brazil. Precambrian Res. 70, 253–268.

Drabon, N., Galic, A., Mason, P.R.D., Lowe, D.R., 2019. Provenance and tectonic implications of the 3.28-3.23 Ga Fig Tree Group, central Barberton greenstone belt, South Africa. Precambrian Res. 325, 1-19.

Duller, P.R., Floyd, J.D., 1995. Turbidite geochemistry and provenance studies in the Southern Uplands of Scotland. Geol. Mag. 132 (5), 557-569.

Feng, R., Kerrich, R., 1990. Geochemistry of fine-grained clastic sediments in the Archean Abitibi greenstone belt, Canada: Implications for provenance and tectonic setting. Geochim. Cosmochim. Acta 54, 1061-1081.

Filgueiras, B.C., Oliveira, C.G., Sousa, I.M.C., Cordeiro, P.F.O., 2020. Further evidence of Rhyacian arc magmatism in the basement of the Brasília Belt. J. S. Am. Earth Sci. 103, 102739.

Floyd, P.A., Leveridge, B.E., 1987. Tectonic environment of the Devonian Gramscatho basin, south Cornwall: framework mode and geochemical evidence from turbiditic sandstones. J. Geol. Soc. London 144, 531–542.

Fortes, P.T.F.O., 1996. Metalogênese dos depósitos auríferos Mina III, Mina Nova e Mina Inglesa, greenstone belt de Crixás, GO. Tese de Doutorado, Instituto de Geociências, Universidade de Brasília, 176 pp.

Fortes, P.T.F.O., Pimentel, M.M., Santos, R.V., Junges, S., 2003. Sm-Nd study of the Crixás greenstone belt, Brazil: implications for the age of deposition of the upper sedimentary rocks and associated Au mineralization. J. S. Am. Earth Sci. 16, 503–512.

Fuck, R.A., Dantas, E.L., Pimentel, M.M., Botelho, N.F., Armstrong, R., Laux, J.H., Junges, S.L., Soares, J.E., Praxedes, I.F., 2014. Paleoproterozoic crust-formation and reworking events in the Tocantins Province, central Brazil: a contribution for Atlantica supercontinent reconstruction. Precambr. Res. 244, 53–74.

Gioia, S. M. C. L., Pimentel, M. M., 2000. The Sm-Nd Isotopic Method in the Geochronology Laboratory of the University of Brasília. An. Acad. Bras. Cienc. 72 (2), 219-245.

Giustina, M.E.S.D., de Oliveira, C.G., Pimentel, M.M., de Melo, L.V., Fuck, R.A., Dantas, E.L., Buhn, B., 2009. U-Pb and Sm-Nd constraints on the nature of the Campinorte sequence and related Palaeoproterozoic juvenile orthogneisses, Tocantins Province, central Brazil. Geol. Soc. Lond. Spec. Publ. 323, 255–269.

Greber, N.D., Dauphas, N., 2019. The chemistry of fine-grained terrigenous sediments reveals a chemically evolved Paleoarchean emerged crust. Geochim. Cosmochim. Acta 255, 247-264.

Greber, N.D., Dauphas, N., Bekker, A., Ptáček, M.P., Bindeman, I.N., Hofmann, A., 2017. Titanium isotopic evidence for felsic crust and plate tectonics 3.5 billion years ago. Science 357 (6357), 1271-1274.

Grisolia, M.F.P., Oliveira, E.P., 2012. Sediment provenance in the Palaeoproterozoic Rio Itapicuru greenstone belt, Brazil, indicates deposition on arc settings with a hidden 2.17 – 2.25 Ga substrate. J. S. Am. Earth Sci. 38, 89-109.

Hartmann A., Endo I., Tadeu M., Suita F., Santos J.O.S., Frantz J.C., Carneiro M.A., McNaughton N.J., Barley M.E., 2006. Provenance and age delimitation of Quadrilátero Ferrífero sandstones based on zircon U-Pb isotopes. J. S. Am. Earth Sci. 20 (4), 273-285.

Hiscott, R., 1984. Ophiolitic source rocks for Taconic-age flysch: trace-element evidence. Geol. Soc. Am. Bull. 95, 1261-1267.

Jackson, S.E., Pearson, N.J., Griffin, W.L., Belousova, E.A., 2004. The application of laser ablation-inductively coupled plasma-mass spectrometry to in situ U-Pb zircon geochronology. Chem. Geol. 211, 47–69.

Jost H., Theodoro S.M.C.H., Figueiredo A.M.G., Boa Ventura G.R. 1996. Propriedades geoquímicas e proveniência de rochas metassedimentares detríticas arqueanas dos greenstone belts de Crixás e Guarinos, Goiás. Rev. Brasil. Geocienc. 26, 151-166.

Jost, H., Apollo, J.F.H., Weber, W., Salles, R.R., Marques, J.C.M., Massucatto, A.J., Costa, D.A., Santos, B.A., 2019. Stratigraphic update, paleotectonic, paleogeographic, and depositional environments of the Crixás Greenstone Belt, Central Brazil. J. S. Am. Earth Sci. 96, 102329.

Jost, H., Carvalho, M.J., Rodrigues, V.G., Martins, R., 2014. Metalogênese dos greenstone belts de Goiás. In: Silva, M.G., Neto, M.B.R., Jost, H., Kuyumjian, R.M. (Orgs.), Metalogênese das províncias tectônicas brasileiras, Belo Horizonte, CPRM, pp. 141-168.

Jost, H., Chemale Jr., F., Dussin, I.A., Tassinari, C.C.G., Martins, R., 2010. A U–Pb zircon paleoproterozoic age for the metasedimentary host rocks and gold mineralization of the Crixás greenstone belt, Goiás, Central Brazil. Ore Geol. Rev. 37, 127–139.

Jost, H., Chemale Jr., F., Fuck, R.A., Dussin, R.A., 2013. Uvá complex, the oldest orthogneisses of the Archean Paleoproterozoic terrane of central Brazil. J. S. Am. Earth Sci. 47, 201-212.

Jost, H., Fuck, R.A., Dantas, E.L., Rancan, C.C., Rezende, D.B., Santos, E., Portela, J.F., Mattos, L., Chiarini, M.F.N., Oliveira, R.C., Silva, S.E., 2005. Geologia e geocronologia do Complexo Uvá, Bloco Arqueano de Goiás. Rev. Brasil. Geocienc. 35, 559-572.

Jost, H., Oliveira, A.M., 1991. Stratigraphy of the greenstone belts, Crixás region, Goiás, Central Brazil. J. S. Am. Earth Sci. 4, 201 -214.

Jost, H., Oliveira, A.M., Vargas, M.C., 1992. Petrography, geochemistry and structural control of trondhjemitic intrusions in greenstone belts of the Crixás region, Central Brazil. In: SBG, Congresso Brasileiro de Geologia, 37, São Paulo. Anais, v. 1. pp. 43-44.

Jost, H., Pimentel, M.M., Fuck, R.A., Danni, J.C., Heaman, L., 1993. Idade U-Pb do Diorito Posselândia, Hidrolina, Goiás. Rev. Brasil. Geocienc. 23, 352-355.

Jost, H., Rodrigues, V.G., Carvalho, N.J., Chemale Jr., F., Marques, J.C., 2012. Estratigrafia e geocronologia do greenstone belt de Guarinos, Goiás. Geol. USP, Sér. Cient. 12 (2), 3-48.

Kuyumjian, R.M., Teixeira, N.A., 1982. Um novo tipo de estrutura em lavas ultramáficas: greenstone belt de Crixás, GO. Rev. Brasil. Geocienc. 12, 572–577.

Ludwig, K.R., 2012. User's Manual for Isoplot 3.75: A geochronological toolkit for Microsoft Excel. Berkeley Geochronology Center Special Publications 5, 75 pp.

Marques, J. C., Jost, H., Creaser, R. A., Frantz, J. C., Osorio, R. G., 2013. Age of arsenopyrite gold-bearing massive lenses of the Mina III and its implications on exploration, Crixás greenstone belt, Goiás, Brazil. In: III Simpósio Brasileiro de Metalogenia, Gramado, extended abstracts.

Martins-Ferreira, M.A.C., Chemale, F., Dias, A.N.C., Campos, J.E.G., 2018. Proterozoic intracontinental basin succession in the western margin of the São Francisco Craton: constraints from detrital zircon geochronology. J. S. Am. Earth Sci. 81, 165–176.

Martins-Ferreira, M.A.C., Dias, A.N.C., Chemale Jr., F., Campos, J.E.G., Seraine, M., Novais-Rodrigues, E., 2020. Multi-stage crustal accretion by magmatic flare-up and quiescence intervals in the western margin

of São Francisco Craton: U-Pb-Hf and geochemical constraints from the Almas Terrane. Gondwana Res. 85, 32-54.

McLennan, S.M., 2001. Relationships between the trace element composition of sedimentary rocks and upper continental crust. Geochem. Geophys. Geosyst. 2, 2000GC000109.

McLennan, S.M., Hemming, S., McDanniel, D.K., Hanson, G.N., 1993. Geochemical approaches to sedimentation, provenance, and tectonics. In: In: Johnsson, M.J., Basu, A. (Eds.), Processes Controlling the Composition of Clastic Sediments. Geol. Soc. Am. Spec. Pap. 285, 21–40.

McLennan, S.M., Taylor, S.R., 1991. Sedimentary rocks and crustal evolution: tectonic setting and secular trends. J. Geol. 99, 1–21.

McLennan, S.M., Taylor, S.R., McCulloch, M.T., Maynard, J.B., 1990. Geochemical and Nd-Sr isotopic composition of deep-sea turbidites: crustal evolution and plate tectonic associations. Geochim. Cosmochim. Acta 54, 2015-2050.

Melezhik, V.A., Huhma, H., Condon, D.J., Fallick, A.E., Whitehouse, M.J., 2007. Temporal constraints on the Paleoproterozoic Lomagundi-Jatuli carbon isotopic event. Geology 35, 655.

Nesbitt, H.W., Young, G.M., 1982. Early Proterozoic climates and plate motions inferred from major element chemistry of lutites. Nature 299, 715-717.

Oliveira, F.V., 2015. Chronus: Um novo suplemento para a redução de dados U-Pb obtidos por LA-MC-ICPMS. Dissertação de Mestrado, Instituto de Geociências, Universidade de Brasília, 91 pp.

Pimentel M.M., Fuck R.A., Jost H., Ferreira Filho C.F., Araújo S.M., 2000. The basement of the Brasília Fold Belt and the Goiás Magmatic Arc. In: Cordani UG, Milani EJ, Thomaz Filho A, Campos DA (eds) Tectonic evolution of South America, international geological congress, Rio de Janeiro, pp 195–232.

Pimentel, M.M., 2016. The tectonic evolution of the Neoproterozoic Brasília Belt, central Brazil: a geochronological and isotopic approach. Braz. J. Geol. 46, 67-82.

Pimentel, M.M., Heaman, L., Fuck, R.A., Marini, O.J., 1991. U–Pb zircon geochronology of Precambrian tin-bearing continental-type acid magmatism in central Brazil. Precambrian Res. 52, 321–335.

Pimentel, M.M., Jost, H., Fuck, R.A., Armstrong, R.A., Dantas, E.L., Potrel, A., 2003. Neoproterozoic anatexis of 2.9 Ga old granitoids in the Goiás-Crixás block, Central Brazil: evidence from new SHRIMP U-Pb data and Sm-Nd isotopes. Geol. USP, Sér. Cient. 3, 1-12.

Pimentel, M.M., Rodrigues, J.B., Giustina, M.E.S.D., Junges, S., Matteini, M., Armstrong, R., 2011. The tectonic evolution of the Neoproterozoic Brasília Belt, central Brazil, based on SHRIMP and LA-ICPMS U-Pb sedimentary provenance data: A review. J. S. Am. Earth Sci. 31, 345-357.

Queiroz, C.L., 2000. Evolução Tectono-Estrutural dos Terrenos Granito-Greenstone Belt de Crixás, Brasil Central. Tese de Doutorado, Instituto de Geociências, Universidade de Brasília, 209 pp.

Queiroz, C.L., Jost, H., Silva, L.C., McNaughton, N.J., 2008. U-Pb SHRIMP and Sm-Nd geochronology of granite-gneiss complexes and implications for the evolution of the central Brazil Archean terrain. J. S. Am. Earth Sci. 26, 100-124.

Reis, L.K.O., Vidotti, R.M., Cordeiro, P., Oliveira, C.G., 2020. The western São Francisco pericraton interpreted from crustal magnetic and gravity sources. J. S. Am. Earth Sci. 103, 102716.

Resende, M.G., Jost, H., Lima, B.E.M., Teixeira, A.A., 1999. Proveniência e idades-modelo Sm-Nd de rochas siliciclásticas arqueanas dos greenstone belts de Faina e Santa Rita, Goiás. Rev. Brasil. Geocienc. 29, 281-290.

Resende, M.G., Jost, H., Osborne, G. A., Mol, A. G., 1998. Stratigraphy of the Goiás and Faina greenstone belts, Central Brazil: a new proposal. Rev. Brasil. Geocienc. 28, 77-94.

Rodrigues, V.G., 2011. Geologia do depósito aurífero do Caiamar, greenstone belt de Guarinos: um raro depósito associado a albitito sódico. Dissertação de Mestrado, Instituto de Geociências, Universidade de Brasília, 79 pp.

Saboia, A.M., Oliveira, C.G., Dantas, E.L., Cordeiro, P., Scandolara, J.E., Rodrigues, J.B., Sousa, I.M.C., 2020. The Siderian crust (2.47–2.3 Ga) of the Goiás Massif and its role as a building block of the São Francisco paleocontinent. Precambrian Res. 350, 105901.

Sabóia, L.A., Teixeira, N., Castro, J.H.G., Teixeira, A.S., 1981. Geologia do greenstone belt de Crixás (GO) e suas implicações geotectônicas. In: Simposium Cráton São Francisco e suas faixas marginais. Salvador, Bahia, Proceedings, pp. 39–50.

Sabóia, L.A., Teixeira, N.A., 1983. Ultramafic flows of the Crixás greenstone belt, Goiás. Precambrian Res. 22, 23–40.

Sharman, G. R., Malkowski, M.A., 2020. Needles in a haystack: Detrital zircon U-Pb ages and the maximum depositional age of modern global sediment. Earth-Sci. Rev. 203, 103109.

Sousa, I.M.C., Giustina, M.E.S.D., Oliveira, C.G., 2016. Crustal evolution of the northern Brasília Belt basement, central Brazil: a Rhyacian orogeny coeval with a pre-Rodinia supercontinent assembly. Precambrian Res. 273, 129–150.

Spencer, C.J., Hoiland, C.W., Harris, R.A., Link, P.K., Balgord, E.A., 2012. Constraining the timing and provenance of the Neoproterozoic Little Willow and Big Cottonwood Formations, Utah: Expanding the sedimentary record for early rifting of Rodinia. Precambrian Res. 204-205, 57-65.

Steinger, R.H., Jäger, E., 1977. Subcomission on geochronology – Convention on the use of decay constants in geo- and cosmochronology. Earth Planet Sc. Lett. 36, 359-362.

Sun, S.S., McDonough, W.F., 1989. Chemical and Isotopic systematics of oceanic basalts, implications for mantle composition and processes. In: Saunders, A.D., Norry, M.J. (Eds.), Magmatism in the Ocean Basins. Geol. Soc. Lond. Spec. Publ. 42. Blackwell Scientific Publication, UK, pp. 313–345.

Tassinari, C.C.G., Jost, H., Santos, J.C., Nutman, A.P., Bennell, M.R., 2006. Pb and Nd isotope signatures and SHRIMP U-Pb geochronological evidence of Paleoproterozoic age for Mina III gold mineralization. In: South American Symposium on Isotope Geology, 5, Pucon, Chile, Proceedings, pp. 615-617.

Taylor, S.R., McLennan, S.M., 1985. The Continental Crust: its Composition and Evolution. Blackwell Scientific, Oxford, Blackwell, pp. 311p.

Toscani, R., Campos, J.E.G., Matos, D.R., Martins-Ferreira, M.A.C., Complex depositional environments on a siliciclastic-carbonate platform with shallow-water turbidites: The Natividade Group, central Brazil, Journal of South American Earth Sciences (2020), doi: https://doi.org/10.1016/j.jsames.2020.102939.

Wiedenbeck, M., Allé, P., Corfu, F., Griffin, W.L., Meier, M., Oberli, F., Von Quadt, A., Roddick, J.C., Spiegel, W., 1995. Three natural zircon standards for U-Th-Pb, Lu-Hf, trace element and REE analyses. Geostandards Newsletter 19, 1-23.

Young, G.M., Long, D.G.F., Fedo, C.M., Nesbitt, H.W., 2001. Paleoproterozoic Huronian basin: product of a Wilson cycle punctuated by glaciations and a meteorite impact. Sediment. Geol. 141, 233-250.

Capítulo III – Artigo 2

Archean to Paleoproterozoic evolution of the Crixás greenstone belt, Central Brazil: Insights from two contrasting assemblies of metaigneous rocks.

Caio C. A. Borges [a, *]; Catarina L. B. Toledo [a]; Adalene M. Silva [a]; Jason Kirk [b]; Joaquin Ruiz [b]; Farid Chemale Jr [c]; Renan G. Souza [d]; Bruno A. Santos [d]; Marcelo P. Campos [d]; Luana M. Campos [a].

[a] Instituto de Geociências, Universidade de Brasília, 70910-900, Brasília, Brasil.

[b] Department of Geosciences, University of Arizona, 85721, Tucson, Arizona, USA.

[c] Departamento de Geologia, Universidade do Vale do Rio dos Sinos, 93022-000, São Leopoldo, RS, Brasil.

[d] AngloGold Ashanti Ltd., Rodovia GO-336, 97000 Km 97, 76510-000, Crixás, GO, Brasil.

* Corresponding author. E-mail address: caioaguiar0@gmail.com. Phone: +55 61 98130-9136

Submitted to Lithos.

Abstract

The Archean-Paleoproterozoic Crixás greenstone belt is one of the most important components of the Crixás-Goiás Domain, the oldest crustal segment of the Central Brazil Goiás Massif. This gold-bearing greenstone comprises amphibolite facies ultramafic-mafic metavolcanic rocks overlaid by a low-grade metasedimentary succession associated with rocks of intermediate composition. We present new integrated geochemical and isotopic data of the metaigneous rocks to characterize the stages of magmatism and delineate the petrogenetic processes and tectonic environment of the different units. The data give important insights into the geological evolution of the Crixás greenstone belt during the Archean and Paleoproterozoic, including that the Crixás greenstone belt consists of genetically and temporal unrelated rocks that are spatially associated in a structural framework marked by stacking and imbrication. Two lithological assemblies were described: i) a Mesoarchean komatiite-tholeiite association formed by heterogeneous mantle plume melting in an oceanic plateau setting, and ii) a Rhyacian intraoceanic arc association. These units are allochthonous and override an Archean crustal basement dominated by granites and gneisses of mostly TTG composition. Chemical composition of the metakomatiites is similar to the Barberton-type Al-depleted komatiites, whilst the metabasalts consist of high-Mg tholeiites with flat chondrite-normalized REE patterns and immobile trace element systematics that resemble Phanerozoic oceanic plateau lavas. Eruption age of the ultramafic and mafic lavas is roughly estimated at ~3.0 Ga, based on previously published Sm-Nd and Pb-Pb isotopic studies, whereas whole-rock Re-Os isotopic data of samples of metakomatiite and metabasalt presented here yield a 2609 ± 65 Ma isochron age. This younger age may reflect a Neoarchean overprinting event associated with metasomatic Re-addition recorded in the lower ultramafic-mafic metavolcanic rocks, possibly related to the late stages of the cratonization of the Crixás-Goiás Domain during the emplacement of the younger granites of the region (~2.7 Ga). Newly described meta-andesites and metadiorites possess a subduction zone fingerprint. LA-ICP-MS U-Pb zircon dating of a meta-andesite sample provided an upper intercept Concordia age of 2172.2 ± 12.7 Ma, constraining the age of the intermediate magmatism. Thus, these rocks are coeval and correlated with the Rhyacian syn-orogenic poorly-sorted metagraywackes and carbonaceous phyllites of the greenstone's upper stratigraphy. Meta-andesites and metadiorites have homogeneous Paleoproterozoic two-stage Nd model ages of 2.28 to 2.26 Ga and positive initial εNd values of +2.34 to +2.69, indicating a juvenile nature for the arc magmatism. Re-Os geochronology of gold-related arsenopyrite from a metasedimentary rock-hosted massive sulfide provided an age of 2137 ± 11 Ma, suggesting that the mineralization is also coeval to the Rhyacian collisional stage.

Keywords: Greenstone Belt, Tocantins Province, Goiás Massif, Al-Depleted Komatiites, Oceanic Plateau.

1. Introduction

Granite-greenstone terranes are a window to explore the tectonic styles acting during the early Earth and how the first continental landmasses grew and stabilized. Several arguments from different perspectives point out the existence of uniformitarian processes controlling the Earth's geodynamics since the Archean Eon (Barley et al., 1984; Wyman, 2013; Kusky et al., 2018; Brenner et al., 2020). Systematically documentation of structural patterns and assemblies of igneous, metamorphic, and sedimentary rocks in ancient terranes have shown similarities to those produced by modern plate tectonics in the Phanerozoic (Cawood et al., 2018; Kusky et al., 2018; Windley et al., 2021).

In this sense, cratons are commonly thought to be composed of accreted terranes. For instance, the Superior Craton comprises oceanic arcs, oceanic plateaus, and sedimentary prisms accreted to older continental fragments (Langford and Morin, 1976; Card, 1990; Kusky and Polat, 1999; Percival et al., 2012); and the early and middle Archean greenstone belts of SW Greenland have been considered one of the best examples of Archean collisional orogenies embracing dismembered fragments of supra-subduction oceanic crust (Polat et al., 2008; Nutman and Friend, 2007, 2009). Accretionary orogenic systems have also been well described in other worldwide cratons such as the Zimbabwe, Yilgarn, Pilbara, and Kaapvaal cratons (Condie, 2007, Kusky et al., 2021; and references therein).

The Crixás-Goiás Domain of the Goiás Massif (Cordeiro and Oliveira, 2017) holds valuable information about Archean and Paleoproterozoic crustal growth processes in Central Brazil. One of the main components of this domain is the Crixás greenstone belt, a metavolcanosedimentary sequence consisted of Mesoarchean amphibolite facies metakomatiites and metabasalts overlaid by a low-grade Paleoproterozoic metasedimentary succession associated with intermediate metaigneous rocks (Borges et al., 2021). Previous studies have addressed the chemical characteristics of the Archean spinifex-textured komatiitic flows (Arndt et al., 1989; Kuyumjian and Jost, 2006), the provenance of the Paleoproterozoic clastic sediments (Jost et al., 2010; Ferreira et al., 2021; Borges et al., 2021), and the main characteristics of the gold deposits (Fortes, 1996; Jost et al., 2014). Nevertheless, the Crixás greenstone belt is still little explored regarding the petrogenetic processes, the tectonic environment of the different metaigneous units, and the space and time relations between the stages of magmatism and the processes of sedimentation and mineralization.

In this contribution, we investigate these rocks with integrated petrographic analysis, whole-rock geochemistry, and radiogenic isotopes. In this multidisciplinary approach, the chemical composition and Sm-Nd isotopic data are present for metakomatiites, metabasalts,

metadiorites, and meta-andesites. We also obtained the first LA-ICP-MS U-Pb zircon dating of the associated intermediate magmatism. Re-Os systematics of the metakomatiites and metabasalts as well as dating of gold-related arsenopyrite are also presented to give further geochronological constraints and context.

In summary, we suggest that the ultramafic and mafic rocks of the Crixás greenstone belt were formed in a ca. 3.0 Ga (Arndt et al., 1989; Fortes et al., 2003) oceanic plateau setting and were tectonically imbricated with ca. 2.2 – 2.1 intraoceanic arc units (arc-related immature sedimentary rocks and intermediate magmatism). This occurred during the collision of a Rhyacian magmatic arc onto the precursor Archean paleocontinent of which the Crixás-Goiás Domain derived, evidencing a complex stacking of temporally and genetically unrelated tectonic units. This orogenic episode is related to the main period of gold mineralization in the region and is treated in the context of the Paleoproterozoic amalgamation of the Goiás Massif, a building component of the western border of the São Francisco-Congo paleocontinent (Cordeiro and Oliveira, 2017; Martins-Ferreira et al., 2020).

2. Geological Background

The Crixás greenstone belt is located in the Crixás-Goiás Domain, which is a part of the Goiás Massif (Cordeiro and Oliveira, 2017; Borges et al., 2021). The massif comprises a complex collage of Archean and Paleoproterozoic distinct terranes that can be divided into four tectonic domains (Cordeiro and Oliveira, 2017) (Fig. 1): i) The Crixás-Goiás Domain, constituted of an association of Archean TTG (tonalite-trondhjemite-granodiorite) and Archean-Paleoproterozoic greenstone belts (Queiroz et al., 2008; Jost et al., 2013; Borges et al., 2017, 2021); ii) The Campinorte Domain, comprising granites, gneisses, granulites and metavolcanosedimentary rocks related to a ca. 2.2 - 2.1 Ga juvenile arc (Campinorte Arc) (Giustina et al., 2009; Cordeiro et al., 2014; Filgueiras et al., 2020); iii) the Cavalcante-Arraias Domain, formed of ca. 2.2 - 2.1 Ga peraluminous granites of the Aurumina Suite intruded in Rhyacian passive margin metasedimentary sequences of the Ticunzal Formation (Botelho et al., 2006; Fuck et al., 2014; Cuadros et al., 2017a, 2017b); and iv) the Almas-Conceição do Tocantins Domain, comprising ca. 2.4 Ga greenstones and 2.4 – 2.1 Ga varied granite-gneissic rocks, including TTG and peraluminous granites (Cruz et al., 2003; Sousa et al., 2016; Fuck et al., 2014; Martins-Ferreira et al., 2020; Saboia et al., 2020).

It is believed that the different domains of the Goiás Massif were amalgamated during successive orogenic cycles and accretion of intraoceanic and continental arcs in the Paleoproterozoic, forming the western margin of the São Francisco-Congo paleocontinent

(see Cordeiro and Oliveira, 2017, Martins-Ferreira et al., 2020, and Borges et al., 2021 for a review). The massif was later involved in Statherian-Calymmian extensional events that resulted in the formation of intracontinental basins, that largely cover the Paleoproterozoic crystalline basement in some regions, and intrusions of anorogenic granites (Pimentel et al., 1991; Martins-Ferreira et al., 2018; Toscani et al., 2021) (Fig. 1). During the Neoproterozoic, the Goiás Massif acted as the continental margin in which the Brasiliano/Pan-African Orogeny took place, building the Western Gondwana supercontinent (Cordeiro and Oliveira, 2017).

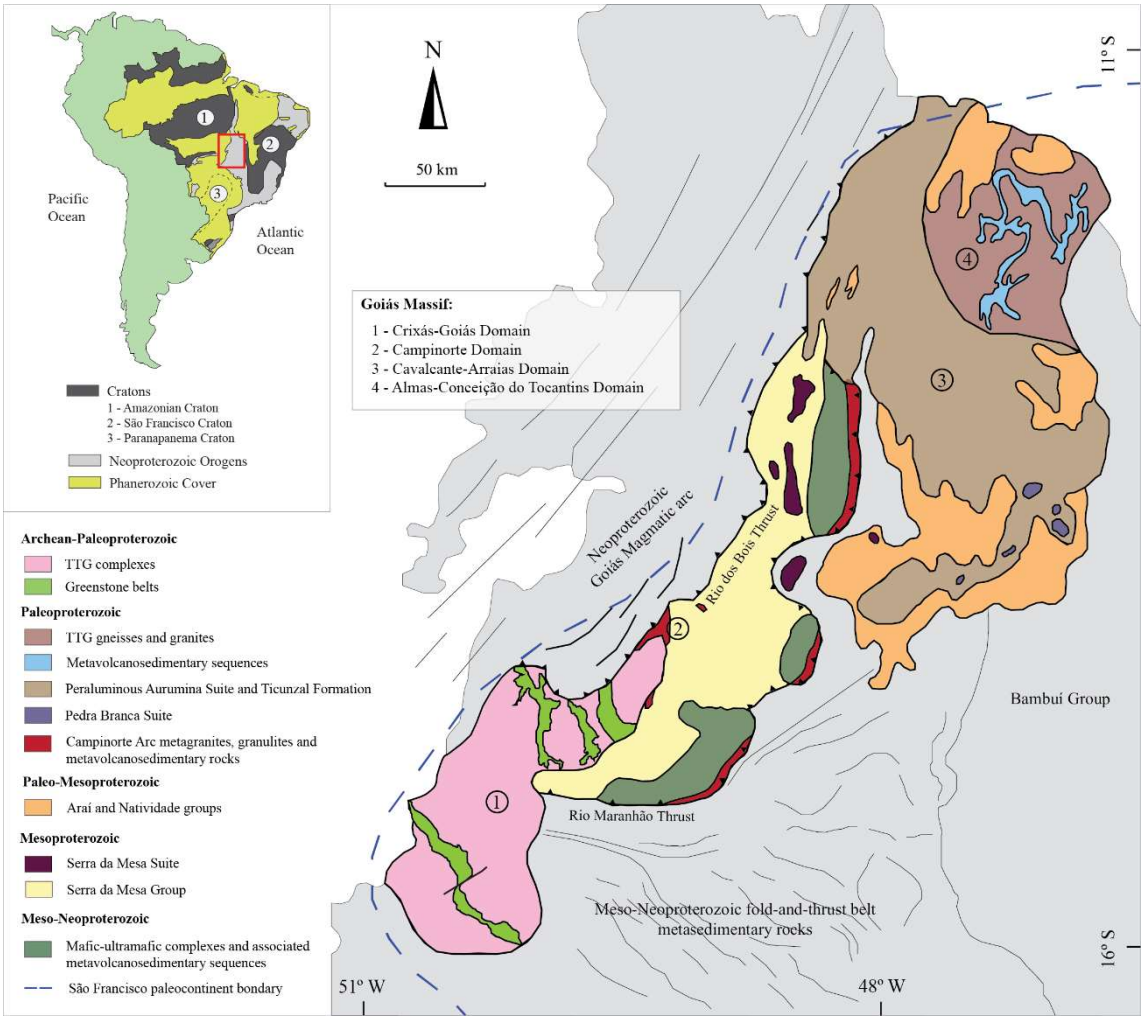

Fig. 1. The central northern part of the Brasília Belt, highlighting the Goiás Massif (modified after Cordeiro and Oliveira, 2017). The Crixás-Goiás Domain is located in the southwesternmost region of the massif.

2.1. The Crixás-Goiás Domain

The Crixás-Goiás Domain contains the oldest crustal fragments of the Goiás Massif. This domain comprises six Archean granite-gneiss complexes (Hidrolina, Moquém, Caiamar, Anta, Caiçara, and Uvá complexes), mostly of TTG composition, and five Archean-

Paleoproterozoic greenstone belts (Crixás, Guarinos, Pilar de Goiás, Faina, and Serra de Santa Rita greenstone belts) (Fig. 2a). Polycyclic stages of magmatic pulses are recorded in the granite-gneiss complexes. The oldest rocks outcrop in the Uvá and Caiçara complexes as ca. 3.1 – 2.9 Ga tonalitic to granodioritic batholiths that are intruded by smaller bodies of ca. 2.8 Ga tonalites, granodiorites, monzogranites, and charnockites (Beghelli Jr, 2012; Jost et al., 2013). The complexes of the northern Crixás-Goiás Domain record two stages of magmatism: the first consists of ca. 2.8 Ga tonalitic and granodioritic gneisses of the Hidrolina, Moquém, and Caiamar complexes, and the second stage consists of ca. 2.7 Ga granodiorites and granites intruded in the Moquém Complex (Queiroz et al., 2008). Various degree of crustal contamination is evidenced by Nd isotopes and inheritance of zircon xenocrysts that show the influence of continental crust as old as ca. 3.3 Ga, of which there is no known exposure so far (Queiroz et al., 2008).

The greenstone belts of the Crixás-Goiás Domain are located between the granite-gneiss complexes and have received increased attention from researchers in the last decades especially because they host different types of gold mineralization and also have the potential for Fe, Cu, and Ni deposits (Jost et al., 2014). In general, the five greenstones are synformal keels formed by basal metavolcanic rocks (mostly metakomatiites and metabasalts) superimposed by contrasting metasedimentary successions (Jost and Oliveira, 1991; Resende et al., 1998).

The age of the ultramafic-mafic volcanism is particularly well constrained in the Faina and Serra de Santa Rita greenstone belts, southern Crixás-Goiás Domain, based on U-Pb zircon dating of amphibolite and chloritite samples that yielded a ca. 2.96 Ga age (Borges et al., 2017). Nevertheless, the current geochronological data of the mafic and ultramafic metavolcanic rocks of the greenstones of the northern Crixás-Goiás Domain are still limited and poorly constrained. In the Crixás greenstone belt, whole-rock Pb-Pb and Sm-Nd data of metakomatiites provided imprecise isochron ages of 2728 ± 140 and 2825 ± 98 Ma, respectively (Arndt et al., 1989). A Mesoarchean age for the ultramafic and mafic volcanism was further reinforced by Fortes et al. (2003), who obtained a whole-rock Sm-Nd "errochron" with an age of 2998 ± 70 Ma.

Conversely, several geochronological data of the metasedimentary successions of the greenstone belts of the Crixás-Goiás Domain are available and have shown provenance from mixed Archean and Paleoproterozoic (predominantly Rhyacian) sources (Resende et al., 1999; Fortes et al., 2003; Tassinari et al., 2006; Jost et al., 2010, 2012, 2014, 2019; Brant et al., 2015; Ferreira et al., 2021; Borges et al., 2021). The variety of sedimentary lithofacies

associations in each greenstone mainly reflect different tectonic settings, depositional environments, and distance to the source areas (Borges et al., 2021).

The region of the Crixás-Goiás Domain also contains an important dike swarm that crosscuts the granite-gneisses and record a period of Siderian crustal extension after the Archean cratonization. The dikes strike mainly NE and correspond to high-Ti and low-Ti diabases, metabasites, and amphibolites emplaced at ca. 2.49 Ga (Corrêa da Costa and Girardi, 2005; Corrêa da Costa et al., 2006). Local Rhyacian felsic-intermediate magmatism is also present and corresponds to ca. 2.14 diorite intrusions near the Hidrolina Complex (Jost et al., 1993), trondhjemite stocks in the Pilar de Goiás greenstone belt (Jost et al., 1992; Queiroz, 2000), and ca. 2.06 Ga syenites in the Faina greenstone belt (Bogossian, 2020). Influences of the Neoproterozoic Brasiliano Orogeny are manifested as ca. 600 Ma granitic intrusions (Pimentel et al., 2003), anatexis and isotopic recycling of Archean orthogneisses (Queiroz et al., 2008; Jost et al., 2013), overgrowth margins in detrital zircon (Ferreira et al., 2021), and hydrothermal alteration (Fortes, 1996; Fortes et al., 2003), possibly causing the remobilization of ore deposits.

2.2. The Crixás Greenstone Belt

The Crixás greenstone belt, where our study is focused, is an NW-trending greenschist- to amphibolite-facies metavolcanosedimentary sequence located in the northern Crixás-Goiás Domain (Fig. 2a). The belt is tectonically limited to the west and east by the Meso-Neoarchean Anta and Caiamar granite-gneissic complexes, respectively, and overthrusted by rocks of the Neoproterozoic Mara Rosa Magmatic Arc to the north (Fig. 2b). In the northeastern sector, an allochthonous fault-bounded supracrustal fragment, named Mina Inglesa Sequence, overrides the metasedimentary rocks of the Crixás greenstone belt (Kuyumjian and Costa, 1999; Jost et al., 2019) (Fig. 2b).

The lowest units of Archean ultramafic and mafic metavolcanic rocks of the Crixás greenstone belt have been well described since the pioneering works of Danni and Ribeiro (1978), Sabóia (1979), Sabóia and Teixeira (1980), and Teixeira et al. (1981). Komatiitic flows, sometimes presenting spinifex textures, comprise the Córrego Alagadinho Formation and are superimposed by mafic lavas of the Rio Vermelho Formation (Sabóia, 1979; Sabóia and Teixeira, 1983; Jost and Oliveira, 1991) (Fig. 2c). Either the metakomatiites and metabasalts may show some intercalations of chert, iron-formation, and carbonaceous schist (Jost and Oliveira, 1991).

The metasedimentary succession of the Crixás greenstone belt consists of thick packages of carbonaceous phyllites with dolomite lenses of the Ribeirão das Antas Formation that gradually transition to metagraywackes of the Córrego Geral Formation, which prevail at the top of the sequence (Jost and Oliveira, 1991; Jost et al., 2019) (Fig. 2c). Petrographic and geochemical aspects of the carbonaceous phyllites and metagraywackes are presented elsewhere (Borges et al., 2021). Extensive U-Pb detrital zircon geochronology of those rocks shows unimodal age spectra, with a dominant peak at ca. 2.2 - 2.1 Ga and incipient contribution of Archean and Siderian grains (Jost et al., 2010; Ferreira et al., 2021; Borges et al., 2021). It was interpreted by Borges et al., (2021) that the poorly-sorted and immature sedimentary protoliths of the Crixás greenstone belt are allochthonous and were derived from the erosion of a rising Rhyacian magmatic arc (named Crixás arc) and originally deposited in a trench or forearc basin. The authors further suggested that the sedimentary rocks were tectonically transported after the collision of the Rhyacian arc and the Archean paleocontinent (formed of TTG and greenstones) of which the current Crixás-Goiás Domain derived.

More recently, it was recognized that the metasedimentary succession of the Crixás greenstone belt is also associated with thin layers of distinct schists, interpreted in this work as meta-andesites (see next sections), as well as to diorite intrusions revealed by deep drilling cores in the central-northern part of the greenstone. Borges et al., 2021 suggested that those rocks might represent the remnants of the Rhyacian magmatic arc that provided the sediments for the synchronous sedimentary rocks.

The present configuration of the different units of the Crixás greenstone belt shows a complex framework developed after tight to isoclinal folding, thin-skinned thrust faulting, duplex structures, and stratigraphic overturning (Fig. 2d) as a consequence of multiphase deformational events (Jost et al., 2010, 2019 and references therein). Low-angle thrust faults control the gold deposits hosted in the metasedimentary rocks. Mineralization occurs as stacked massive lenses, quartz veins, and disseminated orebodies (Jost et al., 2010, 2014). Re-Os dating of arsenopyrite from gold-bearing massive sulfide lenses provided ages of 2126 ± 16 Ma (Marques et al., 2013) and 2137 ± 11 Ma (this work), which may be interpreted either as the approximate timing of the gold mineralization and a minimum depositional age for the hosting sedimentary rocks of the Crixás greenstone belt, showing that the carbonate-siliciclastic basin stage was restricted to a relatively short period since the formation of its main Rhyacian source area (Borges et al., 2021).

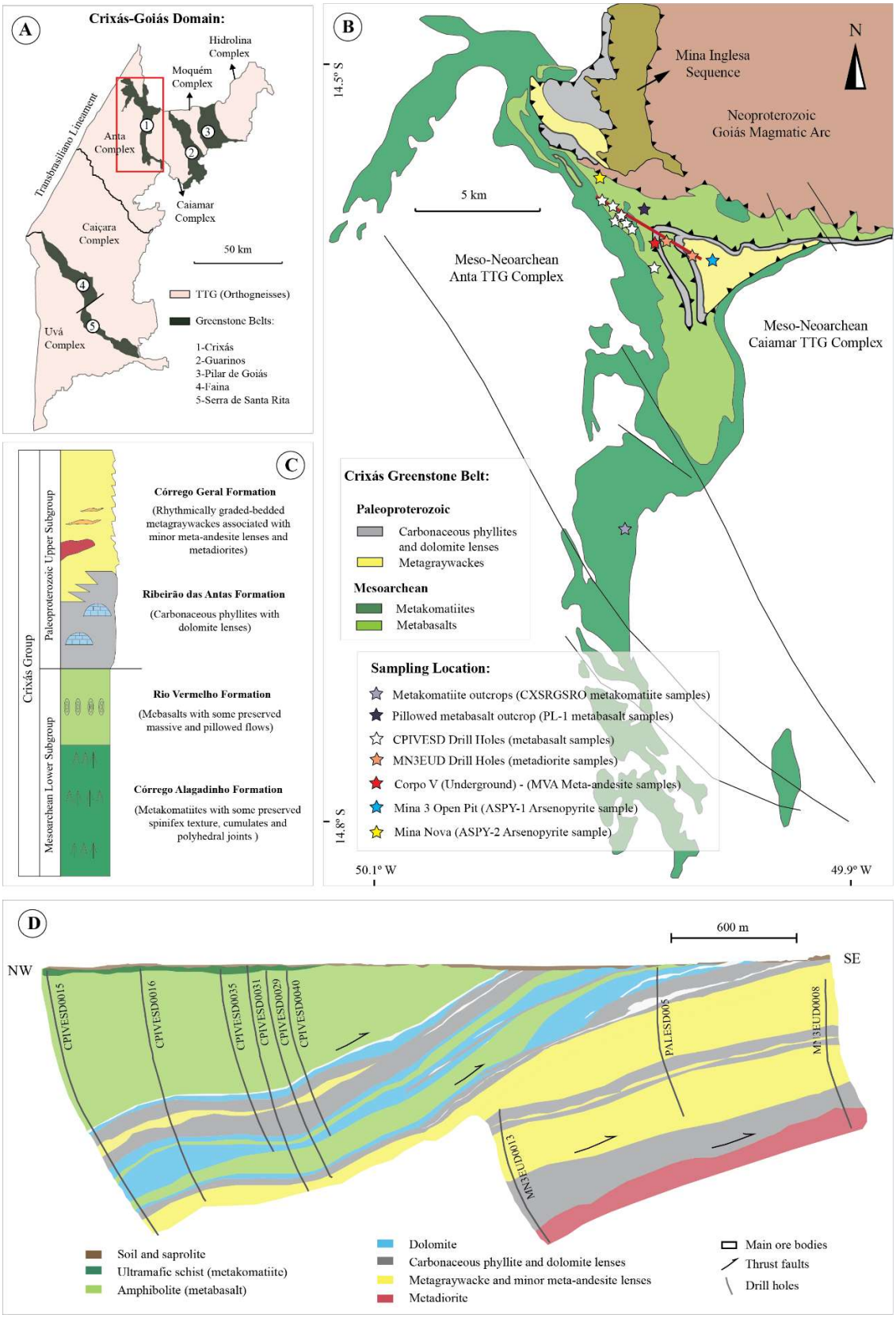

Fig. 2. The Crixás-Goiás Domain and the Crixás greenstone belt. (A) The main components of the Crixás-Goiás Domain (modified after Jost et al. 2010). (B) Geological map of the Crixás greenstone belt (modified after Jost et al., 2019). Sampling locations are highlighted by the star symbols. (C) Simplified tectonostratigraphic column of the Crixás greenstone belt (modified after Jost et al., 2019). (D) NW-SE

schematic section (shown by the red line on the geological map) of the central-northern part of the Crixás greenstone belt, evidencing the tectonic imbrication and repetition of layers due to detachment-thrusting.

3. Methods

3.1. Sampling

Most samples studied in this work were collected from nine drill holes roughly aligned in a NW-SE section located in the central-northern part of the Crixás greenstone belt (Fig. 2b), in the vicinity of the Mineração Serra Grande S.A. – AngloGold Ashanti, an exploration and mining company in the region of Crixás (Goiás State, Central Brazil). Drill cores demonstrate the stratigraphic overturning, as seen by the overriding of metakomatiites onto the metabasalts, which also override the metasedimentary rocks, and the common repetition of layers resulting after successive detachment thrusting (Fig. 2d). Cores were logged and carefully described, and some representative intervals of well-preserved rocks were sampled for petrographical, geochemical, and isotopic analyses. Our work also includes samples from outcrops of spinifex-textured metakomatiites in the southern part of the Crixás greenstone belt (Fig. 3a); samples from an outcrop of pillowed metabasalt in the central-northern part of the belt (Fig. 3b); and samples of meta-andesite collected in underground mine (Fig. 3f).

In total, we selected ten samples of metakomatiite, sixty-two of metabasalt, three of meta-andesite, and eighteen of metadiorites for whole-rock geochemistry. Whole-rock Sm-Nd isotopic analyses were performed in one sample of metakomatiite, seven of metabasalt, one of meta-andesite, and two of metadiorite. To determine the age of the intermediate magmatism, we selected one sample of meta-andesite for LA-ICP-MS U-Pb dating. Additionally, whole-rock Re-Os analyses were conducted in four selected core samples of metabasalt and one outcrop sample of spinifex-textured metakomatiite. Finally, arsenopyrite separates of two samples were selected for Re-Os geochronology: i) a hand sample of sedimentary rock-hosted massive sulfide with coarse-grained arsenopyrite (collected in underground mining of the upper mineralized zone; Mina 3) (Fig. 4); and ii) a ~10 cm thick core sample of strongly foliated sedimentary rock hosting oriented and disseminated arsenopyrite crystals (collected at Mina Nova) (Fig. 4).

All samples used in this study and their respective coordinates, depth, protolith, and type of data provided are listed in Supplementary Material 1. Locations of the samples are also represented in the geological map of Fig. 2b.

3.2. *Whole-rock Geochemistry*

Approximately 15 g of each sample was pulverized and analyzed at the ALS Geochemistry Laboratory. Major elements were determined by ICP-AES. Trace elements, including the rare earth elements (REE), high field strength elements (HFSE), and large ion lithophile elements (LILE), were analyzed by ICP-MS, and the concentrations of the base metals were determined by ICP-AES. Details of the analytical methods and laboratory procedures are available in the Whole Rock Analysis & Lithogeochemistry catalog (Complete Characterization Package CCP-PKG01), accessible on the ALS Geochemistry website (www.alsglobal.com).

Percentages of major element oxides were recalculated to 100 wt. % anhydrous. Chondrite and Primitive Mantle compositions of Sun and McDonough (1989) were used for normalizations. Anomalies of Eu and Ce (Eu/Eu* and Ce/Ce*, respectively) were calculated relative to the neighboring elements on the REE diagrams, following Taylor and McLennan (1985). Major (wt. %) and trace elements (ppm), and their respective detection limits, are listed in Supplementary Material 2.

3.3. *U-Pb Geochronology*

About 5 kg of a meta-andesite sample was crushed, milled, and sieved at the Geochronology Laboratory of the University of Brasília. Non-magnetic heavy concentrates were segregated using a Frantz isodynamic magnetic separator. Zircon grains were individually handpicked using a binocular microscope and mounted in epoxy resin to be polished and cleaned. Cathodoluminescence and back-scatter electron imaging obtained with a FEI Quanta™ 450 Field Emission Scanning Electron Microscope were used to reveal the texture and internal structure of the individual zircon crystals.

The analyses were conducted using an MC-ICP-MS Finnigan Neptune coupled to a New Wave 213 μm Nd-YAG laser equipment at the Geochronology Laboratory of the University of Brasília. Details of the analytical methods are described by Bühn et al (2009). ^{238}U was analyzed in the H4 Faraday cup, ^{232}Th in the H2 Faraday cup, ^{208}Pb in the L3 Faraday cup, and ^{206}Pb in the L4 Faraday cup. ^{207}Pb, $^{204}Hg/^{204}Pb$, and ^{202}Hg were measured using ion counting (IC) fixed in the L4 Faraday cup. Correction of isobaric interference of ^{204}Hg on ^{204}Pb was applied. Laser ablation was performed in 25 μm spots with a frequency of 10 Hz and an intensity of 3.92 J/cm². The pulverized material was carried with a flux of He (-0.38 L/min) and Ar (-1.00 L/min). Signals were collected in a single block of 40 cycles with an

integration time of 1.049 s. ^{202}Hg, $^{204}(Pb + Hg)$, ^{206}Pb, and ^{207}Pb were measured in counts per second (CPS), and ^{232}Th and ^{235}U were measured in millivolts (mV). The sample-standard bracketing technique was used to instrumental mass bias and drift correction.

Two international standards were employed: The GJ-1 zircon was used as the primary standard and has an ID-TIMS age of 608.5 ± 0.4 Ma (Jackson et al., 2004); and the 91,500 zircon was used as the internal secondary standard and has an ID-TIMS age of 1065.4 ± 0.3 Ma (Wiedenbeck et al., 1995). U-Pb data reduction was carried out using the Chronus Add-in for Excel (Oliveira, 2015) and the decay constant values recommended by Steiger and Jäger (1977) were adopted. Concordia age was plotted with the IsoplotR toolbox (Vermeesch, 2018). LA-ICP-MS zircon U-Pb data are listed in Table 1.

3.4. Sm-Nd Isotopes

Whole-rock samples were powdered in a tungsten carbide shatterbox and analyzed at the Geochronology Laboratory of the University of Brasília. For each sample, approximately 100 mg of whole-rock powder was spiked with a ^{150}Nd-^{149}Sm tracer and dissolved with a 5:1 HF-HNO_3 solution in Savillex ® vials. Samples were redissolved with 7 ml of 6N HCl after cooling and evaporation of the 5:1 HF-HNO_3 solution and then immersed in 3 ml of 2.5N HCl. Extraction of Sm and Nd followed the procedures of Gioia and Pimentel (2000). Each sample was loaded with 0.25N H_3PO_4 on Ta and Re filaments for Sm and Nd, respectively.

Isotopic ratios were measured using a Thermo Scientific TRITON™ Plus Thermal Ionization Mass Spectrometer (TIMS) operating in static multicollector mode. We typically collected 100-200 ratios with a 0.5 to 1-V ^{144}Nd beam. Nd ratios were normalized to $^{146}Nd/^{144}Nd = 0.7219$. Repeated analyses of the USGS BHVO-1 standard provided $^{143}Nd/^{144}Nd = 0.512996 \pm 0.000006$ (2SD; n = 7). Average blank values were <100 pg and <500 pg for Sm and Nd, respectively. Blank correction was insignificant for Nd isotopic composition and Sm/Nd ratios. The present-day bulk earth (CHUR) values of $^{147}Sm/^{144}Nd = 0.1967$ and $^{143}Nd/^{144}Nd = 0.512638$ (Jacobsen and Wasserburg, 1980) were adopted. Single-stage Nd model (T_{DM}) and two-stage model age (T_{2DM}) parameters were calculated following DePaolo (1981, 1988) and Liew and Hofmann (1988), respectively. Sm-Nd isotopic data are listed in Table 2.

3.5. Re-Os Isotopes

Initial preparation of the samples and the analytical methods were carried out at the Department of Geosciences of the University of Arizona (Tucson, USA). All samples were firstly wrapped in Texwipe TechniCloth sheets and crushed with a steel hammer, protecting them from metal contact. Samples were then separately handpicked and sieved. Fresh core samples were taken from the inner parts to avoid the edges with drilling marks. For the samples of metabasalt, metakomatiite, only the whole-rock fragments with grain size less than 2 mm were collected. For the individual arsenopyrite separates (hosted in mineralized metasedimentary rocks), only the coarser grains (>0.1 mm) were collected to account for the common Re and Os heterogeneous distribution in sulfide minerals.

Approximately 0.8 g of whole-rock metabasalt and metakomatiite samples, and 0.25 g of arsenopyrite separates were loaded in Carius tubes. Precisely weighed amounts of ^{185}Re and ^{190}Os spikes were added with a mixture of 3ml HCl (10N), 9 ml HNO_3 (16N), and 2 ml H_2O_2, following the procedures described by Shirey and Walker (1995). During this process, each Carius tube was partially submerged in a liquid nitrogen and ethanol slush, so that spikes and reagents were chilled upon introduction into the tubes, retarding potential chemical reactions. Carius tubes were sealed and warmed to room temperature, and later heated in an oven at 240º C for about 48 h to achieve complete dissolution of each sample.

From the resulting solution, separation of Os was treated in a two-stage distillation process (Nägler and Frei, 1997), and a later microdistillation technique (Birck et al., 1997) was used for Os purification. After Os extraction, the remaining solution was dried out and then dissolved with 0.1 N HNO_3. Re was recovered through a two-stage anion exchange chromatography, similar to the procedures described by Morgan and Walker (1989). Purified fractions of Re and Os were loaded on Ni and Pt filaments, respectively. To enhance ionization, 1 µl of $Ba(OH)_2$ and $Ba(NO_3)_2$ salts were loaded on the specific filaments with Re and Os, respectively. All samples were analyzed by Negative Thermal Ion Mass Spectrometry (N-TIMS) on a VG 54 equipment. Os was measured using a Daly collector, and Re using a Faraday collector.

Regression plots were performed using the IsoplotR toolbox (Vermeesch, 2018). ^{187}Re decay constant of 1.666×10^{-11} $year^{-1}$ (Smoliar et al. 1996) was adopted. γ_{Os} is the percentage deviation of the Os isotopic composition between the sample and the reference chondrite reservoir at a specified time (t). T_{MA} refers to the model age calculated as the time of separation from the chondritic mantle evolution curve. For these parameters, we adopted an average $^{187}Re/^{188}Os = 0.40186$ of chondrites and an initial $^{187}Os/^{188}Os = 0.09531$ of the

early solar system, following Shirey and Walker (1998). Re-Os isotopic of data are listed in tables 3 and 4.

4. Results

4.1. Macroscopic Aspects and Petrography

4.1.1. Metakomatiites and Metabasalts

Although the Mesoarchean ultramafic-mafic metavolcanic rocks of the Crixás greenstone belt underwent deformation and metamorphism with a peak at lower amphibolite-facies, well-preserved primary igneous features are still present in some outcrops. Some metakomatiites have spinifex texture (Fig. 3a), and the massive ultramafic flows show relicts of cumulates. Less deformed ultramafic rocks gradually give place to strongly foliated schists (Fig. 3c) and serpentinites lacking primary textures. The metabasalts consist of dark greenish amphibolites that are commonly highly deformed and foliated. However, primary volcanic features, such as amygdales and pillow lavas (Fig. 3b), are locally well-preserved. There is an increase in the grain size of the amphibolites, evidenced in some intervals of the drill cores, where fine-grained rocks gradually progress to massive coarse-grained amphibolites (Fig. 3d). This grain size variation is a primary feature of the protoliths and might be related to the central parts of the thick mafic lava flows, although some coarse-grained rocks also occur as gabbroic sills.

Despite the locally well-preserved primary igneous textures, the rocks are mostly recrystallized and the original mineralogy was fully replaced by metamorphic assemblies. Ultramafic rocks are composed of variable amounts of serpentine, tremolite, chlorite, talc, ilmenite, and carbonate. Spinifex-textured metakomatiites contain parallel platy olivine phenocrysts (now totally transformed into Mg-chlorite) enclosed in a recrystallized fine-grained groundmass consisting mostly of tremolite, talc, carbonate, and opaques (Fig. 5a and 5b); and the cumulate horizons in the layered ultramafic flows are dominantly composed of serpentine aggregates that still preserve the shape of the precursor olivine grains. Ultramafic schists predominate in the high-strain corridors and are characterized by a prominent lepidoblastic texture marked by the preferential orientation of talc and chlorite in one or more directions, and associated nematoblastic domains formed of euhedral tremolite crystals.

Essential minerals of the metabasalts are Mg-hornblende and plagioclase (ranging from oligoclase to andesine; An_{18-32}) (Fig. 5c and 5d), with minor epidote, quartz, carbonate,

ilmenite, sphene, and apatite. The mineral paragenesis is diagnostic of mafic rocks metamorphosed under amphibolite-facies, which marks the metamorphic peak in the region of the Crixás-Goiás Domain. Some amphibole crystals have actinolite cores and Mg-hornblende rims, which suggest a prograde metamorphic reaction from greenschist- to lower amphibolite-facies. Chlorite and biotite substitute the hornblende in various degrees and indicate late processes of hydrothermal alteration or low-grade retrometamorphism. Relics of intergranular texture are also commonly preserved, especially in massive coarse-grained amphibolites, and are characterized by recrystallized plagioclase and quartz filling the interstices between the larger euhedral to subhedral hornblende grains, that are likely pseudomorphs of primary pyroxene (Fig. 5d). Some metabasalts present mm-sized rounded features that resemble amygdales filled with secondary carbonate and quartz. Along the deformed zones, the amphibolites are highly schistose, with a well-marked foliation evidenced by the preferential orientation of Mg-hornblende crystals in a nematoblastic texture, while the plagioclase and quartz grains form stretched granoblastic domains. Carbonate and quartz-filled veinlets, and sulfide dissemination (mainly chalcopyrite and pyrrhotite) are common in all rock types.

4.1.2. Meta-andesites and Metadiorites

Along the upper Rhyacian metasedimentary sequence of the Crixás greenstone belt, some rare layers of biotite-muscovite-plagioclase-quartz schist (Fig. 3f) have been interpreted as felsic/intermediate metavolcanic rocks. These grayish schists have been recognized both in drill core records and underground mining. The schists show a granolepidoblastic texture characterized by a fine-grained groundmass formed of recrystallized plagioclase (mostly albite) and quartz, adjacent to aggregates of oriented biotite and muscovite. Larger grains of plagioclase (albite; An_{1-2}) and quartz are embedded in the groundmass (Fig. 5f), resembling recrystallized and rotated phenocrysts of the precursor volcanic protolith. Rutile, epidote, zircon, and ilmenite are common accessory minerals. Frequently, the rocks are associated with carbonate alteration and pyrrhotite dissemination. As will be discussed in the next sections, the schists have a chemical composition consistent with intermediate rocks and are referred to as meta-andesites in this work. These rocks should not be confused with the immature and poorly-sorted metagraywackes of the Crixás greenstone belt, which can show similar petrographic textures but are distinct by having metamorphic garnet in the modal composition, primary preserved sedimentary textures, and common intercalation with mm-thick carbonaceous phyllite layers (Borges et al., 2021).

Deep drilling in the Crixás greenstone belt has also revealed diorite intrusions that occur just below the detachment zone of the lowest levels of metagraywackes in the central northern part of the belt (Fig. 2d). These are massive to slightly foliated medium- to coarse-grained rocks (Fig, 3e) that occur in tectonic contact with some metasedimentary rocks. Well-preserved massive domains have relics of igneous texture characterized by subhedral pleochroic greenish hornblende crystals with regular contacts, in which the anhedral to subhedral recrystallized grains of plagioclase (albite; An_3) and quartz occur in the interstices (Fig. 5e). Ilmenite, sphene, and apatite are accessory minerals. Hornblende is partially replaced by biotite and chlorite, although primary biotite with euhedral shapes also occurs. Plagioclase shows variable alteration to epidote. Foliation is well developed in some metadiorites and is characterized by the preferential orientation of hornblende, biotite, and chlorite. Late-formed euhedral garnet porphyroblasts can be present.

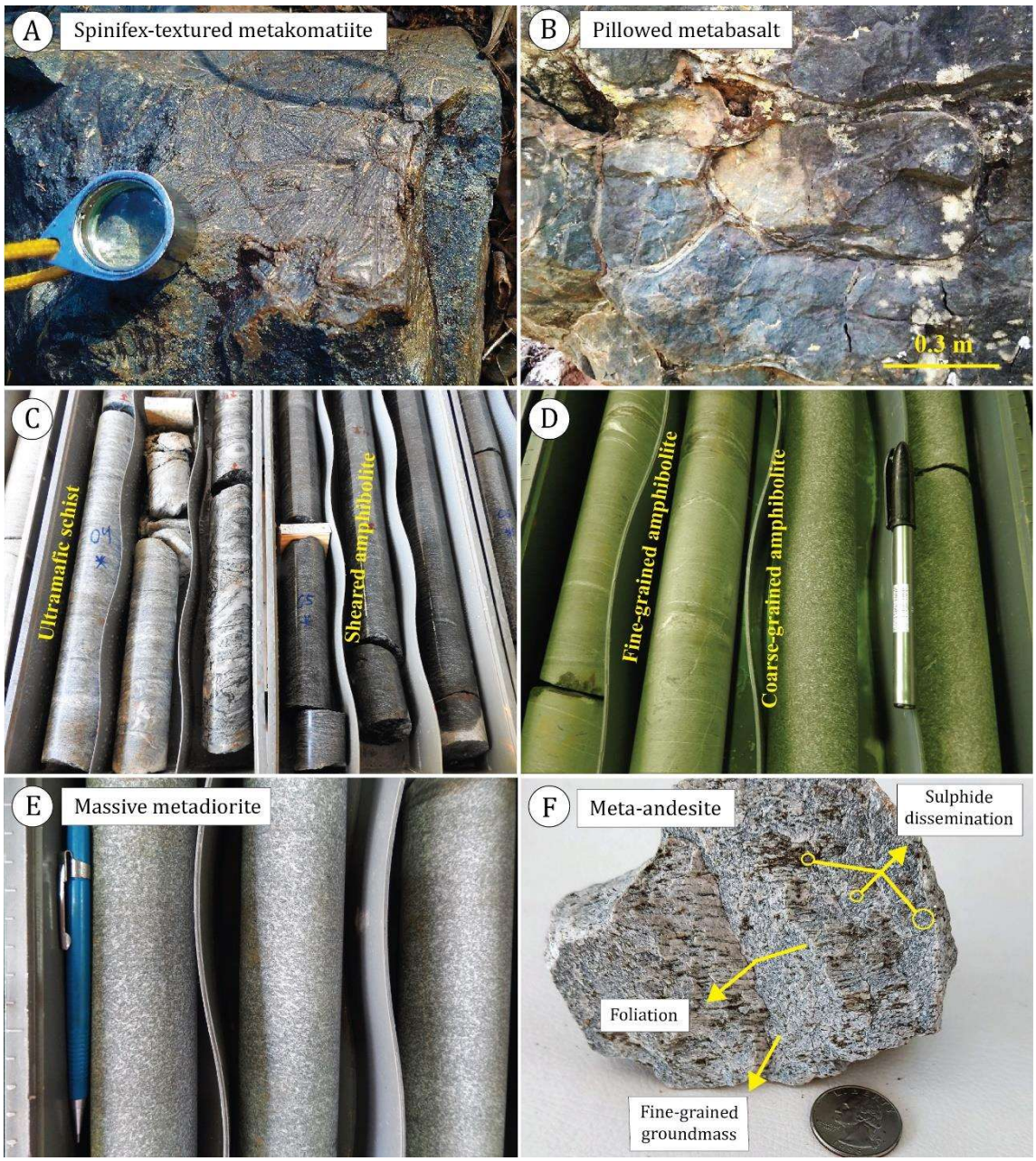

Fig. 3. Macroscopic characteristics of metaigneous rocks of the Crixás greenstone belt. (A) Spinifex-textured metakomatiite. (B) Pillow lavas preserved in amphibolite (metabasalt) outcrop. (C) Drill core aspects evidencing the contact between ultramafic schist (metakomatiite) and sheared amphibolite (metabasalt). (D) Well-preserved amphibolite showing a gradual transition between a fine-grained and a massive coarse-grained rock (increasing depth from the left to right). (E) Drill core aspects of the massive metadiorite. (F) Hand sample of a foliated meta-andesite collected in underground mining (Corpo V).

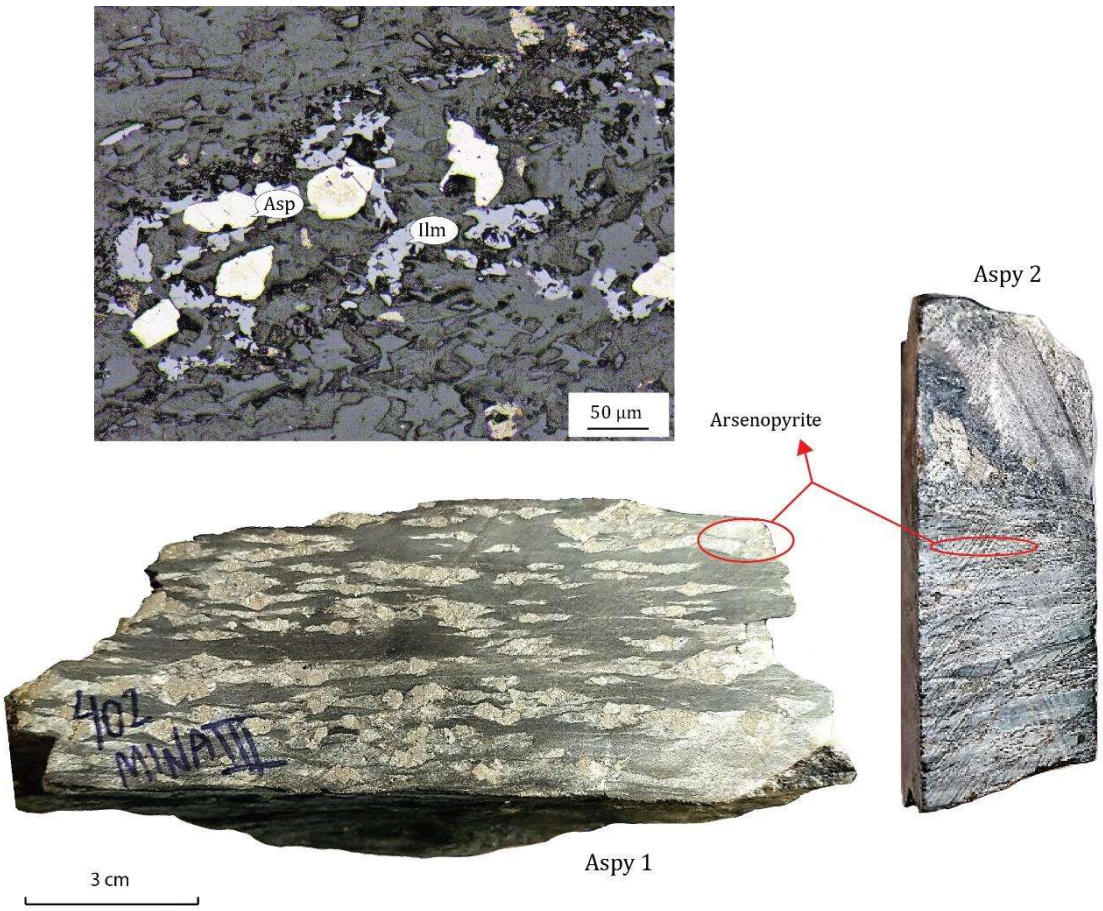

Fig. 4. Macroscopic and microscopic (reflected light) aspects of the arsenopyrite hosted in metasedimentary rocks (carbonaceous phyllites) of the Crixás greenstone belt. Arsenopyrite separates from ASPY-1 (massive sulfide) and ASPY-2 (disseminated sulfide) samples were selected for Re-Os geochronology. Gangue minerals are mostly quartz, muscovite, biotite, ilmenite, and carbonaceous matter. Abbreviations: Aspy (arsenopyrite) and Ilm (ilmenite).

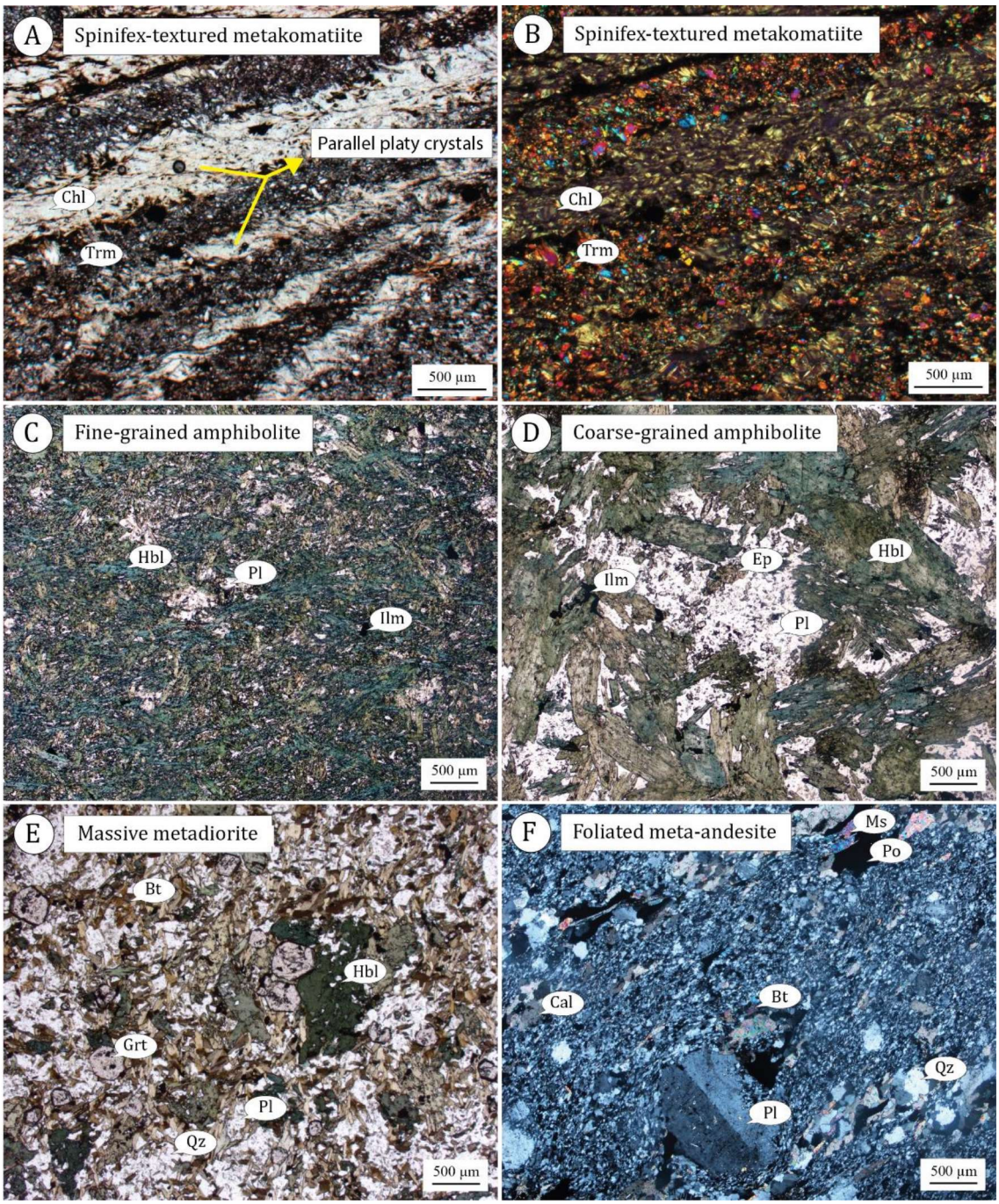

Fig. 5. Photomicrographs of metaigneous rocks of the Crixás greenstone belt. (A and B) Spinifex texture in metakomatiite characterized by relicts of parallel platy olivine phenocrysts (totally transformed into Mg-chlorite) enclosed in a recrystallized fine-grained groundmass composed essentially of tremolite, chlorite, talc, carbonate, and opaques. (C) Fine-grained amphibolite (metabasalt) composed mostly of hornblende and plagioclase. (D) Massive coarse-grained amphibolite with preserved primary intergranular texture. (E) Massive metadiorite composed of hornblende, plagioclase, quartz, biotite, and ilmenite. Rounded euhedral crystals are late-formed garnet. (F) Meta-andesite showing a primary preserved porphyritic texture consisted of euhedral to subhedral plagioclase and quartz crystals embedded in a fine-grained recrystallized groundmass formed of quartz, plagioclase, muscovite, and biotite. Opaque minerals are oxides and/or secondary sulfides. Planar polarized lights: A, C, D, and E. Crossed polarized lights: B and F. Abbreviations: Trm (tremolite), Srp (serpentine), Qz (quartz), Pl (plagioclase), Ms (muscovite), Bt (biotite), Grt (garnet), Ilm (ilmenite), Ep (epidote), Cal (calcite), and Po (pyrrhotite).

4.2. Major and Trace Elements

4.2.1. Metakomatiites and Metabasalts

The metakomatiites of the Crixás greenstone belt have low contents of SiO_2 = 42 – 48 wt%, Al_2O_3 = 2 – 5 wt%, and TiO_2 = 0.3 – 0.5 wt%, very high contents of MgO = 24 – 38 wt%, Fe_2O_3 = 11 – 16 wt%, Cr = 1190 – 2040 ppm, and Ni = 1490 – 2540 ppm, and low and variable contents of CaO = 1 – 8 wt%, Na_2O = 0.02 – 0.29 wt%, and K_2O = 0.01 – 0.04 wt% (Supplementary Material 2). All analyzed samples are consistently classified as komatiites on the Jensen's ternary cationic diagram (Fig. 6a). On chondrite-normalized diagram, the metakomatiites display flat to enriched patterns of LREE (La/Sm_{cn} = 0.91 – 1.96) and markedly depleted patterns of HREE (Gd/Yb_{cn} = 1.26 – 2.20) (Fig. 7a), with the exception of one sample (CXSRGSR06) that possess a flat HREE pattern (Gd/Yb_{cn} = 0.91). Negative anomalies of Zr – Hf and Ti are the most prominent features on the primitive mantle-normalized diagram (Fig. 7b).

The metabasalts (amphibolites) of the Crixás greenstone belt are characterized by SiO_2 = 49 – 55 wt%, MgO = 5 - 14 wt%, Fe_2O_3 = 10 – 16 wt%, Al_2O_3 = 11 – 15 wt%, TiO_2 = 0.6 – 1.6 wt%, CaO = 8 – 13 wt%, Na_2O = 1.3 – 3.6 wt%, K_2O = 0.1 – 0.3 wt%, and a large range of Ni = 28 – 404 ppm, and Cr = 10 – 1250 ppm (Supplementary Material 2). These rocks are classified as basalts on the Nb/Y vs. Zr/Ti diagram (Fig. 6b) and show a typical tholeiitic magmatic affinity, as seen on the Zr/Y vs. Th/Yb diagram (Fig. 7c). The amphibolites plot predominantly in the field of the high-Mg tholeiitic basalts on the Jensen's cationic diagram, with only a few samples plotting in the high-Fe tholeiitic basalt and komatiitic basalt fields (Fig. 6a). On the chondrite-normalized diagram, most metabasalts show flat patterns of LREE, but depleted to slightly enriched patterns are also observed in some samples (La/Sm_{cn} = 0.78-1.66; La/Yb_{cn} = 0.99-2.10) (Fig. 7c). The HREE patterns range from near-flat to slightly fractionated (Gd/Yb_{cn} = 1.20-1.60). On the primitive-mantle normalized diagram, the metabasalts show near-flat patterns without significant anomalies (Fig. 7d).

4.2.2. Meta-andesites and Metadiorites

The meta-andesites of the Crixás greenstone belt are characterized by SiO_2 = 60 – 62 wt%, MgO = 1.9 – 2.4 wt%, Fe_2O_3 = 6.0 – 6.4 wt%, Al_2O_3 = 16 – 17 wt%, TiO_2 = 0.7 – 0.8 wt%, CaO = 2.3 – 3.5 wt%, Na_2O = 8.2 – 9.2 wt%, K_2O = 0.4 – 0.7 wt%, P_2O_5 = 0.1 – 0.2

wt%, Ni = 37 – 45 ppm, and Cr = 90 – 120 ppm. In comparison to the meta-andesites, the metadiorites of the Crixás greenstone belt show generally lower SiO_2 (51 – 65 wt%), Na_2O (2.6 – 4.9 wt%), Ni (4 – 52 ppm), and Cr (10 – 70 ppm); moderately higher MgO (1.4 – 5.1 wt%), Fe_2O_3 (6 – 13 wt%), TiO_2 (0.8 – 1.4 wt%), CaO (1.7 – 6.7 wt%), and K_2O (0.3 – 2.7 wt%); and similar Al_2O_3 (14 – 17 wt%), and P_2O_5 (0.17 – 0.31 wt%) (Supplementary Material 2).

The meta-andesites and metadiorites plot in the andesite field on the Nb/Y vs. Zr/Ti diagram, although few samples of metadiorite plot in the basalt field (Fig. 6b). An intermediate composition for both groups is also evidenced on Jensen's ternary cationic diagram, where most samples plot in the andesite field (Fig. 6a). The meta-andesites show a calc-alkaline magmatic affinity according to the Zr/Y vs. Th/Yb diagram, while the metadiorites plot mostly in the transitional field (Fig. 6c). The meta-andesites and metadiorites of the Crixás greenstone belt display similar trace element systematics on the chondrite- and primitive mantle-normalized diagrams. Samples are characterized by LREE-enriched patterns (La/Sm_{cn} = 2.06 – 4.00) and flat to slightly depleted HREE patterns (Gd/Yb_{cn} = 1.06 – 1.90) (Fig. 8a and 8c). Various magnitudes of Eu negative anomalies are present (Eu/Eu* = 0.68 – 0.93) (Fig. 8a and 8c). Samples also show prominent negative anomalies of Nb and Ti and incipient negative anomalies of Zr (Fig. 8b and 8d).

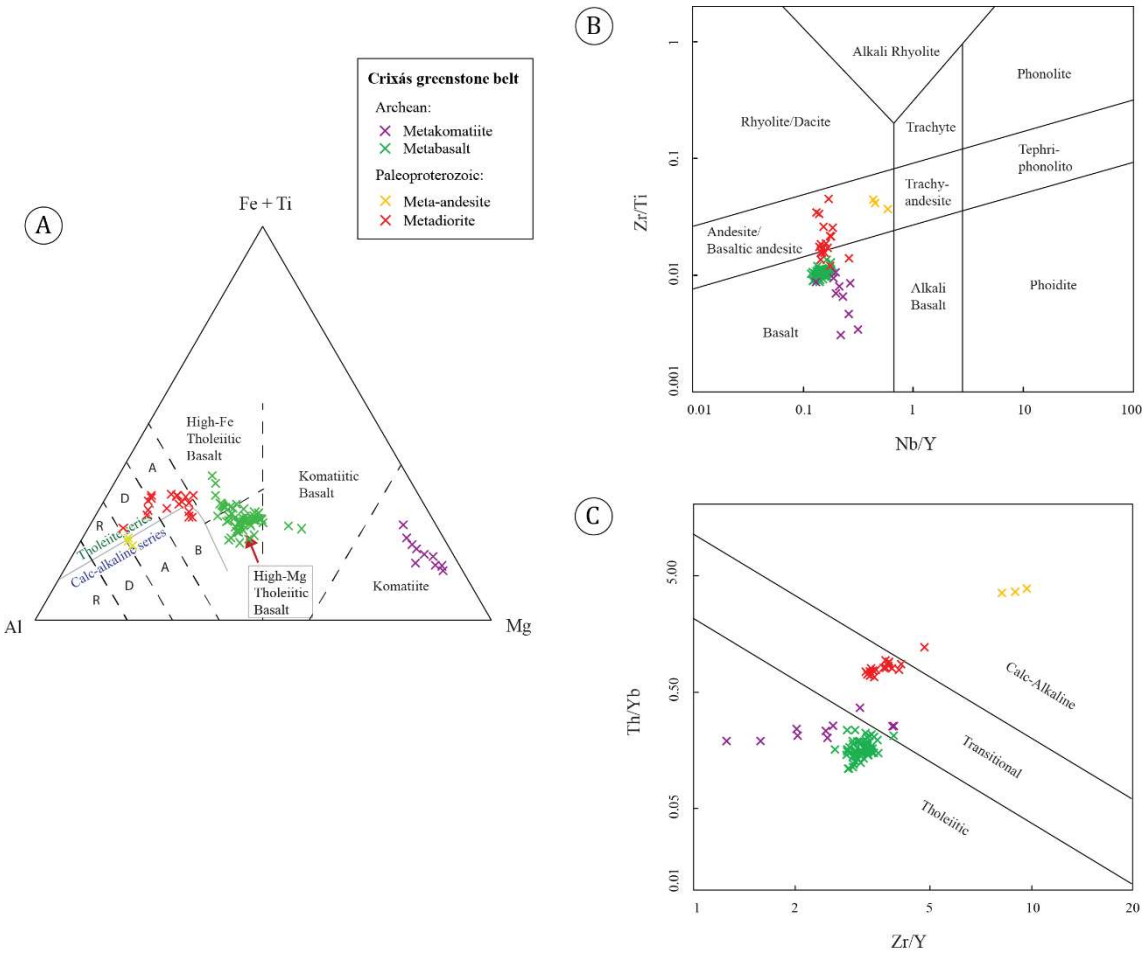

Fig. 6. Classification diagrams for the metaigneous rocks of the Crixás greenstone belt. (A) Ternary cationic proportion diagram (Jensen, 1976). (B) Nb/Y vs. Zr/Ti diagram (Pearce, 1996 after Winchester and Floyd, 1977). (C) Zr/Y vs. Th/Yb diagram (Ross and Bédard, 2009).

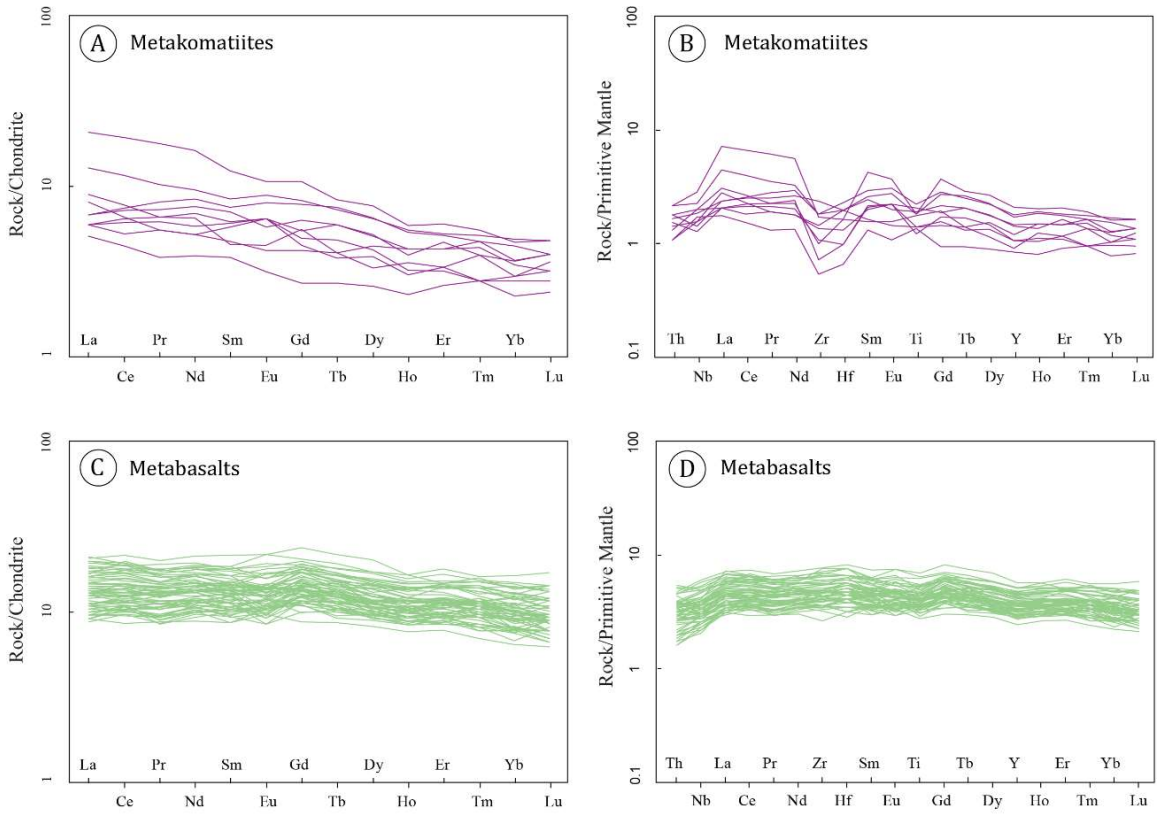

Fig, 7. Chondrite- and primitive mantle-normalized diagrams for the metakomatiites (A and B) and metabasalts (C and D) of the Crixás greenstone belt. Normalization values are those of Sun and McDonough (1989).

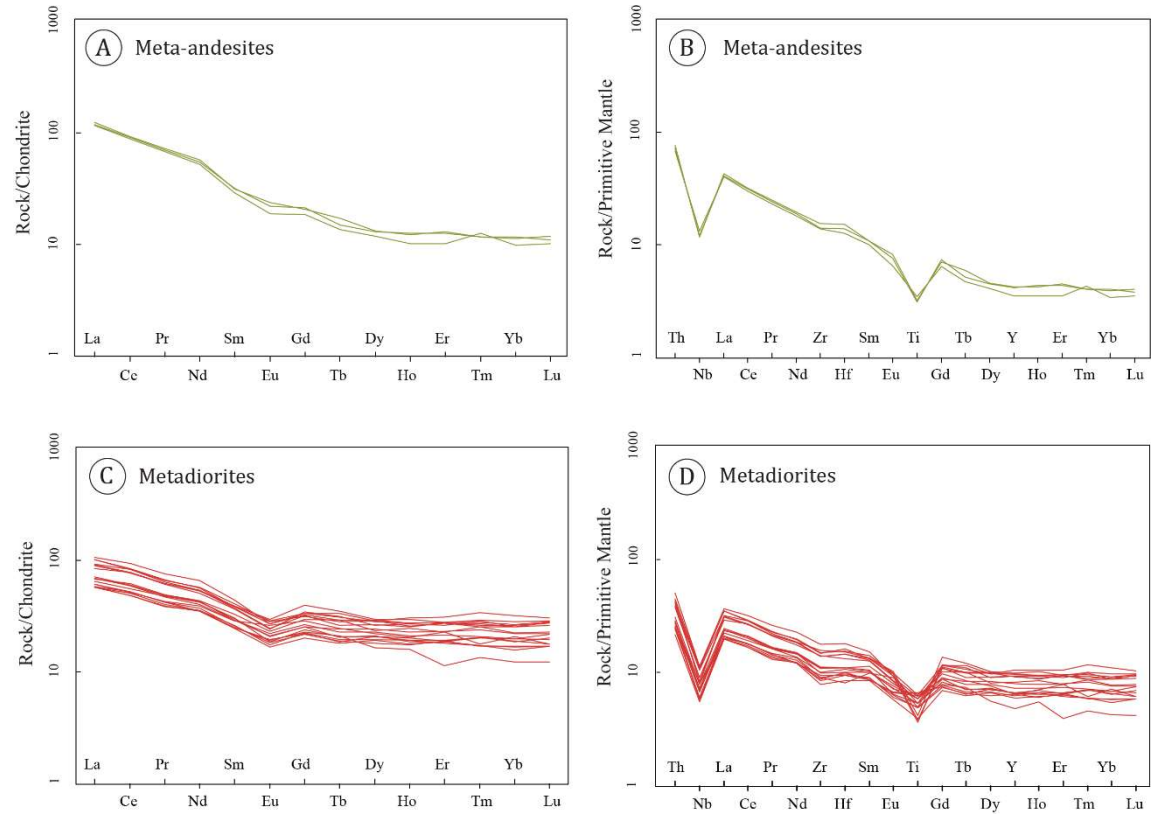

Fig, 8. Chondrite- and primitive mantle-normalized diagrams for the meta-andesites (A and B) and metadiorites (C and D) of the Crixás greenstone belt. Normalization values are those of Sun and McDonough (1989).

4.3. Zircon U-Pb Geochronology

Zircon crystals recovered from the meta-andesite sample (MVA-1A) consist of euhedral prismatic and sub-rounded grains with internal growth zoning. Th/U ratios of the individual grains range from 0.46 to 1.38 (Table 1), typical of magmatic zircon values (e.g. Rubatto and Gebauer, 2000). U-Pb analytical data (Table 1) from nine zircon grains were plotted on a Concordia diagram and defined the upper intercept age of 2172.2 ± 12.7 Ma and a lower intercept age of 501 ± 249 Ma (MSWD = 1.4) (Fig. 9).

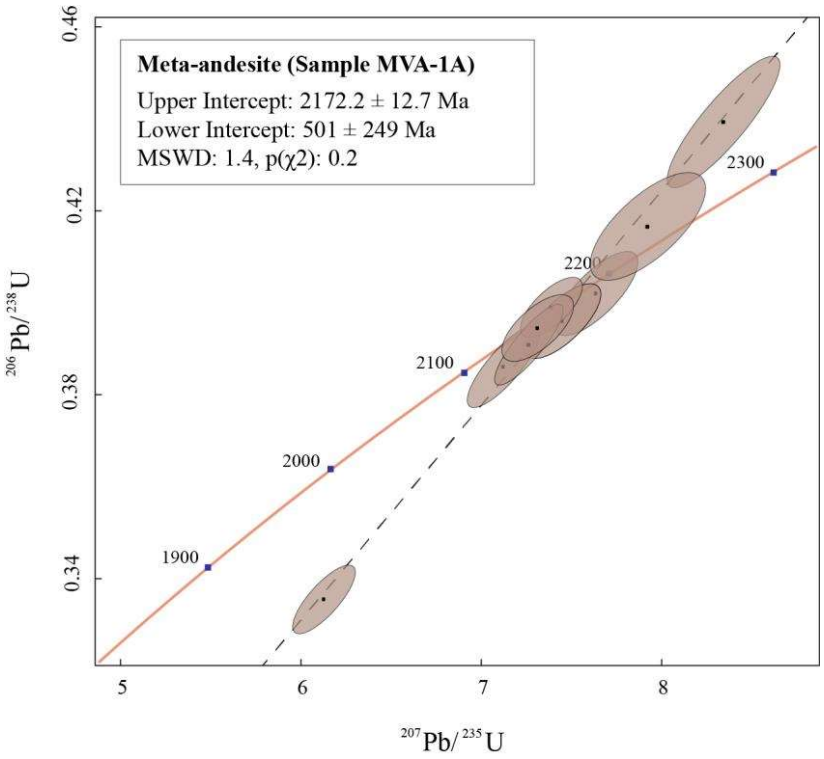

Fig. 9. U-Pb Concordia plot for the sample of meta-andesite (MVA-1A) of the Crixás greenstone belt.

Table 1. U-Pb zircon data from the sample of meta-andesite of the Crixás greenstone belt (MVA-1A).

					Isotope ratios									Ages (Ma) [2]						
Spot ID	206* (%)	^{204}Pb cps	^{206}Pb mV [1]	Th/U	^{206}Pb/^{204}Pb	1σ (%)	^{207}Pb/^{206}Pb	1σ (%)	^{207}Pb/^{235}U	1σ (%)	^{206}Pb/^{238}U	1s %	Rho	^{207}Pb/^{206}Pb	2σ abs	^{206}Pb/^{238}U	2σ abs	^{207}Pb/^{235}U	2σ abs	U-Pb disc. (%) [3]
003-ZR1	0.0110	7	0.0028	0.463	136626	12.47	0.13776	0.73	7.637	1.24	0.4020	0.93	0.75	2199	25	2178	34	2189	22	0.95
007-ZR5	0.2153	59	0.0036	1.380	7085	39.18	0.13248	0.61	6.128	1.16	0.3355	0.91	0.79	2131	21	1865	30	1994	20	12.49
012-ZR9	0.0150	5	0.0019	0.634	100557	7.96	0.13644	0.72	7.450	1.17	0.3960	0.84	0.72	2183	25	2151	31	2167	21	1.46
019-ZR14	0.0397	29	0.0040	0.894	38154	41.47	0.13379	0.55	7.123	1.15	0.3861	0.94	0.82	2148	19	2105	34	2127	20	2.02
020-ZR15	0.0157	13	0.0025	0.446	95521	18.03	0.13773	0.65	8.344	1.53	0.4393	1.33	0.87	2199	23	2348	52	2269	28	-6.76
023-ZR18	0.0040	3	0.0043	0.437	373939	35.61	0.13432	0.57	7.389	0.95	0.3990	0.67	0.70	2155	20	2164	24	2160	17	-0.42
027-ZR20	0.0092	8	0.0040	0.767	164988	16.44	0.13477	0.39	7.264	1.07	0.3909	0.92	0.86	2161	14	2127	33	2144	19	1.58
028-ZR21	0.0234	9	0.0016	0.463	64388	19.42	0.13795	1.13	7.924	1.65	0.4166	1.15	0.70	2202	39	2245	44	2222	30	-1.96
029-ZR22	0.0150	5	0.0020	0.701	100973	9.21	0.13445	0.73	7.313	1.11	0.3945	0.75	0.67	2157	25	2143	27	2150	20	0.62
004-ZR2	0.2796	63	0.0038	0.548	5454	13.46	0.13759	0.56	6.439	1.02	0.3394	0.77	0.75	2197	19	1884	25	2038	18	14.26
008-ZR6N	0.1112	172	0.0054	0.751	13738	52.76	0.15190	0.95	6.857	1.84	0.3274	1.53	0.83	2367	32	1826	48	2093	32	22.88
010-ZR7	0.3199	61	0.0025	0.544	4745	20.20	0.14270	0.66	7.253	1.25	0.3686	0.99	0.80	2260	23	2023	34	2143	22	10.50
011-ZR8	1.0227	307	0.0048	0.648	1501	14.06	0.16070	1.56	6.362	2.83	0.2871	2.33	0.82	2463	52	1627	67	2027	49	33.94
018-ZR13	0.9887	187	0.0038	0.760	1524	8.97	0.15407	0.80	8.733	1.38	0.4111	1.06	0.77	2392	27	2220	40	2310	25	7.18

[1] Conversion factor from mV to CPS is 62500000.
[2] Not corrected for common-Pb.
[3] Discordance calculated as (1-(^{206}Pb/^{238}U age/^{207}Pb/^{206}Pb age)) *100.
Decay constants of Steiger and Jäger (1977) were used.

4.4. Sm-Nd Isotopes

Samples of metakomatiite and metabasalt presented in this study have high $^{147}Sm/^{144}Nd$ ratios of 0.1835 to 0.2012 (Table 2), reflecting strong Sm/Nd fractionation. Nd model ages were not calculated for these samples as their evolution curves become sub-parallel to the mantle evolution curve, thus yielding unreliable ages. These samples form a tight cluster on a $^{147}Sm/^{144}Nd$ vs. $^{143}Nd/^{144}Nd$ diagram, without sufficient spread to yield an isochron (not shown). Therefore, we have calculated the initial values of ε_{Nd} for our samples of metakomatiite and metabasalt assuming t = 2998 Ma (Fortes et al., 2003) and obtained the positive values of +1.30 to +4.39.

The analyzed sample of meta-andesite has a $^{147}Sm/^{144}Nd$ ratio of 0.1917, substantially higher than those of the metadiorites ($^{147}Sm/^{144}Nd$ = 0.1440 – 0.1444). We have hence calculated two-stage Nd model ages (T_{2DM}; Liew and Hofmann, 1988) for those samples and obtained coherent and homogeneous values of 2.28 – 2.26 Ga. Single-stage Nd model ages (T_{DM}; De Paolo, 1981, 1988) are also presented in Table 2 for comparison. The values of T_{DM} and T_{2DM} are similar for the metadiorites (T_{DM} = 2.24 Ga; T_{2DM} = 2.25 Ga) but differ significantly for the meta-andesite sample (T_{DM} = 2.52 Ga; T_{2DM} = 2.28 Ga). A three-point isochron provided by the samples of meta-andesite and metadiorite yields an age of 2117 ± 50 Ma (MSWD = 0.24) (not shown). We opted to calculate the initial values of ε_{Nd} for all samples of meta-andesite and metadiorite at t = 2172 Ma (U-Pb zircon age of the meta-andesite presented in this study) and obtained positive values between +2.34 and +2.69 (Table 2).

Table 2. Sm-Nd data of the metaigneous rocks of the Crixás greenstone belt.

Sample	Type	Sm (ppm)	Nd (ppm)	$^{147}Sm/^{144}Nd$	$^{143}Nd/^{144}Nd \pm 2\sigma$	t (Ma)	ƐNd (t) [1]	T_{DM} (Ga)[2]	T_{2DM} (Ga) [3]
CXSRGSRO1	Metakomatiite	2.753	9.070	0.1835	0.512600 ± 13	2998	+4.39	-	-
PL-1	Pillowed metab.	3.814	11.863	0.1943	0.512710 ± 12	2998	+2.33	-	-
CPIVESD0016-3	Metabasalt	2.319	7.181	0.1952	0.512750 ± 9	2998	+2.79	-	-
CPIVESD0016-8	Metabasalt	2.698	8.231	0.1982	0.512733 ± 14	2998	+1.30	-	-
CPIVESD0029-1	Metabasalt	3.213	9.820	0.1978	0.512795 ± 14	2998	+2.65	-	-
CPIVESD0031-114	Metabasalt	2.473	7.432	0.2012	0.512831 ± 16	2998	+2.06	-	-
CPIVESD0031-186	Metabasalt	1.794	5.550	0.1954	0.512804 ± 11	2998	+3.77	-	-
CPIVESD0035-7	Metabasalt	3.120	9.817	0.1921	0.512752 ± 18	2998	+4.03	-	-
MVA-1	Meta-andesite	2.428	7.657	0.1917	0.512686 ± 11	2172	+2.34	2.52	2.28
MN3EUD008-8	Metadiorite	5,165	21,616	0.1444	0.512027 ± 3	2172	+2.69	2.24	2.26
MN3EUD0013-6	Metadiorite	4,923	20,665	0.1440	0.512020 ± 5	2172	+2.67	2.24	2.26

[1] Initial values of ƐNd were calculated at t = 2998 Ma (Fortes et al., 2003) for the metakomatiites and metabasalts, and at t = 2172 Ma (this study) for the meta-andesites and metadiorites.
[2] Nd model ages were calculated using the model of DePaolo (1981, 1988).
[3] Two-stage model ages were calculated following Liew and Hofmann (1988).
Present-day reference values for CHUR: $^{147}Sm/^{144}Nd = 0.1967$ and $^{143}Nd/^{144}Nd = 0.512638$ (Jacobsen and Wasserburg, 1980).

4.5. Re-Os Isotopes

Whole-rock Re-Os data of the metabasalt samples of the Crixás greenstone belt show large variation in the Re and Os concentration (Re = 1.23 – 0.27 ppb; Os = 0.27 – 0.04 ppb), and especially in the isotopic ratios ($^{187}Re/^{188}Os = 409.8 – 17.96$; $^{187}Os/^{188}Os = 18.24 – 0.86$) (Table 3). The analyzed sample of metakomatiite possesses lower Re and higher Os contents (0.12 ppb and 0.53 ppb, respectively), and substantially lower $^{187}Re/^{188}Os$ and $^{187}Os/^{188}Os$ ratios (1.11 and 0.15, respectively) (Table 3). Samples display a negative correlation between Re and Os (Fig. 10a), and a relatively good-fitting regression on a $^{187}Re/^{188}Os$ vs. $^{187}Os/^{188}Os$ plot. The isochron yielded a 2609 ± 65 Ma age (MSWD = 7; n = 5) and an initial $^{187}Os/^{188}Os$ ratio of -0.0085 ± 0.082 (Fig. 10b).

Three analyses were conducted in arsenopyrite samples (Table 4). The Os budget of the analyzed arsenopyrite separates is almost exclusively radiogenic (Rad. Os ~ 100 – 99%), and can be classified as "low-level highly radiogenic sulfides" (sulfide samples that can be evaluated similarly as molybdenite, i.e. very low common Os in relation to their high radiogenic ^{187}Os content resulting from decay of Re; see Stein et al., 2000). As the common Os is virtually absent relative to the radiogenic ^{187}Os in these minerals, a single analysis may provide accurate and geological meaningful ages, much like the approach used for the molybdenite geochronometer (Stein et al., 2000; 2014). Thus, Re-Os data in Table 4 are pre-

sented in terms of ^{187}Re and ^{187}Os concentrations, and age could be calculated for each analysis. Arsenopyrite from ASPY1 sample (Re = 0.032 ppm; Os = 0.72 ppb) is more enriched in both Re and Os when compared to arsenopyrite from ASPY2 sample (Re = 0.010 – 0.009 ppm; Os = 0.18 – 0.15 ppb). A single analysis for the ASPY1 sample provided a 2137 ± 11 Ma age. For the ASPY2 sample, two analyses provided largely varied and younger ages of 1893 ± 9 and 1367 ± 7 Ma.

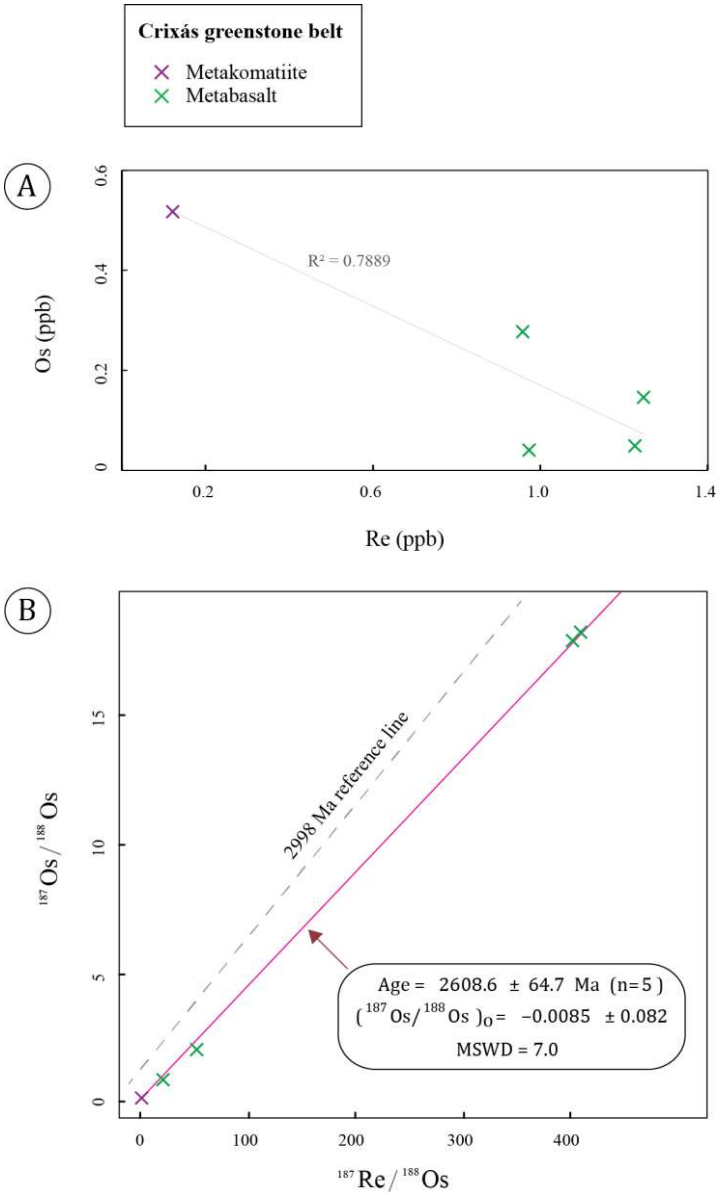

Fig. 10. Re vs. Os (A) and $^{187}Re/^{188}Os$ vs. $^{187}Os/^{188}Os$ (B) plots for the metakomatiite and metabasalt samples of the Crixás greenstone belt. Isochron (Model 3) was built using IsoplotR toolbox (Vermeesch, 2018).

Table 3. Re-Os data of ultramafic and mafic metavolcanic rocks of the Crixás greenstone belt.

Sample	Type	Re (ppb)	Os (ppb)	$^{187}Re/^{188}Os$	2σ (abs)	$^{187}Os/^{188}Os$	2σ (abs)	Rho	γOs (t = 2998 Ma)	T_{MA} (Ga)
CXSRGSRO1	Metakomatiite	0.12	0.53	1.110	0.056	0.150	0.006	0.38	-101	1.93
CPIVESD0031-170	Metabasalt	1.25	0.15	51.622	0.927	2.062	0.050	0.57	-169	2.23
CPIVESD0031-171	Metabasalt	0.95	0.28	17.960	0.258	0.859	0.014	0.54	-117	2.45
CPIVESD0031-121	Metabasalt	0.97	0.04	409.852	5.401	18.242	0.233	0.55	-386	2.60
CPIVESD0031-506	Metabasalt	1.23	0.05	402.404	5.462	17.934	0.351	0.42	-378	2.60

Table 4. Re-Os data of arsenopyrite grains of the Crixás greenstone belt.

Sample	Type	Re (ppm)	^{187}Re (ppm)	^{187}Os (ppb)	Re-Os age (Ma)
ASPY-1	Arsenopyrite 1	0.0316	0.0198	0.7207	2137 ± 11
ASPY-2A	Arsenopyrite 2	0.0090	0.0056	0.1806	1893 ± 9
ASPY-2B	Arsenopyrite 2	0.0103	0.0065	0.1496	1367 ± 7

5. Discussion

5.1. Element Mobility

The rocks of the Crixás greenstone belt have undergone metamorphism with a peak at amphibolite facies and various extent of hydrothermal alteration (e.g. silicate and carbonate alteration) that were responsible for the replacement of the original igneous mineralogy and stabilization of newly formed mineral phases. Therefore, even though in this work we have tried to carefully sample the most well-preserved rocks, it is necessary to discuss the alteration processes and the extent to which the chemical composition of the metaigneous rocks of the Crixás greenstone belt might reflect the primary composition of their protoliths and provide petrogenetic information.

Loss on ignition associated with the metakomatiites are variable and possess the highest values (LOI = 4 – 10 wt%; Supplementary Material 2), consistent with varying degrees of volatile component enrichment due to the formation of hydrated metamorphic assemblies (e.g chlorite, tremolite, talc, and serpentine). Two samples show minor positive anomalies of Eu (Eu/Eu* = 1.21 – 1.23) (Fig. 7a), which, when occurring in ultramafic rocks, has been generally attributed to post-magmatic alteration (e.g. Siepierski and Ferreira Filho, 2016; Singh et al., 2019). Highly altered igneous rocks also frequently show Ce anomalies, which could indicate LREE mobility (Polat and Hofmann, 2003). Nevertheless, Ce anomalies are not present in samples of metakomatiites of the Crixás greenstone (Fig. 7a). The metabasalts have generally low and homogeneous loss on ignition, ranging from 0.72 – 3.19 wt%, but mostly around 1 - 2 wt% (Supplementary Material 2). The metadiorites are also associated with low LOI values, ranging from 0.48 – 3.04 wt%, but largely lower than 1 wt% (Supplementary Material 2). On the other hand, the samples of meta-andesite show higher LOI (3.39 – 4.29 wt%; Supplementary Material 2), indicating volatile component enrichment, likely related to hydrothermal alteration, which is consistent with the common presence of secondary minerals (carbonate, sulfides, and rutile), explicit in petrographic analysis (Fig. 5f). Among all mafic and intermediate rocks, only two samples of metabasalt have slightly positive Ce anomalies (Ce/Ce* = 1.19 and 1.22).

Major and trace elements were plotted vs. Zr (Fig. 11 and 12), one of the most immobile elements, which is useful to understand igneous differentiation and post-magmatic alteration. In general, SiO_2 and Al_2O show a good to moderate positive correlation with Zr, MgO show a good negative correlation, while Fe_2O_3, CaO, K_2O, and Na_2O data are highly dispersed, showing weak to no correlation with Zr.

Distinct trends are evidenced on the TiO_2 vs. Zr plots: A good positive correlation is shown for the metakomatiites and metabasalts, and a weak negative correlation is shown for the meta-andesites and metadiorites (Fig. 11). A strong positive correlation of selected trace elements (Th, Nb, La, Sm, Lu, and Y) vs. Zr is evidenced in Fig. 12, while Cr and Ni show fairly negative trends with Zr, as expected. Zr also correlates moderately well with Re (positive correlation; Fig. 13a) and Os (negative correlation; Fig. 13c) in the samples of ultramafic and mafic rocks analyzed for Re-Os isotopes. Furthermore, different trends are highlighted by some trace elements (especially Th and La) vs. Zr, distinguishing a low-slope trend defined by the metakomatiites and metabasalts, and a higher slope trend defined by the meta-andesites and metadiorites. It is worth noting that the meta-andesite samples do not share a continuous trend with the metadiorite samples in some trace element bivariant plots (Th, Lu, and Y vs. Zr) (Fig. 12).

Trace element distribution on the chondrite- and primitive mantle-normalized diagrams of each group of samples consistently show relatively smooth and coherent patterns (Fig. 7 and 8). With all those considerations, we believe that even some major elements of the metaigneous rocks of the Crixás greenstone belt have experienced limited post-magmatic remobilization (e.g. Al_2O_3, TiO_2, and MgO). However, the relatively immobile trace elements (e.g. the REE and HFSE) appear to reflect the original composition of the protoliths more accurately and, therefore, will be emphasized in this work for subsequent petrogenetic interpretations and discussions. Careful must be taken, nevertheless, for the samples of meta-andesite, as they showed the highest aspects of alteration.

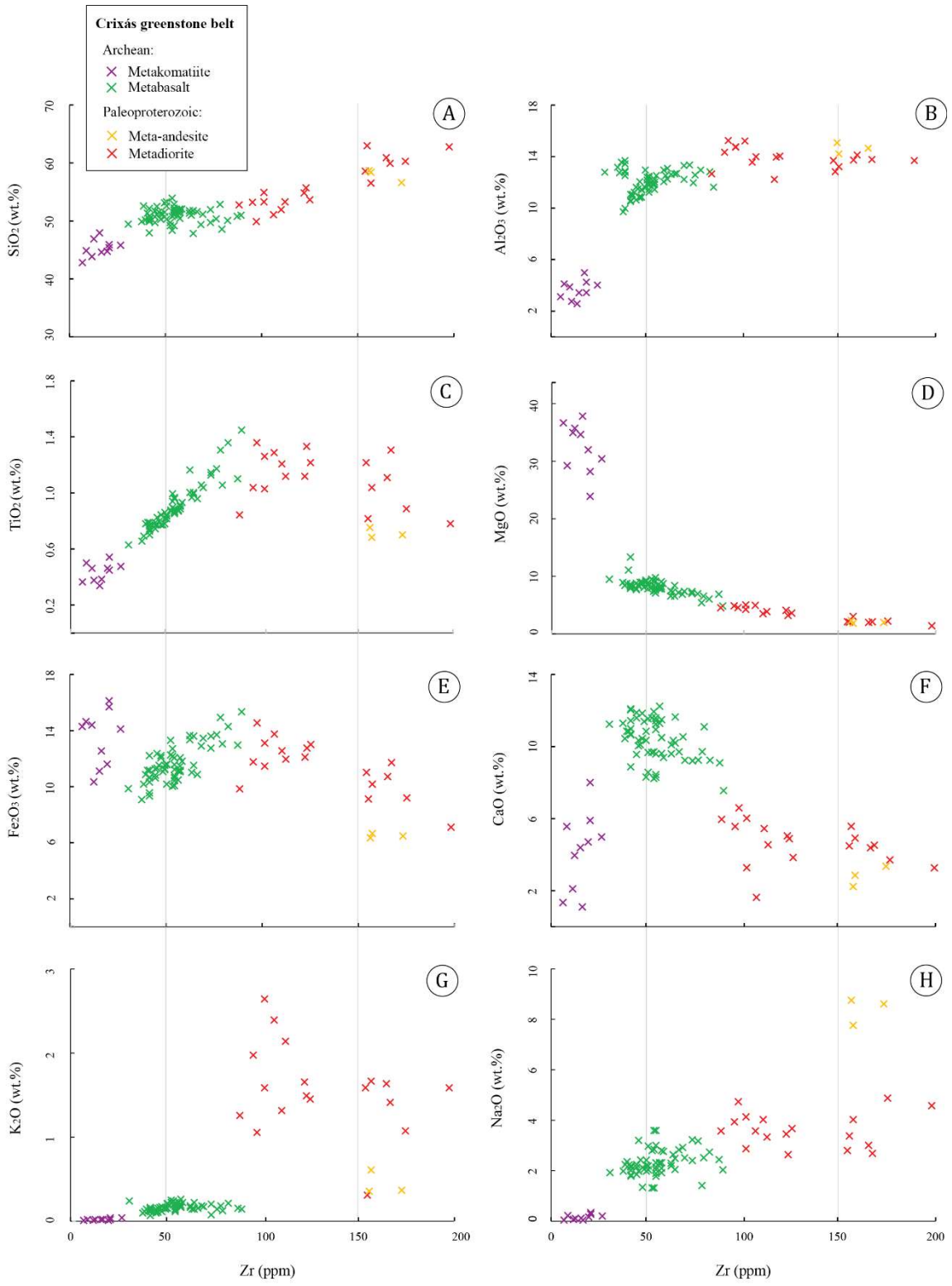

Fig. 11. Plots of Zr vs. major elements for the metakomatiites, metabasalts, meta-andesites, and metadiorites of the Crixás greenstone belt.

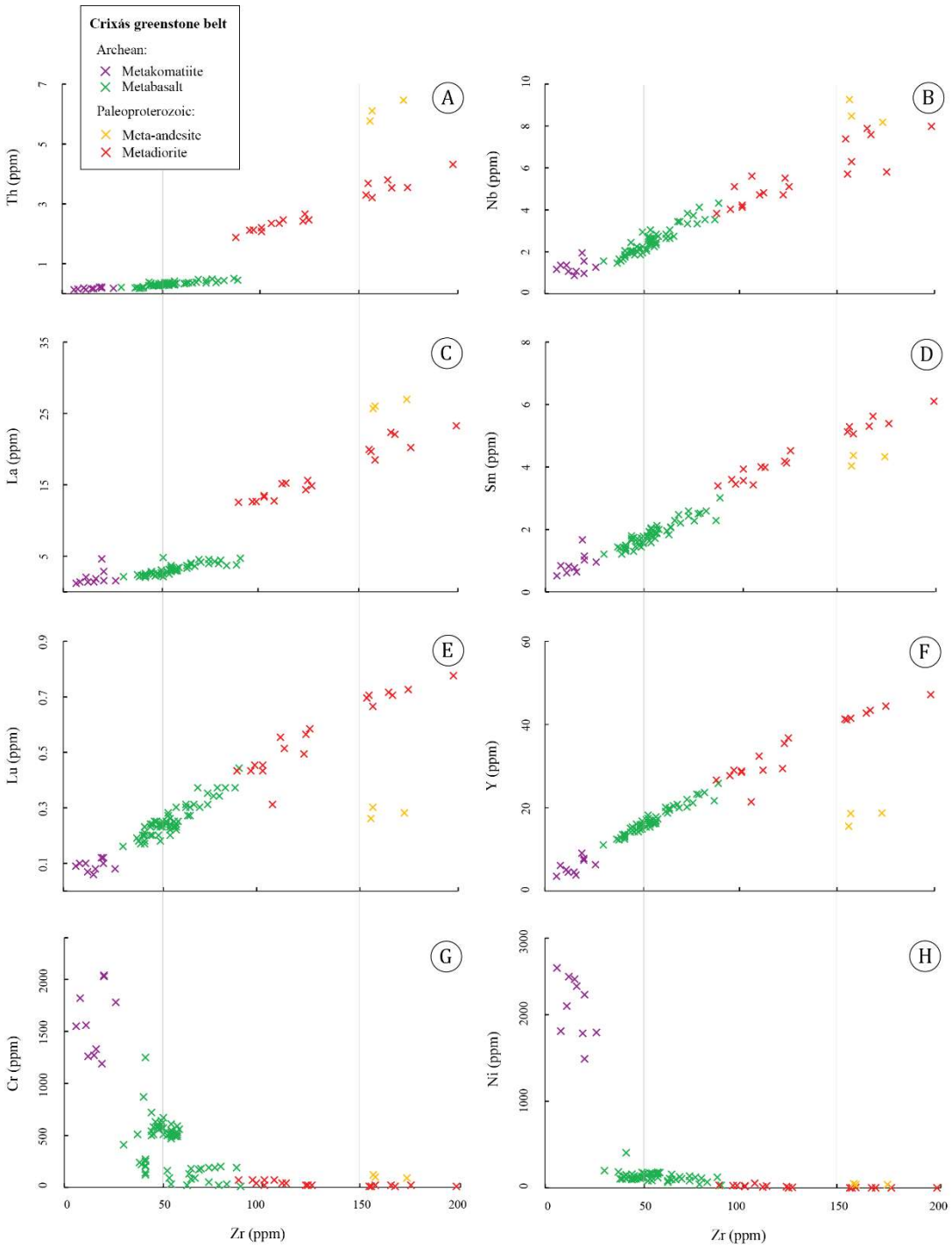

Fig. 12. Plots of Zr vs. selected trace elements for the metakomatiites, metabasalts, meta-andesites, and metadiorites of the Crixás greenstone belt.

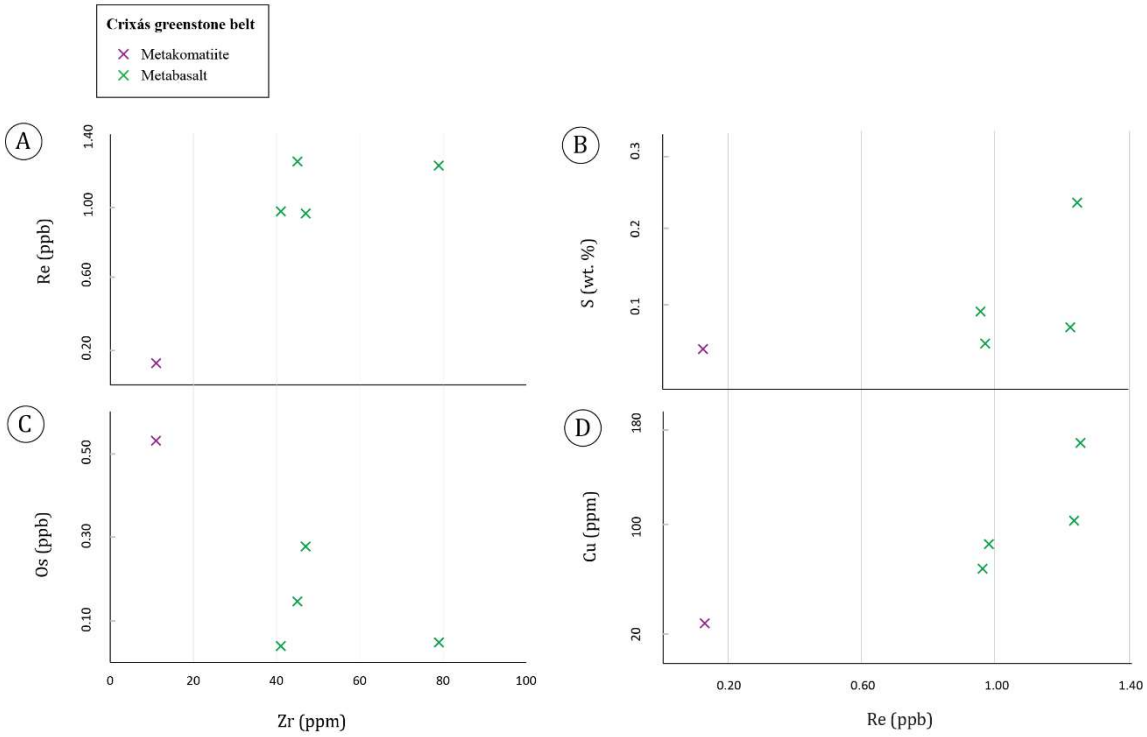

Fig. 13. Bivariant plots of Zr vs. Re (A) and Os (B), and Re vs. S (C) and Cu (D) for samples of the metakomatiite and metabasalt of the Crixás greenstone belt.

5.2. Re-Os Isotopic Systematics of the Ultramafic-Mafic Metavolcanic Rocks and Arsenopyrite of the Crixás Greenstone Belt: Geochronological Constraints

5.2.1. *Ultramafic-Mafic Metavolcanic Rocks*

Re-Os isotopic systematics of mantle-derived peridotites and volcanic rocks, which are strongly controlled by the presence of sulfide minerals in those rocks, trace the isotopic evolution of the mantle through time and give potential information on ancient melt-depletion events (Carlson 2005). High-precision data have been increasingly reported for several lower- to medium-grade komatiites and basalts in worldwide greenstone belts.

For instance, the Late Archean komatiites of Western Australia define a whole-rock Re-Os isochron with an age with a close agreement with robust previous U-Pb zircon ages (~2.7 Ga) and a near-chondritic initial $^{187}Os/^{188}Os$ (0.10889 ± 0.00035), showing that the Re-Os system remained closed since the emplacement of the volcanic flows (Foster et al., 1996). Re-Os elemental systematics were also shown to be a primary magmatic feature of many ca. 2.7 Ga komatiites in the Abitibi greenstone belt, even after large-scale alteration and lower greenschist metamorphism, where samples display Re-Os isochron age in general

agreement with previously determined U–Pb zircon ages of associated felsic rocks and also with Sm-Nd and Pb–Pb isochron ages of the same flows (Gangopadhyay and Walker, 2003). Komatiites, komatiitic basalts, and chromite separates of the Abitibi greenstone belt display essentially chondritic initial Os isotopic composition (Gangopadhyay and Walker, 2003; Gangopadhyay et al., 2005; Puchtel et al., 2009), which has also been reported in the ca. 2.7 Ga komatiites of the Belingwe greenstone belt (Puchtel et al., 2009), ca. 3.48 – 3.26 Ga komatiites of the Komati and Weltevreden systems in the Barberton greenstone belt (Puchtel et al., 2014), and many others. Thus, it has been suggested that the combined Re-Os data of komatiites indicate that the mantle sources of most Archean mantle-derived rocks evolved with essentially uniform long-term Re/Os ratios within the chondritic range, and are similar to the chondritic composition of the contemporaneous convective upper mantle (Gangopadhyay and Walker, 2003; Gangopadhyay et al., 2005; Puchtel et al., 2014).

Exceptions occur, however, as pointed out by the Re-Os systematics of ultramafic-hosted chromites from the Isua supracrustal belt (West Greenland), one of the oldest oceanic crust remnants on Earth, that roughly display a suprachondritic initial $^{187}Os/^{188}Os$ composition at ca. 3.81 Ga (average $\gamma_{Os} = +1.3 \pm 2.5$), possibly related to enriched subduction components or core-mantle interaction (Frei and Jensen, 2003), and also by komatiites from the Kostomuksha greenstone belt in the Baltic Shield, characterized by a coupled ^{186}Os–^{187}Os enrichment at the time of lava emplacement at ca. 2.8 Ga ($\gamma_{Os} = +2.5 \pm 0.6$), which origin has been linked to the outer core in a rising mantle plume context (Puchtel et al., 2005). Enrichment related to crustal contamination is also sensitively monitored by the Re-Os isotopic system as Os is highly concentrated in the mantle relative to crustal rocks. Thus, the continental crust evolves with high Re/Os ratios and, consequently, high radiogenic Os in comparison to mantle-derived rocks. Lahaye et al., 2001 reported that the ca. 2.7 Ga komatiites associated with Ni-Cu sulfide deposits from Alexo, Texmond, and Hart in the Abitibi greenstone belt have highly radiogenic Os isotopic composition ($\gamma_{Os} = +20.2$ and $+33.2$), suggesting that the ultramafic flows were contaminated by crustal-derived materials, likely Os-rich black shales.

The large variation on the Re and Os contents (Re = 1.23 – 0.12 ppb; Os = 0.53 – 0.04 ppb) (Table 3) of our samples of metakomatiite and metabasalt of the Crixás greenstone belt are within the range of the average Re and Os concentrations of komatiites and basalts (Shirey and Walker, 1998; Carlson 2005). However, the isotopic ratios ($^{187}Re/^{188}Os = 409.8 – 1.11$; $^{187}Os/^{188}Os = 18.24 – 0.15$) (Table 3) are substantially higher than those shown by the komatiites and basalts that have been interpreted to reflect their primary magmatic com-

position ($^{187}Os/^{188}Os$ generally lower than 0.20; e.g. Pegram and Allègre, 1992; Gangopadhyay and Walker, 2003; Gangopadhyay et al., 2005; Puchtel et al., 2014). Our samples provide substantially varied T_{MA} (^{187}Os model-ages calculated in reference to a chondritic mantle evolution curve; Shirey and Walker, 1998) of 2.60 – 1.93 Ga (Table 3). Initial values of γ_{Os} calculated at the currently most cited age estimate for the ultramafic-mafic volcanism of the Crixás greenstone belt (t = 3.0 Ga; Fortes et al., 2003) are also varied and range from -101 and -386 (Table 3).

These features could suggest that the original Re-Os isotopic composition of the ultramafic-mafic metavolcanic rocks of the Crixás greenstone belt has not remained undisturbed since the eruption. This is a common situation as many rocks are often susceptible to various extents of open-system behavior of the Re-Os isotopes due to a range of post-magmatic processes. For example, matrix ore and mineral separates from the Alexo komatiites of the Abitibi greenstone belt are aligned along a 1.2 Ga reference isochron, which is related to a Re-Os disturbance during the Greenville orogeny (Lahaye et al., 2001). Whole-rock Re-Os systematics of Archean-Paleoproterozoic komatiite-hosted Ni-Cu-PGE sulfide deposits in Finland indicates resetting of the Re-Os isotopic system at ~1.87-1.83 Ga as a consequence of the Svecofennian orogeny (Moilanen et al., 2019). In the western-northwestern sector of the Isua belt, whole-rock Re-Os data have extremely varied γOs (ranging from -8500 to +9), which were interpreted to reflect early to late Archean metamorphic events associated with the emplacements of tonalites into the supracrustal sequences and consequently Re-additions carried by metasomatic fluids (Frei and Jensen, 2003).

When plotted in bivariant diagrams that could give further shreds of evidence of possible element mobility, the samples of the Crixás greenstone belt display a moderate negative correlation between Re and Os (Fig. 10a), a moderate positive correlation between Zr and Re (Fig. 13a), and a negative correlation between Zr and Os (Fig. 13c). Positive correlations are also present with Re vs. S (Fig. 13b) and Cu (Fig. 13d) contents, indicating that its abundance is controlled by sulfides in the rocks (mostly chalcopyrite). A relatively good-fitting regression is shown on a $^{187}Re/^{188}Os$ vs. $^{187}Os/^{188}Os$ plot, yielding an isochron age of 2609 ± 65 Ma (MSWD = 7; n = 5) with an initial $^{187}Os/^{188}Os$ ratio of -0.0085 ± 0.082 (γ_{Os} = -100) (Fig. 10b), suggesting the absence of initial radiogenic Os in the system at ~2.6 Ga. A 2998 Ma reference line (assuming a chondritic initial Os isotopic composition of the volcanic protoliths) was also plotted in Fig. 10b for comparison. This reference isochron refers to the presumable age of the ultramafic-mafic volcanic flows of the Crixás greenstone belt (based on a Sm-Nd "errochron" presented by Fortes et al., 2003).

In this sense, one possible interpretation is that the 2609 ± 65 Ma age provided by the whole-rock Re-Os isochron (Fig. 10b) indicates the timing of a hydrothermal-metasomatic event associated with Re addition that overprinted the original Re-Os isotopic composition of the protoliths. If this assumption is correct, it brings direct implications for the age of the ultramafic-mafic volcanism itself, since the ~2.6 Ga metasomatic event confirms that the hosting metavolcanic rocks are older, favoring previous suggestions of a Mesoarchean age for the volcanism (Arndt et al., 1989; Fortes et al., 2003). The youngest Archean granodiorites and granites of the region were emplaced at ~2709-2704 Ma (Queiroz et al., 2008), marking the late stages of the Neoarchean cratonization of the block, which remained stable until the Paleoproterozoic (Jost et al., 2014; Borges et al., 2021). Considering the age uncertainty of the Re-Os isochron, it could be argued that the ~2.6 Ga hydrothermal-metasomatic event in the ultramafic-mafic volcanic rocks of the Crixás greenstone belt reflects the late stage of this continental amalgamation period and was responsible for the Neoarchean isotopic resetting of the Re-Os system.

It is nevertheless important to stress that limitations to this interpretation arise when we consider the possibility that the Re-Os isochron provided by the metakomatiite and metabasalt samples (Fig. 10b) could represent a mixing line between sulfides of different generations at whole-rock scale, as the Archean rocks in the region has also been affected by orogenic events in the Paleoproterozoic (Borges et al., 2021) and Neoproterozoic (Pimentel et al., 2003; Queiroz et al., 2008; Jost et al., 2013).

5.2.2. Arsenopyrite

The Re-Os age provided by the coarse-grained arsenopyrite separates of sample ASPY1 (2137 ± 11; Table 4) (Fig. 4) is similar to the Re-Os age (2126 ± 16) of the arsenopyrite grains analyzed by Marques et al. (2013), which was collected in massive sulfide lenses of the Crixás greenstone belt, thus supporting a Rhyacian age for the arsenopyrite and gold mineralization, and also constraining a minimum depositional age for the hosting metasedimentary rocks (see Borges et al., 2021). Our Re-Os data for the two analyses of arsenopyrite separates from sample ASPY2 (Fig. 4) are somewhat varied and younger (1893 ± 9 and 1367 ± 7 Ma). Arsenopyrite from this sample is disseminated, oriented, and deformed with the hosting metasedimentary rock, thus indicating that the Re-Os isotopic system has not remained closed after the Rhyacian mineralization in some parts of the Crixás greenstone belt, yielding to local Re and/or Os loss due to metamorphism and deformation.

5.3. Metakomatiites and Metabasalts of the Crixás Greenstone Belt: Remnants of an Archean Oceanic Plateau

Chemical composition of the Crixás metakomatiites has been formerly examined by few studies (Arndt et al., 1989; Costa Jr et al., 1997; Kuyumjian and Jost, 2006), while geochemical data regarding the metabasalts are even more scarce (Kuyumjian and Araújo Filho, 1991). A peculiar feature observed by Arndt et al. (1989) is that the metakomatiites of the Crixás greenstone belt have "hump-shaped" chondrite-normalized REE patterns, with both depletion of LREE and HREE in the spinifex-textured horizons, contrasting from the cumulate zones of the same flows, that are more enriched in LREE. These unusual geochemical patterns were speculated by those authors to reflect element migration after hydrothermal alteration or metamorphism, even though those komatiites were still considered to be likely of the Al- and HREE-depleted type (Arndt et al., 1989), which was also suggested by Kuyumjian and Jost (2006).

Samples of metakomatiite investigated in our work have low ratios of Al_2O_3/TiO_2 (7 to 11) (Fig. 14), flat to enriched patterns of LREE (La/Sm_{cn} = 0.91 – 1.96), fractionated patterns of HREE (Gd/Yb_{cn} typically higher than 1.26, and reaching extreme values of 2.27) (Fig. 7a), and prominent negative anomalies of Zr and Hf on the primitive-mantle normalized diagram (Fig. 7b). These characteristics have striking similarities with those of the Al-depleted komatiites (ADK) (Arndt et al., 2008; Dostal, 2008) (Fig. 14). In contrast, when compared to the metakomatiites, the metabasalts of the Crixás greenstone belt have much varied and mostly higher Al_2O_3/TiO_2 ratios (8 - 23) (Fig. 14), display mostly flat patterns of LREE, with only a few samples showing LREE depletion or enrichment (La/Sm_{cn} = 0.78 – 1.66) (Fig. 7c), display near-flat to variably depleted patterns of HREE (Gd/Yb_{cn} = 1.20 – 1.60) (Fig. 7c), and lack the prominent negative anomalies of Zr and Hf on the primitive-mantle normalized diagram (Fig. 7d).

The above geochemical differences likely reflect a combination of heterogeneous mantle source, variable depth of mantle melting, and variable degree of partial melting. It is generally a consensus that the abundant occurrence of komatiites associated with high-Mg tholeiites implies anomalously hot melting temperatures (1600 – 1900º C) that have been linked to deep-seated anhydrous mantle plumes (e.g. Campbell et al., 1989; Campbell, 1998). We, therefore, suggest that the komatiites of the Crixás greenstone belt are the product of mantle melting of the anomalous hot core of the plume, at sufficient depth to retain residual majorite garnet in the source, whilst the basalts were formed by lower degrees of partial

melting at shallower depths (plume head), involving more depleted parts of the mantle. This interpretation is consonant with the zoned and heterogeneous mantle plume model to account for the origin of some genetically related komatiites and basalts in other greenstone belts (e.g. Campbell et al., 1989; Dostal and Mueller, 2013). Moreover, the occurrence of pillow lavas indicates submarine eruption.

On the Nb/Yb vs. Th/Yb discriminant diagram (Pearce, 2008), the metakomatiites and metabasalts of the Crixás greenstone belt form a cluster between the N-MORB and E-MORB components within the MORB-OIB array (Fig. 15). The metabasalts plot around the primitive mantle composition and the metakomatiites tend to plot closer to the E-MORB (Fig. 15). No imprint of subduction-derived fluids or crustal contamination is evidenced by neither metakomatiites and metabasalts on this diagram. This is consistent with the low Th/Nb ratios of the samples (~0.1), the lack of negative anomalies of Nb on the primitive mantle-normalized immobile trace element plot (Figs. 7b), the positive values of $\varepsilon_{Nd}(t)$ (Table 2), and the absence of inherited zircon xenocrysts (based on numerous attempts performed by the present authors to recover any zircon grain from those rocks). It is thus inferred that the komatiitic and basaltic lavas of the Crixás greenstone belt were not generated by melting of a subduction-zone metasomatized mantle wedge, and neither interacted with older continental crust.

Mantle domain components can be further investigated using the relationship between HFSE and REE ratios expressed on the diagrams of Fig. 16 (Condie, 2003, 2005). The metakomatiites and metabasalts of the Crixás greenstone belt plot predominantly in the oceanic plateau field (OPB) on the three diagrams. Metabasalt samples are arranged in clusters close to the primitive mantle composition (PM), whereas the metakomatiite samples are sparser. A distinct trend is visualized on the Nb/Th vs. Zr/Nb diagram, where some metakomatiite samples plot toward the OIB deep mantle component due to their low Zr/Nb ratios (Fig. 16a). A steep vertical trend from OPB toward N-MORB is present by the metabasalts on the La/Yb vs. Th/Ta diagram (Fig. 16b), which suggest a variable contribution of a shallow depleted mantle (DM) component, based on the low Th/Ta ratios of some mafic samples. Once more, the interelement ratios reveal the absence of interaction with continental crust or subcontinental lithosphere, since no samples of metakomatiite and metabasalt plot close to the enriched component (EN) (Fig. 16).

Oceanic plateaus are large areas of over-thickened (>30 km) ocean floor, which, unlike normal oceanic crust, are not a primary product of seafloor spreading. Instead, the formation of oceanic plateaus has been widely attributed to the decompression melting of hot mantle plumes (Kerr, 2014). Indeed, the mafic metavolcanic rocks of the Crixás greenstone

belt share many geochemical similarities with volcanic rocks of Phanerozoic oceanic plateaus. Most basaltic lavas from the Caribbean and Ontong Java plateaus typically possess flat chondrite-normalized REE patterns, often defined as T-MORB (transitional composition between the depleted and enriched types), whereas the high-magnesian lavas (picrites and komatiites) from the Caribbean Plateau are more chemically heterogeneous in terms of trace elements (Kerr et al., 2000; Revillon et al., 2000; Serrano et al., 2011). This is believed to reflect the heterogeneity of the mantle plume source, whilst the origin of the chemically homogeneous mafic lavas results from the entrapment of earlier primitive and heterogeneous magma either in the melting column or in large chambers and subsequent mixing, crystal fractionation, and homogenization (Kerr et al., 1997, 2000).

This correlation is also highlighted by the interrelation between the Th/Nb and Ce/Nb ratios, as visualized in Fig. 17, where the metabasalts and metakomatiites of the Crixás greenstone belt plot in the field defined by ultramafic and mafic volcanic rocks of the Caribbean Plateau. Several worldwide Archean and Proterozoic terranes have also been interpreted to contain fragments of oceanic plateaus, particularly regarding komatiites and tholeiites in greenstone belts, which origin has often been considered analogs to the modern representatives (e.g. Puchtel et al., 1998; Arndt et al., 2001; Condie et al., 2002; Chavagnac, 2004; Velásquez et al., 2011; Maier et al., 2013; Schneider et al., 2019).

5.4. Meta-andesites and Metadiorites of the Crixás Greenstone Belt: Records of a Rhyacian Magmatic Arc

The ca. 2.17 Ga meta-andesites and metadiorites of the Crixás greenstone belt present an obvious arc signature as evidenced by the HFSE depletion on the primitive mantle-normalized diagrams (Figs. 8b and 8d) and the trace element systematics on the tectonic discriminant diagrams of Figs. 15, 16, and 17. A juvenile character of the intermediate arc magmatism is indicated by the positive and homogeneous values of $\varepsilon_{Nd\,(t)} = +2.34$ to $+2.69$ (Table 2).

However, in addition to the mineralogical differences between the meta-andesites and metadiorites, some geochemical characteristics of the two groups are distinct: The meta-andesites display higher average SiO_2 and lower MgO than the metadiorites. The former is also more enriched in LREE and generally shows higher depletion of HREE than the metadiorites (Figs. 7c and 7e). Moreover, the meta-andesites and metadiorites do not share the sample trends on the bivariant plots of Zr vs. immobile trace elements (Fig. 12). Conjointly, these characteristics can indicate that the protoliths of the meta-andesites and metadiorites,

although likely cogenetic, might not represent the same parental magma batch and that the andesitic lavas represent a more evolved magma than the dioritic intrusions, denoting the variability of the magmatism of intermediate composition in the Crixás greenstone belt. However, as discussed earlier in this work, hydrothermal alteration could also have overprinted some of the major and trace element characteristics specifically of the meta-andesites.

The ca. 2.2 - 2.1 Ga is marked by crustal compression and is considered the main metallogenic epoch in the Crixás-Goiás Domain (Jost et al., 2010; 2014). It was interpreted by Borges et al. (2021) that the protoliths of the upper metasedimentary succession of the Crixás greenstone belt, consisting mostly of poorly-sorted metagraywackes and carbonaceous phyllites, are allochthonous and formed after rapid erosion of a rising juvenile Rhyacian magmatic arc and originally deposited as turbidites in a forearc or trench type basin. Unimodal age spectra of the detrital zircon U-Pb data performed by Borges et al. (2021) constrained the age range of the proximal arc source area, between 2213.4 ± 5.6 and 2162.2 ± 9.2 Ma, and the geochemical composition of the metagraywackes and carbonaceous phyllites indicated a mixed mafic and felsic provenance, which is also consistent with contribution from arc rocks of intermediate composition.

Interestingly, no known occurrences of extensive Rhyacian crust outcrop in the region of the Crixás-Goiás Domain. This has led to different interpretations regarding the origin of the Rhyacian provenance of the metasedimentary rocks of the Crixás greenstone belt. For instance, Jost et al. (2019) suggested an external arc source area occurring to the west of the Crixás-Goiás Domain, possibly the basement of the Araguaia or the Paraguay belts, while Cordeiro et al. (2014) suggested a provenance from the Campinorte Arc (Campinorte Domain), located at northeast of the Crixás-Goiás Domain (see Fig. 1).

Alternatively, Borges et al. (2021) interpreted that a distinct Rhyacian juvenile arc (named Crixás Arc) formed adjacent to the Archean paleocontinent of which the “proto” Crixás-Goiás Domain crust derived. *Syn*-orogenic sedimentary rocks were tectonically transported during docking of the intraoceanic arc onto the TTG-greenstone continental crust. The authors pointed out that the arc-related sedimentary basin occurring in the upper Crixás greenstone belt (and possibly also in the other greenstones of the Crixás-Goiás Domain) currently provides the best evidence of this Rhyacian orogeny since most of the magmatic arc was buried, eroded, or obliterated. Remnants of this arc magmatism are nonetheless possibly preserved as local outcrops of ca. 2.15 Ga diorites (Jost et al., 1993) and trondhjemites (Queiroz, 2000) within the Hidrolina TTG Complex and Pilar de Goiás greenstone belt, respectively. Queiroz (2000) also reported a ca. 2.15 Ga U-Pb SHRIMP age of metamorphic sphene from Archean tonalitic gneiss of the Caiamar Complex.

In summary, the ca. 2.17 Ga metadiorites and meta-andesites characterized in this work are suggested to represent the first documentation of Rhyacian magmatism within the Crixás greenstone belt tectonostratigraphy. These intermediate rocks can be correlated with the Rhyacian Crixás Arc (Borges et al., 2021), giving a further piece of evidence of the ca. 2.2 – 2.1 Ga crustal growth of the Crixás-Goiás Domain. This indicates that occurrences of Rhyacian arc-related magmatic rock remnants in the region of the Crixás-Goiás Domain are higher than previously thought, and it should be better recognized and detailed in the future with more work focused on geological mapping associated with geochronology.

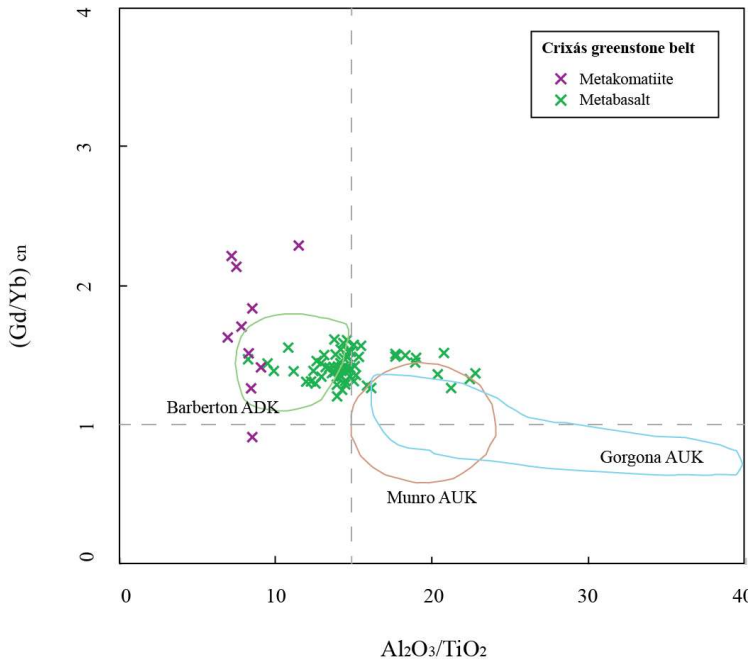

Fig. 14. Al_2O_3/TiO_2 vs. $(Gd/Yb)_{cn}$ classification diagram for the metakomatiites and metabasalts of the Crixás greenstone belt. Fields for the average composition of the Barberton (ADK), Munro (AUK), and Gorgona (AUK) komatiites are from Arndt et al (2008).

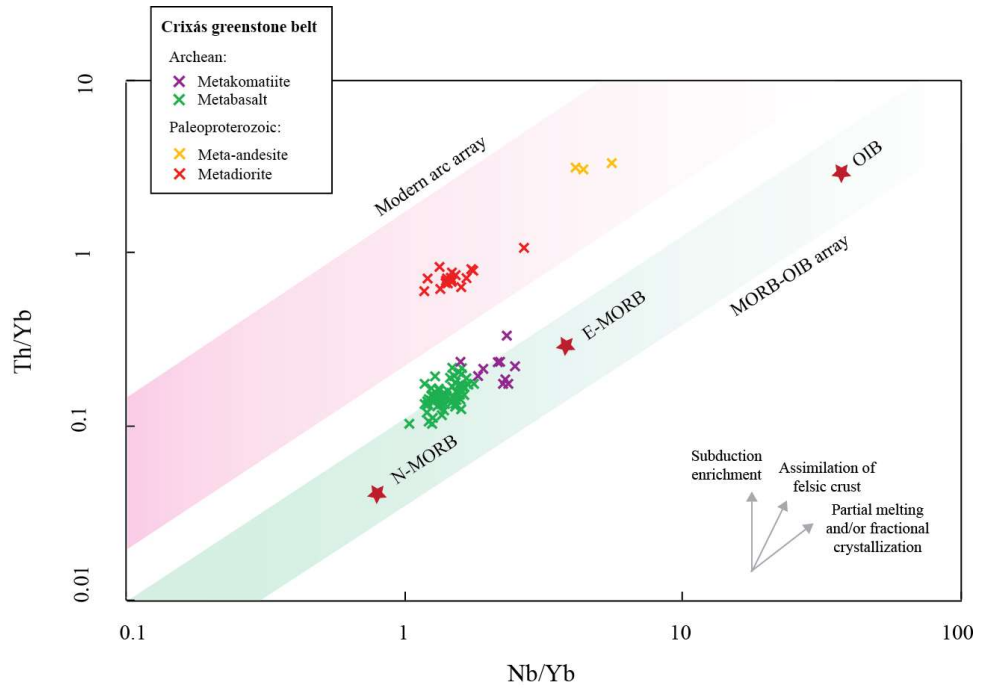

Fig. 15. Nb/Yb vs. Th/Yb tectonic discriminant diagram (Pearce, 2008) for the metaigneous rocks of the Crixás greenstone belt.

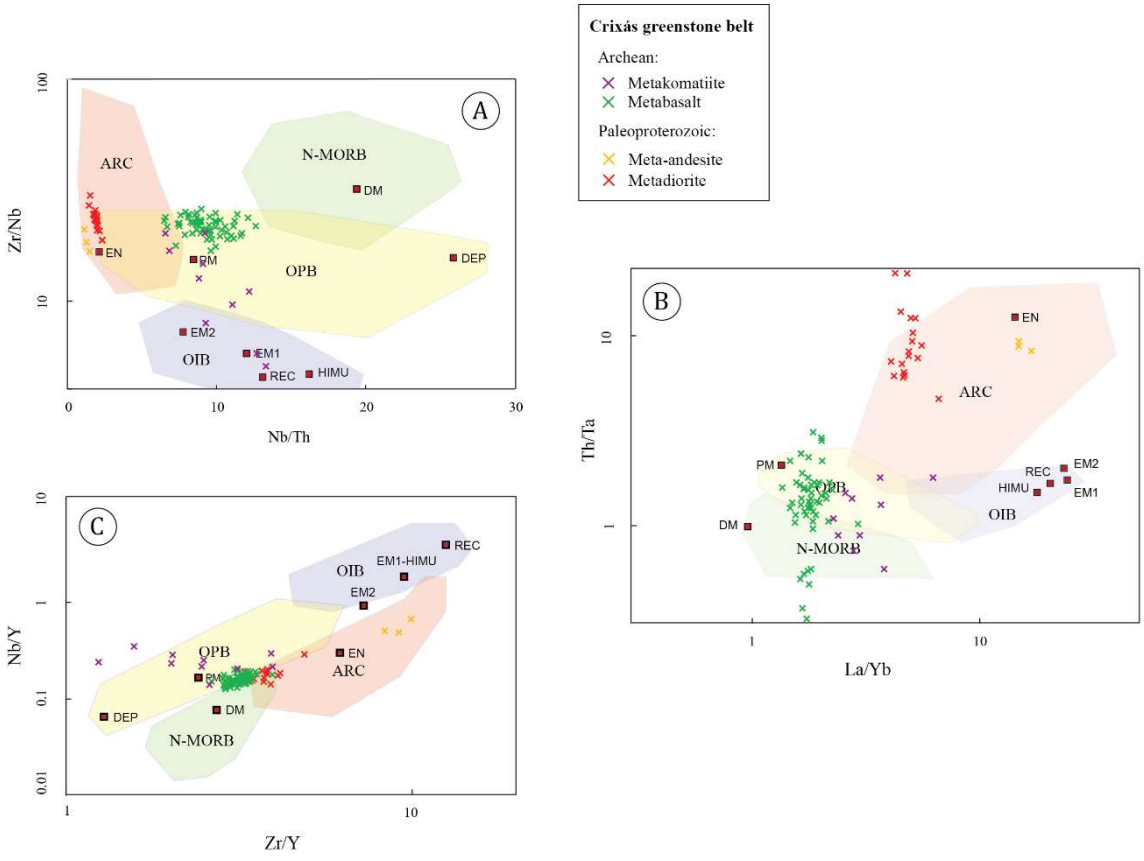

Fig. 16. Plots of the metaigneous rocks of the Crixás greenstone belt on the (A) La/Yb vs. Th/Ta, (B) Nb/Tb vs. Zr/Nb, and (C) Zr/Y vs. Nb/Y discriminant diagrams. Abbreviations: OPB (oceanic plateau basalts), ARC (arc-related rocks), N-MORB (normal ocean ridge basalts), OIB (oceanic island basalts), PM (primitive mantle), DM (depleted mantle),

HIMU (high mu U/Pb source), EM1 and EM2 (enriched mantle sources), DEP (deep depleted mantle), EN (enriched component), and REC (recycled component). References: Weaver (1991); Condie (2003, 2005).

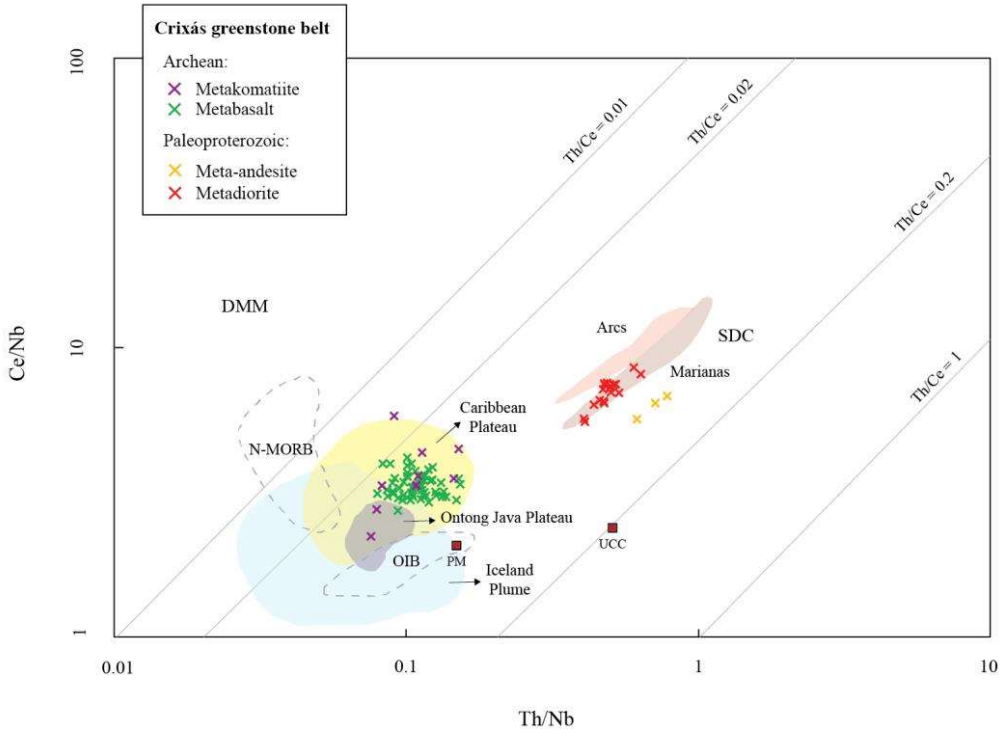

Fig. 17. Plots of the metaigneous rocks of the Crixás greenstone belt on the Th/Nb vs. Ce/Nb diagram (Saunders et al., 1988). Abbreviations: N-MORB (normal ocean ridge), OIB (oceanic island basalts), SDC (supra-subduction zone), DMM (depleted MORB mantle component), PM (primitive mantle), and UCC (upper continental crust). Compositional data of komatiites and basalts of the Caribbean Plateau are from Arndt et al. (1997), Revillon et al. (2000), and Hastie et al. (2008). Compositional data of basalts of the Ontong-Java Plateau are from Mahoney et al. (1993) and Fitton and Godard (2004).

5.5. Implications to the Evolution of the Crixás Greenstone Belt and the Northern Crixás-Goiás Domain

The above discussions have characterized two different units of rocks formed in distinct tectonic settings in the Crixás greenstone belt: i) A Mesoarchean (~3.0 – 2.8 Ga; Arndt et al., 1989; Fortes et al., 2003) plume-related komatiites and basalts (high-Mg tholeiites) with a strong oceanic affinity, interpreted to have formed in an oceanic plateau environment, and ii) a juvenile Paleoproterozoic (Rhyacian) magmatic arc assembly comprising andesites, diorites, and *syn*-orogenic poorly-sorted immature sedimentary rocks deposited in an arc-related basin (Borges et al., 2021; this work). Despite being genetically and temporal unrelated, those rocks are spatially associated (Fig. 2b), and their

structural framework indicates stacking and imbrication as an outcome of horizontal accretionary tectonics and multiple thrusting (Fig. 2d). Furthermore, those units are allochthonous and override an Archean crustal basement dominated by granites and gneisses of mostly TTG composition.

Oceanic plateaus are substantially thicker and more buoyant than normal oceanic crust and often interact with subduction zones. During this interaction, buoyant oceanic plateaus typically resist subduction and are readily accreted onto the margins of continents. It is believed that these terrains have performed an important contribution to the continental crustal growth throughout Earth's history as accretionary processes favor the preservation of dismembered oceanic plateaus in the geological record (Kerr and Mahoney, 2007; Kerr et al., 2000, Kerr, 2015).

In this context, assuming that uniformitarian processes have operated since the Archean, we propose a geological evolution model for the Crixás greenstone belt and the northern Crixás-Goiás Domain as follows (Fig. 18): A Mesoarchean oceanic plateau was formed above an upwelling mantle plume and accreted to the Archean granite-gneissic complexes of the northern part of the Crixás-Goiás Domain, although the exact timing of this accretion can only be roughly estimated between 2.8 and 2.7 Ga, on the basis of the current geochronological data. Polydeformed granite-gneissic complexes of the northern part of the Crixás-Goiás Domain (Fig. 2a) record a dominant juvenile stage of TTG magmatism emplaced at ca. 2.84 – 2.78 Ga. However, the existence of older sialic crust is indicated by inherited zircon xenocrysts as old as 3.3 Ga identified in the hosting Mesoarchean orthogneisses (Queiroz et al., 2008). The juvenile crustal growth stage was followed by ca. 2.71 Ga granitic magmatism characterized by crustal rework in the Moquém Complex, interpreted as the final stage of the orogenic systems. Titanite grains hosted in ca. 2.82 Ga orthogneisses were dated at ca. 2.71 Ga, constraining the age of the final Archean metamorphism and deformation, which was interpreted by Queiroz et al. (2008) to register the cratonization period of the region. Considering the associated error, we believe that this period is also related to the hydrothermal-metasomatic event that overprinted the original Re-Os systematics of the ultramafic-mafic metavolcanic rocks of the Crixás greenstone belt, which records a ~2.6 Ga isochron.

After the cratonization of the Archean crustal segment of the Crixás-Goiás Domain, the region remained stable until the Siderian, when it experienced extensional regime after regional uplift and cooling, marked by intrusions of NE (and less frequent NW) high- and low-Ti mafic dike swarms derived from a heterogeneous mantle source and crystallized at ca. 2.49 Ga (Corrêa da Costa and Girardi, 2005; Corrêa da Costa et al.,

2006). In the Rhyacian, the Crixás-Goiás Domain was involved in an important convergent process that can be correlated with the Paleoproterozoic amalgamation of the Goiás Massif, during successive collages of arc-related terranes (see Cordeiro et al., 2017; Martins-Ferreira et al., 2020; Borges et al., 2021). As proposed by Borges et al. (2021), a ca. 2.2 -2.1 Ga magmatic arc (Crixás Arc) was formed in an intraoceanic setting and collided with the Archean paleocontinent referred to in this work as the proto-crust of the Crixás-Goiás Domain (consisted of Meso-Neoarchean granite-gneisses and Mesoarchean ultramafic-mafic volcanic flows of the greenstone). Arc-continent collision was accompanied by accretion and tectonic transport of the magmatic arc units onto the Archean continental crust, resting on the older terranes. This is also the main metallogenic epoch in the region, as shown by Re-Os ages of gold-related arsenopyrite (Marques et al., 2013; this work).

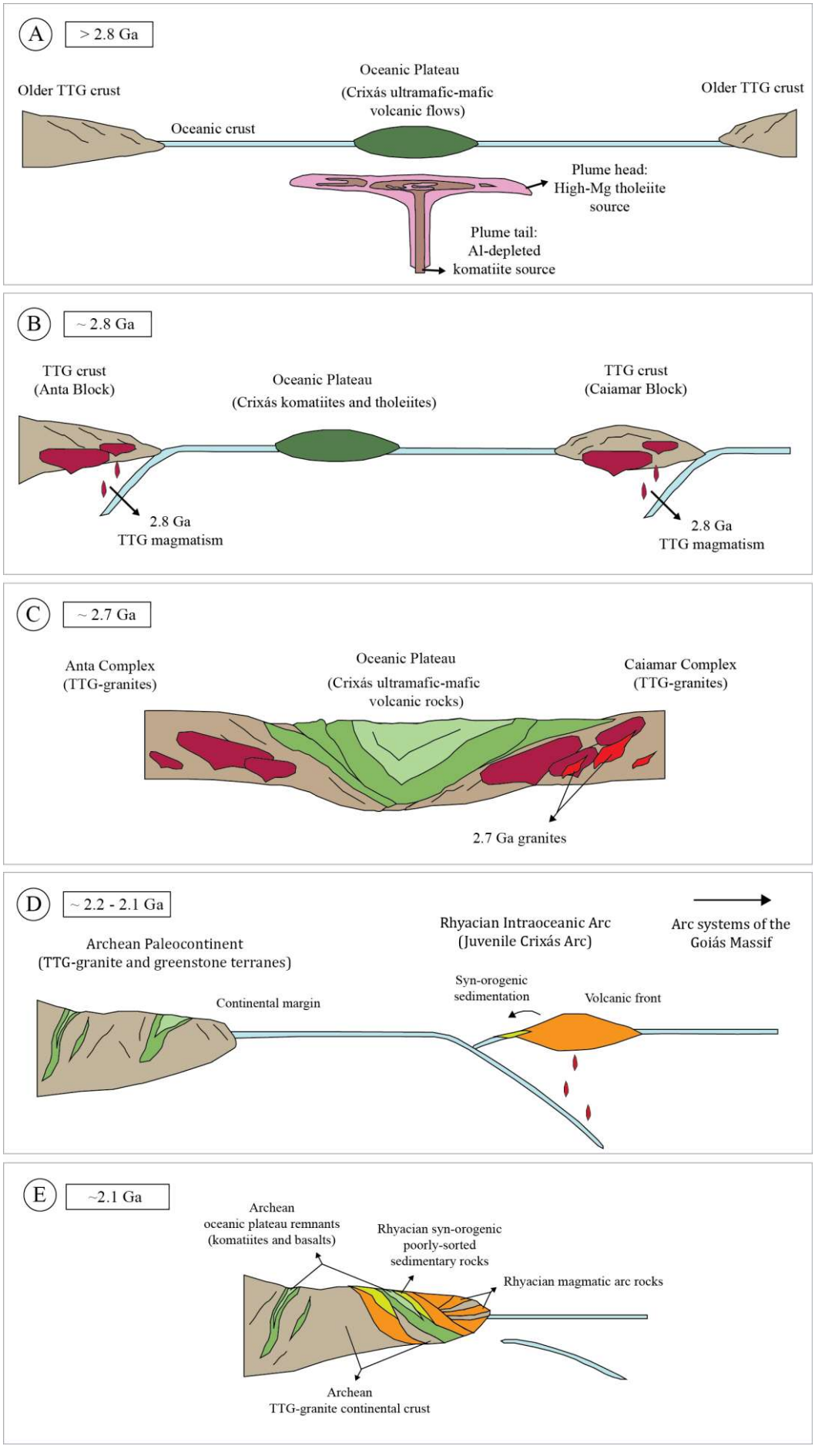
A
> 2.8 Ga
Older TTG crust
Oceanic Plateau
(Crixás ultramafic-mafic
volcanic flows)
Older TTG crust
Oceanic crust
Plume head:
High-Mg tholeiite
source
Plume tail:
Al-depleted
komatiite source
B
~ 2.8 Ga
TTG crust
(Anta Block)
Oceanic Plateau
(Crixás komatiites and tholeiites)
TTG crust
(Caiamar Block)
2.8 Ga
TTG magmatism
2.8 Ga
TTG magmatism
C
~ 2.7 Ga
Anta Complex
(TTG-granites)
Oceanic Plateau
(Crixás ultramafic-mafic
volcanic rocks)
Caiamar Complex
(TTG-granites)
2.7 Ga granites
D
~ 2.2 - 2.1 Ga
Archean Paleocontinent
(TTG-granite and greenstone terranes)
Rhyacian Intraoceanic Arc
(Juvenile Crixás Arc)
Arc systems of the
Goiás Massif
Continental margin
Syn-orogenic
sedimentation
Volcanic front
E
~2.1 Ga
Archean
oceanic plateau remnants
(komatiites and basalts)
Rhyacian syn-orogenic
poorly-sorted
sedimentary rocks
Rhyacian magmatic arc rocks
Archean
TTG-granite continental crust

Fig. 18. Schematic diagrams illustrating the evolution of the Crixás greenstone belt throughout the Archean and Paleoproterozoic. (A) Mesoarchean (>2.8 Ga) Al-depleted komatiites and high-Mg tholeiites were derived from heterogeneous mantle plume melting in an oceanic plateau setting. Komatiites were formed at high melting degrees at great depth, in the presence of residual garnet, whist the basalts were formed at shallower depths. (B) Generation of ca. 2.8 Ga TTG magmatism that comprises most of the gneissic complexes of the northern Crixás-Goiás Domain. In the figure, the precursor Anta and Caiamar blocks are represented (see Fig. 2a). This juvenile TTG magmatism interacted with older continental crust, as reveled by inherited zircon as old as 3.3 Ga (Queiroz et al., 2008). (C) After the accretion of the oceanic plateau onto the the ca. 2.8 Ga TTG rocks of the Anta and Caiamar blocks, cratonization of the region occurred at ca. 2.7 Ga and followed crustal reworking and emplacement of ca. 2.7 granites (currently recognized only in the Moquém Complex, located at east of the Caiamar Complex; Queiroz et al., 2008). (D) Formation of a Rhyacian (2.2 - 2.1 Ga) intraoceanic arc adjacent to the Archean paleocontinent (stabilized TTG-greenstone terranes; proto Crixás-Goiás Domain). This is inserted in the context of the arc systems of the Goiás Massif (Cordeiro and Oliveira, 2017; Borges et al., 2021). (E) Accretion of the Rhyacian intraoceanic arc onto the Archean paleocontinent resulted in tectonic transport of the arc units (arc volcanics and intrusives, and syn-orogenic sedimentary rocks) and imbrication with the older Archean terranes, such as the oceanic plateau remnants (Crixás komatiites and basalts).

6. Conclusion

The Crixás greenstone belt consists of temporal unrelated rock units formed in different geological environments, with a complex tectonostratigraphy that includes two contrasting assemblies of rocks: Archean metakomatiites and metabasalts overlaid by Paleoproterozoic metagraywackes and carbonaceous phyllites associated with newly recognized meta-andesites and metadiorites.

Metakomatiites are chemically similar to the Al-depleted type komatiites (ADK), while the metabasalts are high-Mg tholeiites with mostly flat patterns of REE, and a trace element systematics analogous to Phanerozoic oceanic plateau basalts. An origin from a heterogeneous mantle plume is proposed for the komatiite-tholeiite association of the Crixás greenstone belt, in which the komatiites were formed at high degrees of partial melting at greater depths, and the basalts derived from lower degrees of partial mantle melting at shallower depths. It is believed that this oceanic plateau was formed in the Mesoarchean, based on previous Sm-Nd and Pb-Pb isotopic data (~3.0 – 2.8 Ga; Arndt et al., 1998; Fortes et al., 2003). However, we highlight the necessity of more robust geochronological data to give further constraints on the time of eruption of the komatiite and basalt flows. Whole-rock Re-Os data of the ultramafic-mafic metavolcanic rocks yield an isochron of 2609 ± 65 Ma (MSWD = 7; n = 5). This age is interpreted to reflect a Neoarchean overprinting event associated with hydrothermal-metasomatic Re-addition recorded in the lower ultramafic-mafic

metavolcanic rocks, possibly related to the late stages of the cratonization of the Crixás-Goiás Domain during the emplacement of the younger Archean granodiorites and granites of the region (~2.7 Ga).

LA-ICP-MS U-Pb zircon geochronology of a meta-andesite sample provided an upper intercept Concordia age of 2172.2 ± 12.7 Ma (MSWD = 1.4), interpreted as the age of the intermediate magmatism. Samples have homogeneous Paleoproterozoic two-stage Nd model ages (2.28 to 2.26 Ga), positive initial εNd values (+2.34 to +2.69), and geochemical fingerprinting of subduction zone. These rocks are interpreted to have formed in a Rhyacian juvenile magmatic arc setting and correlated with the *syn*-orogenic metagraywackes and carbonaceous phyllites occurring in the upper succession of the Crixás greenstone belt (see Borges et al., 2021). Two samples of gold-related arsenopyrite hosted in metasedimentary rocks were analyzed for Re-Os geochronology. Coarse-grained arsenopyrite separates from a massive sulfide sample provided a Re-Os age of 2137 ± 11 Ma, in agreement with previous works that support a Rhyacian age for the gold mineralization (e.g. Marques et al., 2013; Jost et al., 2010, 2014). Although it is possible that post-Paleoproterozoic events could have been responsible for remobilization of some ore deposits. Arsenopyrite separates from a foliated drill core sample yielded younger and varied ages (1893 ± 9 and 1367 ± 7 Ma), which likely indicate local disturbance of the Re-Os isotopic system in the sheared zones.

7. Acknowledgments

We are grateful to Mineração Serra Grande S.A. for providing the drill cores and supporting the field works and analytical data acquisition. We thank Dr. Hardy Jost for the innumerous and precious geological discussions about the Crixás greenstone belt and the Crixás-Goiás Block. A.M. Silva, C.L.B. Toledo, and F. Chemale Jr. acknowledge the Conselho Nacional de Desenvolvimento Científico e Tecnológico (CNPq) for their respective research grants. This work was financed by the Coordenação de Aperfeiçoamento de Pessoal de Nível Superior - Brasil (CAPES) - Finance Code 001, CAPES-PrInt (Grant Number: 88881.312018/2018-01), and CNPq (MCTIC/CNPq 28/2018 – Grant Number: 420308/2018-0). The first author thanks CAPES for the PhD scholarship (PROEX – Grant Number: 88882.347184/2019-01).

8. References

Arndt, N.T., Bruzak, G., Reischmann, T., 2001. The oldest continental and oceanic plateaus: geochemistry of basalts and komatiites of the Pilbara craton, Australia. Spec. Pap. Geol. Soc. Am. 352, 359-387.

Arndt, N.T., Kerr, A.C., Tarney, J., 1997. Dynamic melting in plume heads: the formation of Gorgona komatiites and basalts. Earth Planet. Sci. Lett. 146, 289-301.

Arndt, N.T., Lesher, C.M., Barnes, S.-J., 2008. Komatiite. Cambridge University Press, 465 p.

Arndt, N.T., Teixeira, N.A., White, W.M., 1989. Bizarre geochemistry of komatiites from the Crixás Greenstone belt, Brazil. Contr. Mineral. Petrol. 74, 549-564.

Barley, M.E., Sylvester, G.C., Groves, D.I., Borley, G.D., Rogers, N., 1984. Archaean calc-alkaline volcanism in the Pilbara Block, Western Australia. Precambrian Res. 24, 285–319.

Beghelli Junior, L.P., 2012. Charnockitos e ortognaisses da porção centro-oeste do Bloco Arqueano de Goiás: Dados geoquímicos e isotópicos. Dissertação de Mestrado, Instituto de Geociências, Universidade de Brasília, 87 pp.

Birck, J. L., Barman M. R. and Capmas F., 1997. Re-Os isotopic measurements at the femtomole level in natural samples. Geostand. Newslett. 21, 19–27.

Bogossian, J., 2020. Gold systems in the Faina greenstone belt and crustal evolution of the southern Goiás Archean Block, central Brazil. PhD thesis, School of Earth Sciences, The University of Western Australia, 246 pp.

Borges, C.C.A., Toledo, C.L.B., Silva, A.M., Chemale, F., Jost, H., Lana, C.C., 2017. Geochemistry and isotopic signatures of metavolcanic and metaplutonic rocks of the Faina and Serra de Santa Rita greenstone belts, Central Brazil: evidence for a Mesoarchean intraoceanic arc. Precambrian Res. 292, 350-377.

Borges, C.C.A., Toledo, C.L.B., Silva, A.M., Chemale, F., Santos, B.A., Figueiredo, F.L., Zacchi, E.N.P., 2021. Unraveling a hidden Rhyacian magmatic arc through provenance of metasedimentary rocks of the Crixás greenstone belt, Central Brazil. Precambrian Res. 353, 106022. https://doi.org/10.1016/j.precamres.2020.106022

Botelho, N.F., Fuck, R.A., Dantas, E.L., Laux, J.L., Junges, S.L., 2006. The Paleoproterozoic peraluminous Aurumina granite suite, Goiás and Tocantins: whole rock geochemistry and Sm–Nd isotopic constraints. In: The Paleoproterozoic Record of the São Francisco Craton, Brazil, IGCP 509, Brazil, September 9–21.

Brant, R.A.P., Souza, V.S., Dantas, E.L., Jost, H., Rodrigues, V.G., Carvalho, M.J., Araújo, K.C., 2015. Contribuição ao estudo de proveniência sedimentar com base em dados U-Pb para o greenstone belt de Faina, Goiás. In: SBG, XIV Simpósio de Geologia do Centro-Oeste, Brasília, Anais, pp. 30-33.

Brenner, A.R., Fu, R.R., Evans, D.A.D., Smirnov, A.V., Trubko, R., Rose, I.R., 2020. Paleomagnetic evidence for modern-like plate motion velocities at 3.2 Ga. Science Advances 6, eaaz8670. https://doi.org/10.1126/sciadv.aaz8670.

Bühn, B., Pimentel, M.M., Matteini, M., Dantas, E.L., 2009. High spatial resolution analysis of Pb and U isotopes for geochronology by laser ablation multi-collector inductively coupled plasma mass spectrometry (LA-MC-ICP-MS). An. Acad. Bras. Cienc. 81, 1–16.

Campbell, I. H., 1998, The mantle's chemical structure: insights from the melting products of mantle plumes, in Jackson, I., ed., The Earth's mantle: Composition, structure, and evolution: Cambridge, Cambridge University Press, p. 259–310.

Campbell, I.H., Griffiths, R.W., Hill, R.I., 1989. Melting in an Archean mantle plume: Heads it is basalts and tails it is komatiites. Nature 339, 697-699.

Card, K. D., 1990. A review of the Superior Province of the Canadian Shield, a product of Archean accretion, Precambrian Res. 48, 99–156.

Carlson, R.W., 2005. Application of the Pt-Re-Os isotopic system to mantle geochemistry and geochronology. Lithos 82, 249-272.

Cawood, P.A., Hawkesworth, C.J., Pisarevsky, S.A., Dhuime, B., Capitanio, F.A., Nebel, O., 2018. Geological archive of the onset of plate tectonics. Phil. Trans. R. Soc. A 376, 20170405. http://dx.doi.org/10.1098/rsta.2017.0405.

Chavagnac, V., 2004. A geochemical and Nd isotopic study of Barberton komatiites (South Africa): implication for the Archean mantle. Lithos 74, 253-281.

Condie, K.C., 2003. Incompatible element ratios in oceanic basalts and komatiites: tracking deep mantle sources and continental growth rates with time. Geochem. Geophys. Geosyst. 4 (1), 1-28.

Condie, K.C., 2005. High field strength element ratios in Archean basalts: a window to evolving sources of mantle plumes? Lithos 79, 491-504.

Condie, K.C., 2007. Accretionary orogens in space and time. Geological Society of America Memoir, 200, 145158.

Condie, K.C., Frey, B.A., Kerrich, R. 2002. The 1.75-Ga Iron King Volcanics in west central Arizona: a remnant of an accreted oceanic plateau derived from a mantle plume with a deep depleted component. Lithos 64, 49-62.

Cordeiro P.F.O., Oliveira. C.G., 2017. The Goiás Massif: Implications for a pre-Columbia 2.2–2.0 Ga continent-wide amalgamation cycle in central Brazil. Precambrian Res. 288, 403-420.

Cordeiro, P.F.O., Oliveira, C.G., Giustina, M.E.S.D., Dantas, E.L., dos Santos, R.V., 2014. The Paleoproterozoic Campinorte Arc: Tectonic evolution of a Central Brazil pre-Columbia orogeny. Precambrian Res. 251, 49–61.

Corrêa da Costa, P.C., Giradi, V.A.V., 2005. Petrology, geochemistry and Sr-Nd isotopes of the Paleoproterozoic mafic dykes from the Goiás-Crixás Archean Block, Goiás State, Brazil. Rev. Brasil. Geociênc. 35 (1), 135-150.

Corrêa da Costa, P.C., Giradi, V.A.V., Teixeira, W., 2006. 40Ar/39Ar and Rb/Sr Geochronology of the Goiás-Crixás Dike Swarm, Central Brazil: Constraints on the Neoarchean–Paleoproterozoic Tectonic Boundary in South America, and Nd-Sr Signature of the Subcontinental Mantle. Int. Geol. Rev. 48, 547-560.

Costa Jr., C.N., Ferreira Filho, C.F., Osborne, G.A., Araújo, S.M., Lopes, R.O., 1997. Geology and geochemistry of the Boa Vista nickel sulfide deposit, Crixás greenstone belt, Central Brazil. Rev. Brasil. Geociênc. 27 (4), 365-376.

Cruz, E.L.C.C., Kuyumjian, R.M., Boaventura, G.R., 2003. Low-K calc-alkaline granitic series of southeastern Tocantins state: chemical evidence for two sources for the granite-gneissic complexes in the Paleoproterozoic Almas-Dianópolis terrane. Rev. Brasil. Geociênc. 33, 125–136.

Cuadros, F.A., Botelho, N.F., Fuck, R.A., Dantas, E.L., 2017a. The peraluminous Aurumina granite suite in central Brazil: an example of mantle-continental crust interaction in a Paleoproterozoic cordilleran hinterland setting? Precambrian Res. 299, 75–100.

Cuadros, F.A., Botelho, N.F., Fuck, R.A., Dantas, E.L., 2017b. The Ticunzal Formation in central Brazil: record of Rhyacian sedimentation and metamorphism in the western border of the São Francisco Craton. J. S. Am. Earth Sci. 79, 307–325.

Danni, J.C.M., Ribeiro, C.C., 1978. Caracterização Estratigráfica da Sequência Vulcanossedimentar de Pilar de Goiás e de Guarinos, Goiás. In: SBG, Congresso Brasileiro de Geologia, 30, Recife, Anais, v. 2, pp. 582 596.

DePaolo D., 1981. Neodymiun isotopes in the Colorado Front Range and crust-mantle evolution in the Proterozoic. Nature 291, 193-196.

DePaolo, D.J., 1988. Neodymium Isotope Geochemistry: An Introduction. Springer Verlag, New York.

Dostal, J., 2008. Komatiites. Geoscience Canada 35, 21-31

Dostal, J., Mueller, W.U., 2013. Deciphering and Archean mantle plume: Abitibi greenstone belt, Canada. Gondwana Res. 23, 493-505.

Ferreira, B.F., Marques, J.C., Frantz, J.C., de Souza, R.G., Campos, M.P., Figueiredo, F.L.A.R., Padilha, N.L., 2021. Stratigraphy and U–Pb detrital zircon provenance, Crixás Greenstone Belt, Goiás-Brasil: Gold-bearing vs barren siliciclastic rocks. J. S. Am. Earth Sci. 105, 102994. https://doi.org/10.1016/j.jsames.2020.102994.

Filgueiras, B.C., Oliveira, C.G., Sousa, I.M.C., Cordeiro, P.F.O., 2020. Further evidence of Rhyacian arc magmatism in the basement of the Brasília Belt. J. S. Am. Earth Sci. 103, 102739.

Fitton, J.G., Godard, M., 2004. Origin and evolution of the magmas on the Ontong Java Plateau. Geol. Soc. Spec. Publ. 229, 151-178. https://doi.org/10.1144/GSL.SP.2004.229.01.10

Fortes, P.T.F.O., 1996. Metalogênese dos depósitos auríferos Mina III, Mina Nova e Mina Inglesa, greenstone belt de Crixás, GO. Tese de Doutorado, Instituto de Geociências, Universidade de Brasília, 176 pp.

Fortes, P.T.F.O., Pimentel, M.M., Santos, R.V., Junges, S., 2003. Sm-Nd study of the Crixás greenstone belt, Brazil: implications for the age of deposition of the upper sedimentary rocks and associated Au mineralization. J. S. Am. Earth Sci. 16, 503–512.

Foster, J. G., Lambert D. D., Frick L. R., Maas R. 1996. Re–Os isotopic evidence for genesis of Archaean nickel ores from uncontaminated komatiites. Nature 382(6593), 703–706.

Frei, R., Jensen, 2003. Re–Os, Sm–Nd isotope- and REE systematics on ultramafic rocks and pillow basalts from the Earth's oldest oceanic crustal fragments (Isua Supracrustal Belt and Ujaragssuit nunât area, W Greenland). Chem. Geol. 196, 163-191.

Fuck, R.A., Dantas, E.L., Pimentel, M.M., Botelho, N.F., Armstrong, R., Laux, J.H., Junges, S.L., Soares, J.E., Praxedes, I.F., 2014. Paleoproterozoic crust-formation and reworking events in the Tocantins Province, central Brazil: a contribution for Atlantica supercontinent reconstruction. Precambrian Res. 244, 53–74.

Gangopadhyay A., Sproule R. A., Walker R. J. and Lesher C. M., 2005. Re-Os systematics of komatiites and komatiitic basalts at Dundonald Beach, Ontario, Canada: evidence for a complex alteration history and implications of a late-Archean chondritic mantle source. Geochim. Cosmochim. Acta 69, 5087–5098.

Gangopadhyay, A., Walker, R.J., 2003. Re-Os systematics of the ca. 2.7-Ga komatiites from Alexo, Ontario, Canada. Chem. Geol. 196 (1–4), 147– 162.

Gioia, S. M. C. L., Pimentel, M. M., 2000. The Sm-Nd Isotopic Method in the Geochronology Laboratory of the University of Brasília. An. Acad. Bras. Cienc. 72 (2), 219-245.

Giustina, M.E.S.D., de Oliveira, C.G., Pimentel, M.M., de Melo, L.V., Fuck, R.A., Dantas, E.L., Buhn, B., 2009. U-Pb and Sm-Nd constraints on the nature of the Campinorte sequence and related Palaeoproterozoic juvenile orthogneisses, Tocantins Province, central Brazil. Geol. Soc. Lond. Spec. Publ. 323, 255–269.

Hastie, A.R., Kerr, A.C., Mitchell, S.F., Millar, I.L., 2008. Geochemistry and petrogenesis of Cretaceous oceanic plateau lavas in eastern Jamaica. Lithos 101, 323-343.

Jackson, S.E., Pearson, N.J., Griffin, W.L., Belousova, E.A., 2004. The application of laser ablation-inductively coupled plasma-mass spectrometry to in situ U-Pb zircon geochronology. Chem. Geol. 211, 47–69.

Jacobsen, S.B., Wasserburg, G.J., 1980. Sm–Nd isotopic evolution of chondrites. Earth Planet. Sci. Lett. 50, 139–155.

Jensen , L. 1976 . A New Cation Plot for Classifying Subalkalic Volcanic Rocks; Ontario Div. Mines, MP 66, 22p.

Jost, H., Apollo, J.F.H., Weber, W., Salles, R.R., Marques, J.C.M., Massucatto, A.J., Costa, D.A., Santos, B.A., 2019. Stratigraphic update, paleotectonic, paleogeographic, and depositional environments of the Crixás Greenstone Belt, Central Brazil. J. S. Am. Earth Sci. 96, 102329.

Jost, H., Carvalho, M.J., Rodrigues, V.G., Martins, R., 2014. Metalogênese dos greenstone belts de Goiás. In: Silva, M.G., Neto, M.B.R., Jost, H., Kuyumjian, R.M. (Orgs.), Metalogênese das províncias tectônicas brasileiras, Belo Horizonte, CPRM, pp. 141-168.

Jost, H., Chemale Jr., F., Dussin, I.A., Tassinari, C.C.G., Martins, R., 2010. A U–Pb zircon paleoproterozoic age for the metasedimentary host rocks and gold mineralization of the Crixás greenstone belt, Goiás, Central Brazil. Ore Geol. Rev. 37, 127–139.

Jost, H., Chemale Jr., F., Fuck, R.A., Dussin, R.A., 2013. Uvá complex, the oldest orthogneisses of the Archean Paleoproterozoic terrane of central Brazil. J. S. Am. Earth Sci. 47, 201-212.

Jost, H., Oliveira, A.M., 1991. Stratigraphy of the greenstone belts, Crixás region, Goiás, Central Brazil. J. S. Am. Earth Sci. 4, 201 -214.

Jost, H., Oliveira, A.M., Vargas, M.C., 1992. Petrography, geochemistry and structural control of trondhjemitic intrusions in greenstone belts of the Crixás region, Central Brazil. In: SBG, Congresso Brasileiro de Geologia, 37, São Paulo. Anais, v. 1. pp. 43-44.

Jost, H., Pimentel, M.M., Fuck, R.A., Danni, J.C., Heaman, L., 1993. Idade U-Pb do Diorito Posselândia, Hidrolina, Goiás. Rev. Brasil. Geociênc. 23, 352-355.

Jost, H., Rodrigues, V.G., Carvalho, N.J., Chemale Jr., F., Marques, J.C., 2012. Estratigrafia e geocronologia do greenstone belt de Guarinos, Goiás. Geol. USP, Sér. Cient. 12 (2), 3-48.

Kerr A.C., 2015. Oceanic Plateaus. In: Harff, J., Meschede, M., Petersen, S., Thiede, J. (eds) Encyclopedia of Marine Geosciences. Springer, Dordrecht. https://doi.org/10.1007/978-94-007-6644-0_21-1

Kerr, A. C., 2014. Oceanic plateaus. In: Rudnick, R. (ed.), The Crust. Chapter 18. Treatise on Geochemistry, 2nd edn (Holland, H. C., and Turekian, K. (Series eds.)). Elsevier, Amsterdam, Vol. 4, pp. 631–667.

Kerr, A. C., Mahoney, J. J., 2007. Oceanic plateaus: problematic plumes, potential paradigms. Chem. Geol. 241, 332–353.

Kerr, A. C., Tarney, J., Marriner, G. F., Nivia, A., and Saunders, A. D., 1997. The Caribbean-Colombian Cretaceous igneous province: the internal anatomy of an oceanic plateau. In Mahoney, J. J., and Coffin, M. (eds.), Large Igneous Provinces: Continental, Oceanic and Planetary Flood Volcanism. Washington, DC: American Geophysical Union. American Geophysical Union Monograph, 100, pp. 45–93.

Kerr, A. C., White, R. V., Saunders, A. D., 2000. LIP reading: recognizing oceanic plateaux in the geological record. J. Petrol. 41, 1041–1056.

Kusky, T. M., Polat, A., 1999. Growth of granite–greenstone terranes at convergent margins, and sta-bilization of Archean cratons. Tectonophysics 305, 43–73.

Kusky, T. M., Windley, B. F., Polat, A., 2018. Geological evidence for the operation of plate tectonics throughout the Archean: Records from Archean Paleo-Plate Boundaries. J. Earth Sci. 29 (6), 1291–1303.

Kusky, T.M., Windley, B.F., Polat, A., Wang, L., Ning, W., Zhong, Y., 2021. Archean dome-and-basin style structures form during growth and death of intraoceanic and continental margin arcs in accretionary orogens. Earth-Sci. Rev. 103725.

Kuyumjian, R.M., Araújo Filho, J.O., 1991. Implicações genéticas das variações de alguns elementos-traço incompatíveis nos basaltos komatiíticos de Crixás, Goiás. Rev. Brasil. Geociênc. 21 (4), 301-304.

Kuyumjian, R.M., Costa, A.L.L., 1999. Geologia, geoquímica e mineralizações auríferas da Sequência Mina Inglesa, greenstone belt de Crixás, Goiás. Rev. Bras. Geociênc. 29, 313–318.

Kuyumjian, R.M., Jost, H., 2006. Low-and high-alumina komatiites of Goiás, Central Brazil. J. S. Am. Earth Sci. 20, 315–326.

Lahaye, Y., Barnes, S.-J., Frick, L.R., Lambert, D.D., 2001. Re–Os isotopic study of komatiitic volcanism and magmatic sulfide formation in the southern Abitibi greenstone belt, Ontario, Canada. Can. Mineral. 39, 473– 490.

Langford, F. F., Morin, J. A., 1976. The development of the Superior Province of northwestern Ontario by merging island arcs, Am. J. Sci. 276, 1023–1034.

Liew, T., Hofmann, A., 1988. Precambrian crustal components, plutonic associations, plate environment of the Hercynian Fold Belt of central Europe: indications from a Nd and Sr isotopic study. Contrib. to Mineral. Petrol. 98, 129–138.

Mahoney, J.J., Storey, M., Duncan, R.A., Spencer, K.J. and Pringle, M. 1993. Geochemistry and age of the Ontong Java Plateau. In: Pringle, M.S. (ed.), The Mesozoic Pacific: 1737 Geology, Tectonics and Volcanism. American Geophysical Union, Geophysical Monograph 77, pp. 233-261.

Maier, W.D., Peltonen, P., Halkoaho, T., Hanski, E., 2013. Geochemistry of komatiites from the Tipasjärvi, Kuhmo, Suomussalmi, Ilomantsi and Tulppio greenstone belts, Finland: Implications for tectonic setting and Ni sulphide prospectivity. Precambrian Res. 228, 63-84.

Marques, J. C., Jost, H., Creaser, R. A., Frantz, J. C., Osorio, R. G., 2013. Age of arsenopyrite gold-bearing massive lenses of the Mina III and its implications on exploration, Crixás greenstone belt, Goiás, Brazil. In: III Simpósio Brasileiro de Metalogenia, Gramado, extended abstracts.

Martins-Ferreira, M.A.C., Chemale, F., Dias, A.N.C., Campos, J.E.G., 2018. Proterozoic intracontinental basin succession in the western margin of the São Francisco Craton: constraints from detrital zircon geochronology. J. S. Am. Earth Sci. 81, 165–176.

Martins-Ferreira, M.A.C., Dias, A.N.C., Chemale Jr., F., Campos, J.E.G., Seraine, M., Novais-Rodrigues, E., 2020. Multi-stage crustal accretion by magmatic flare-up and quiescence intervals in the western margin of São Francisco Craton: U-Pb-Hf and geochemical constraints from the Almas Terrane. Gondwana Res. 85, 32-54.

Moilanen, M., Hanski, E., Konnunaho, J., Yang, S-H., Törmänen, T., Li, C., Zhou, L.M., 2019. Re-Os isotope geochemistry of komatiite-hosted Ni-Cu-PGE deposits in Finland. Ore Geol. Rev. 105, 102-122.

Morgan, J. W., Walker, R. J., 1989. Isotopic determinations of rhenium and osmium in meteorites by using fusion, distillation and ion-exchange separations. Analytica Chimica Acta, 222, 291-300.

Nägler, T.F., Frei, R., 1997. Plug in plug osmium distillation. Schweiz. Mineral. Petrogr. Mitt. 77, 123–127.

Nutman, A.P., Friend, C.R.L., 2007. Adjacent terranes with ca. 2715 and 2650 Ma high-pressure metamorphic assemblages in the Nuuk region of the North Atlantic Craton, southern West Greenland: complexities of Neoarchaean collisional orogeny. Precambrian Res. 155, 159–203.

Nutman, A.P., Friend, C.R.L., 2009. New 1:20,000 scale geological maps, synthesis and history of investigation of the Isua supracrustal belt and adjacent orthogneisses, southern West Greenland: A glimpse of Eoarchean crust formation and orogeny. Precambrian Res. 172, 189–211.

Oliveira, F.V., 2015. Chronus: Um novo suplemento para a redução de dados U-Pb obtidos por LA-MC-ICPMS. Dissertação de Mestrado, Instituto de Geociências, Universidade de Brasília, 91 pp.

Pearce, J.A., 1996. A users guide to basalt discrimination diagrams. In: Wyman DA, editor. Trace Element Geochemistry of Volcanic Rocks: Applications for Massive Sulphide Exploration. Short Course Notes 12. St. John's, Canada: Geological Association of Canada, pp. 79-113.

Pearce, J.A., 2008. Geochemical fingerprinting of oceanic basalts with applications to ophiolite classification and the search for Archean oceanic crust. Lithos 100, 14–48.

Pegram, W.J., Allègre, C.J., 1992. Osmium isotopic compositions from oceanic basalts. Earth Planet. Sci. Lett. 111, 59-68.

Percival, J., Skulski, T., Sanborn-Barrie, M., Stott, G., Leclair, A.D., Corkery, M. T., Boily, M., 2012. Geology and tectonic evolution of the Superior Province, Canada, in Tectonic Styles in Canada: The Lithoprobe Perspective, Special Paper, vol. 49, edited by J. Percival, F. Cook, and R. Clowes, pp. 321–378, Geological Association of Canada, St John's, NF, Canada.

Pimentel, M.M., Heaman, L., Fuck, R.A., Marini, O.J., 1991. U–Pb zircon geochronology of Precambrian tin-bearing continental-type acid magmatism in central Brazil. Precambrian Res. 52, 321–335.

Pimentel, M.M., Jost, H., Fuck, R.A., Armstrong, R.A., Dantas, E.L., Potrel, A., 2003. Neoproterozoic anatexis of 2.9 Ga old granitoids in the Goiás-Crixás block, Central Brazil: evidence from new SHRIMP U-Pb data and Sm-Nd isotopes. Geol. USP, Sér. Cient. 3, 1-12.

Polat, A., Frei, R., Apple, P. W. U., Dilek, Y., Fryer, B., Ordonez-Calderon, J. C., Yang, Z., 2008. The origin and compositions of Mesoarchean oceanic crust: Evidence from the 3075 Ma Ivisaartoq greenstone belt, SW Greenland. Lithos 100, 293–321.

Polat, A., Hofmann, A.W., 2003. Alteration and geochemical patterns in the 3.7–3.8 Ga Isua green-stone belt, West Greenland. Precambrian Res. 126, 197–218.

Puchtel, I. S., Brandon A. D., Humayun M., Walker R. J., 2005. Evidence for the early differentiation of the core from Pt–Re–Os isotope systematics of 2.8-Ga komatiites. Earth Planet. Sci. Lett. 237 (1–2), 118–134.

Puchtel, I. S., Walker R. J., Brandon A. D. and Nisbet E. G., 2009. Pt–Re–Os and Sm–Nd isotope and HSE and REE systematics of the 2.7 Ga Belingwe and Abitibi komatiites. Geochim. Cosmochim. Acta 73(20), 6367–6389.

Puchtel, I. S., Walker R. J., Touboul M., Nisbet E. G., Byerly G. R., 2014. Insights into Early Earth from the Pt–Re-Os isotope and Highly Siderophile Element abundance systematics of Barberton komatiites. Geochim. Cosmochim. Acta 125, 394–413.

Puchtel, I.S., Hofmann, A.W., Mezger, K., Jochum, P.K., Scipansky, A.A., Samsanov, A.V., 1998. Oceanic plateau model for continental crustal growth in the Archean: a case study from the Kostomuksha greenstone belt, NW Baltic Shield. Earth Planet. Sci. Lett. 155, 57–74.

Queiroz, C.L., 2000. Evolução Tectono-Estrutural dos Terrenos Granito-Greenstone Belt de Crixás, Brasil Central. Tese de Doutorado, Instituto de Geociências, Universidade de Brasília, 209 pp.

Queiroz, C.L., Jost, H., Silva, L.C., McNaughton, N.J., 2008. U-Pb SHRIMP and Sm-Nd geochronology of granite-gneiss complexes and implications for the evolution of the central Brazil Archean terrain. J. S. Am. Earth Sci. 26, 100-124.

Resende, M.G., Jost, H., Lima, B.E.M., Teixeira, A.A., 1999. Proveniência e idades-modelo Sm-Nd de rochas siliciclásticas arqueanas dos greenstone belts de Faina e Santa Rita, Goiás. Rev. Brasil. Geociênc. 29, 281-290.

Resende, M.G., Jost, H., Osborne, G. A., Mol, A. G., 1998. Stratigraphy of the Goiás and Faina greenstone belts, Central Brazil: a new proposal. Rev. Brasil. Geociênc. 28, 77-94.

Revillon, S., Arndt, N.T., Chauvel, C., Hallot, E., 2000. Geochemical study of ultramafic volcanic and plutonic rock from Gorgona Island, Colombia: the plumbing system of an oceanic plateau. J. Petrol. 41, 1127-1153.

Ross, P.-S., Bédard, J.H., 2009. Magmatic affinity of modern and ancient subalkaline volcanic rocks determined from trace-element discriminant diagrams. Can. J. Earth Sci. 46, 823–839.

Rubatto, D., Gebauer, D., 2000. Use of cathodoluminescence for U–Pb zircon dating by ion microprobe: some examples from the Western Alps. In: Pagel M, Barbin V, Blanc P, Ohnenstetter D (eds) Cathodoluminescence in geosciences. Springer, Berlin, Heidelberg, pp 373–400.

Saboia, A.M., Oliveira, C.G., Dantas, E.L., Cordeiro, P., Scandolara, J.E., Rodrigues, J.B., Sousa, I.M.C., 2020. The Siderian crust (2.47–2.3 Ga) of the Goiás Massif and its role as a building block of the São Francisco paleocontinent. Precambrian Res. 350, 105901.

Sabóia, L.A., 1979. Os greenstone be1ts de Crixás e Goiás, GO. Sociedade Brasileira de Geologia. Núcl. Centro-Oeste, Goiâ., Boletim Inf. 9, 43–72.

Sabóia, L.A., Teixeira, N.A., 1980. Lavas ultrabásicas da unidade basal do "greenstone belt" de Crixás (GO): uma nova classe de rochas ultrabásicas no Estado de Goiás. Rev. Bras. Geociênc. 10, 28-42.

Sabóia, L.A., Teixeira, N.A., 1983. Ultramaphic flows of the Crixás greenstone belt, Goiás. Precambrian Res. 22, 23–40.

Saunders, A.D., Norry, M.J., Tarney, J., 1988. Origin of MORB and chemically depleted mantle reservoirs: trace element constraints. J. Petrol. (Special Lithosphere Issue), 415–445.

Schneider, K.P., Hoffmann, J.E., Münker, C., Patyniak, M., Sprung, P., Roerdink, D., Schönberg, D.G., Kröner, A., 2019. Petrogenetic evolution of metabasalts and metakomatiites of the lower Onverwacht Group, Barberton Greenstone Belt (South Africa). Chem. Geol. 511, 152-177.

Serrano, L., Ferrari, L., Martínez, M.L., Petrone, C.M., Jaramillo, C., 2011. An integrative geologic, geochronologic and geochemical study of Gorgona Island, Colombia: Implications for the formation of the Caribbean Large Igneous Province. Earth Planet. Sci. Lett. 309, 324-336.

Shirey, S. B., Walker R. J., 1998. The Re-Os isotope system in cosmochemistry and high-temperature geochemistry. Annu. Rev. Earth Planet. Sci. 26, 423–500.

Shirey, S., Walker, R., 1995. Carius tube digestion for low-blank rhenium-osmium analysis. Anal. Chem. 67, 2136–2141.

Siepierski, L., Ferreira Filho, C.F., 2016. Spinifex-textured komatiites in the south border of the Carajás Ridge, Selva Greenstone Belt, Carajás Province, Brazil. J. Earth Sci. 66, 41-55.

Singh, P.K., Verma, S.K., Moreno, J.A., Singh, V.K., Malviya, V.P., Oliveira, E.P., Mishra, S., Arima, M., 2019. Geochemistry and Sm-Nd isotope systematics of mafic-ultramafic rocks from the Babina and Mauranipur greenstone belts, Bundelkhand Craton, India: Implications for tectonic setting and Paleoarchean mantle evolution. Lithos 330-331, 90-107.

Smoliar, M. I., Walker R. J. and Morgan J. W., 1996. Re-Os ages of Group IIA, IIIA, IVA, and IVB iron meteorites. Science 271, 1099–1102.

Sousa, I.M.C., Giustina, M.E.S.D., Oliveira, C.G., 2016. Crustal evolution of the northern Brasília Belt basement, central Brazil: a Rhyacian orogeny coeval with a pre-Rodinia supercontinent assembly. Precambrian Res. 273, 129–150.

Stein, H.J., 2014. Dating and Tracing the History of Ore Formation, in: Turekian, H.D.H.K. (Ed.), Treatise on Geochemistry (Second Edition). Elsevier, Oxford, pp. 87-118.

Stein, HJ, Morgan, J.W, Scherstén, A., 2000. Re–Os dating of low-level highly radiogenic (LLHR) sulfides: The Harna¨s gold deposit, southwest Sweden records continental scale tectonic events. Econ. Geol. 95, 1657–1671.

Steinger, R.H., Jäger, E., 1977. Subcomission on geochronology – Convention on the use of decay constants in geo- and cosmochronology. Earth Planet Sc. Lett. 36, 359-362.

Sun, S.S., McDonough, W.F., 1989. Chemical and Isotopic systematics of oceanic basalts, implications for mantle composition and processes. In: Saunders, A.D., Norry, M.J. (Eds.), Magmatism in the Ocean Basins. Geol. Soc. Lond. Spec. Publ. 42. Blackwell Scientific Publication, UK, pp. 313–345.

Tassinari, C.C.G., Jost, H., Santos, J.C., Nutman, A.P., Bennell, M.R., 2006. Pb and Nd isotope signatures and SHRIMP U-Pb geochronological evidence of Paleoproterozoic age for Mina III gold mineralization. In: South American Symposium on Isotope Geology, 5, Pucon, Chile, Proceedings, pp. 615-617.

Taylor, S.R., McLennan, S.M., 1985. The Continental Crust: its Composition and Evolution. Blackwell Scientific, Oxford, Blackwell, pp. 311p.

Teixeira, N.A., Saboia, L.A., Ferreira, M.C.B., Teixeira, A.S., Castro, J.H.G., 1981. Estruturas e texturas das lavas ultrabásicas e básicas do greenstone belt de Crixás, Goiás, Brasil. SBG, Núcleo do Centro-Oeste, Boletim Informativo 10, 33-87.

Tomlinson, K.Y., Condie, K.C., 2001, Archean mantle plumes: Evidence from greenstone belt geochemistry, in Ernst, R.E., and Buchan, K.L., eds., Mantle Plumes: Their Identification Through Time: Boulder, Colorado, Geological Society of America Special Paper 352, p. 341–357.

Toscani, R., Campos, J.E.G., Matos, D.R., Martins-Ferreira, M.A.C., 2021. Complex depositional environments on a siliciclastic-carbonate platform with shallow-water turbidites: The Natividade Group, central Brazil. J. S. Am. Earth Sci. 107, 102939. https://doi.org/10.1016/j.jsames.2020.102939.

Velásquez, G., Béziat, D., Salvi, S., Tosiani, T., Bebat, P., First occurrence of Paleoproterozoic oceanic plateau in the Guiana Shield: The gold-bearing El Callao Formation, Venezuela. Precambrian Res. 186, 181-192.

Vermeesch, P., 2018, IsoplotR: a free and open toolbox for geochronology. Geoscience Frontiers 9, 1479-1493. doi: 10.1016/j.gsf.2018.04.001.

Weaver, B.L., 1991. Trace element evidence for the origin of ocean-island basalts. Geology 19, 123–126.

Wiedenbeck, M., Allé, P., Corfu, F., Griffin, W.L., Meier, M., Oberli, F., Von Quadt, A., Roddick, J.C., Spiegel, W., 1995. Three natural zircon standards for U-Th-Pb, Lu-Hf, trace element and REE analyses. Geostandards Newsletter 19, 1-23.

Winchester, J.A., Floyd, P.A., 1977. Geochemical discrimination of different magma series and their differentiation products using immobile elements. Chem. Geol. 20, 325–343.

Windley, B.F., Kusky, T., Polat, A., 2021. Onset of plate tectonics by the Eoarchean. Precambrian Res. 352, 105980. https://doi.org/10.1016/j.precamres.2020.105980

Wyman, D. A., 2013. A critical assessment of Neoarchean ‘plume only’ geodynamics: evidence from the Superior Province. Precambrian Res. 229, 3–19.

Capítulo IV - Conclusão

1. Considerações Finais

A abordagem multidisciplinar deste trabalho possibilitou uma melhor caracterização das diferentes unidades estratigráficas que compõe o *greenstone belt* Crixás. Com os dados coletados, integrados com informações disponíveis na literatura, foi possível elaborar um modelo evolutivo para o *greenstone belt* Crixás e fornecer implicações em âmbito regional, no contexto do Domínio Crixás-Goiás e do Maciço de Goiás.

Como discutido no segundo artigo, os metakomatiitos da base do *greenstone belt* Crixás são quimicamente semelhantes aos komatiitos depletados em Al (Arndt et al., 2008; Dostal, 2008). Essas características incluem as baixas razões Al_2O_3/TiO_2, a depleção nos padrões de elementos terras-raras (ETR) pesados, e as anomalias negativas em Zr-Hf. Tal correlação já havia sido proposta em trabalhos anteriores (Arndt et al., 1989; Kuyumjian & Jost, 2006). No entanto, os dados geoquímicos de metakomatiitos apresentados neste trabalho permitem apontar algumas diferenças importantes em relação aos dados anteriores; por exemplo, a ausência de padrões depletados em ETR leves, que, junto aos padrões depletados de ETR, levaram Arndt et al. (1989) a caracterizar os padrões convexos de ETR (*hump-shaped REE patterns*) dos komatiitos do *greenstone belt* Crixás, interpretados por aqueles autores como possível evidência de alteração pós-magmática. Por outro lado, Kuyumjian & Jost (2006) interpretaram que esses padrões de ETR refletiam as características da fonte mantélica: i.e., fusão parcial do manto depletado, gerando depleção em ETR leves, e retenção da granada no manto residual, gerando depleção também nos ETR pesados. Entretanto, os dados do presente trabalho mostram apenas padrões planos a enriquecidos em ETR leves, e depletados em ETR pesados, e se assemelham mais aos dos típicos komatiitos depletados em Al (ex: do tipo Barberton), que apresentam maior concentração de elementos incompatíveis (ex: ETR leves, Th) quando comparados aos komatiitos não-depletados em Al (Dostal, 2008).

Os primeiros dados geoquímicos de alta qualidade referentes aos metabasaltos do *greenstone belt* Crixás também são apresentados no segundo artigo. Essas rochas são classificadas como basaltos toleíticos de alto Mg metamorfizados em fácies anfibolito e possuem predominantemente padrões planos de ETR. As razões de elementos traço relativamente imóveis e os diagramas discriminantes permitem correlacionar os

metabasaltos com platôs oceânicos. Deste modo, os protólitos vulcânicos dos metakomatiitos e metabasaltos do *greenstone belt* Crixás são interpretados como gerados devido a ação de uma pluma mantélica. As assinaturas geoquímicas mostram que as lavas ultramáficas foram formadas sob altas taxas de fusão parcial nas porções mais profundas do manto, com retenção de granada como mineral residual, enquanto os basaltos toleíticos foram formados em taxas de fusão parcial menores e em profundidades mais rasas. Além disso, de acordo com os dados geoquímicos e isotópicos apresentados, essas rochas não interagiram com crosta continental mais antiga, o que contrasta com modelos propostos anteriormente para a bacia do *greenstone* (ex: Jost et al., 2019; Ferreira et al., 2021).

No entanto, a idade da sequência metavulcânica ultramáfica-máfica do *greenstone belt* Crixás ainda pode ser apenas estimada de maneira imprecisa, com base em dados isotópicos publicados de Pb-Pb e Sm-Nd, que resultaram em "errócronas" com as idades ~2.8 Ga (Arndt et al., 1989) e ~3.0 Ga (Fortes et al., 2003). É importante ressaltar que durante este trabalho inúmeras tentativas de obter cristais de zircão nas rochas máficas para datação U-Pb foram realizadas; infelizmente sem êxito. Tal dificuldade não é incomum, tendo em vista que o zircão raramente é uma fase mineral acessória encontrada em rochas ultramáficas e máficas. Os dados Re-Os em rocha total de amostras de metakomatiito e metabasalto, no entanto, forneceram uma isócrona de ~2.6 Ga, interpretada como um evento de reequilíbrio do sistema isotópico Re-Os, o que representaria uma idade mínima do vulcanismo ultramáfico e máfico, e confirmaria que essas rochas são de fato arqueanas. Apesar disso, destaca-se a necessidade de profunda investigação geocronológica dos metakomatiitos e metabasaltos.

Após as primeiras publicações que reportaram que a sequência metassedimentar do *greenstone belt* Crixás não é de idade arqueana (Fortes et al., 2003; Tassinari et al., 2006; Jost et al., 2010), como originalmente interpretada (ex: Sabóia, 1979; Jost & Oliveira, 1991), o primeiro artigo deste trabalho possibilitou uma melhor caracterização dessas rochas e investigação das potenciais áreas-fonte com base na integração de dados petrográficos, geoquímicos, isotópicos (Sm-Nd) e geocronológicos (datação U-Pb em zircão detrítico). Os protólitos sedimentares apresentam baixa maturidade textural e mineralógica, como destacado especialmente nas metagrauvacas. A composição química sugere erosão de áreas-fonte predominantemente de composição intermediária e relacionada a um arco magmático. Idades modelo Sm-Nd são em torno de 2.4 e 2.3 Ga, e os valores de ε_{Nd} (t = 2.1 Ga) variam entre valores aproximadamente condríticos e valores positivos (-0.27 a +1.25). Os dados U-Pb em zircão detrítico decorrente de amostragem sistemática de metagrauvacas e filitos carbonosos em diferentes profundidades de testemunhos de sondagem apresentam

distribuição unimodal (2.2 – 2.1 Ga), com contribuição apenas incipiente de fontes do Sideriano (~2.4 Ga) e Arqueano (~2.7 Ga). As rochas ainda apresentam sistemática de elementos traço coerente com bacias sedimentares relacionadas a arco magmático.

Foi realizada uma tentativa de datação da deposição dos protólitos sedimentares ricos em matéria orgânica pelo método Re-Os em amostras bem preservadas de filito carbonoso. No entanto, como ressaltado no relatório presente em anexo neste trabalho, os dados de concentração dos elementos Re-Os e as razões isotópicas apresentam baixa correlação e provavelmente indicam alteração pós-deposicional, impossibilitando a datação por este método. Por outro lado, a datação Re-Os de cristais de arsenopirita provenientes de sulfeto maciço hospedado em filitos carbonosos forneceu a idade de 2137 ± 11 Ma, semelhante a idade previamente reportada por Marques et al. (2013). Essa idade pode ser considerada como uma idade mínima para a sedimentação no *greenstone belt* Crixás e é relativamente próxima a idade máxima de sedimentação calculada a partir dos cristais de zircão detrítico mais jovens (2149 ± 4 Ma). Portanto, os dados geocronológicos indicam que as rochas sedimentares são relativamente síncronas com a principal área-fonte do Riaciano e foram depositadas em uma bacia relacionada a um arco magmático intraoceânico (denominado Arco de Crixás). Sugere-se que as rochas sedimentares são alóctones e foram transportadas tectonicamente sobre um embasamento arqueano (granitos e gnáisses TTG, e vulcânicas ultramáficas e máficas) durante a colisão do arco magmático com um paleocontinente arqueano (referido neste trabalho como uma proto-crosta do Domínio Crixás-Goiás, i.e. a dominante parte Arqueana do bloco). Neste trabalho, essa orogênese é correlacionada com a amalgamação do Maciço de Goiás durante o Paleoproterozoico, ao longo de sucessivas colisões entre arcos intraoceânicos e continentais na formação do paleocontinente São Francisco (Cordeiro & Oliveira, 2017).

A caracterização deste arco magmático foi feita no primeiro artigo deste trabalho com base nas evidências indiretas fornecidas pelos registros sedimentares, tendo em vista a ausência de crosta continental riaciana significativa aflorante dentro do Domínio Crixás-Goiás. Tal fato levou a sugestão de que a maior parte deste arco magmático foi erodido, obliterado e/ou encontra-se encoberto. No entanto, o segundo artigo deste trabalho também apresenta os primeiros registros e descrições de meta-andesitos e metadioritos associados à sequência metassedimentar do *greenstone belt* Crixás. A datação U-Pb em cristais de zircão provenientes de uma amostra de meta-andesito forneceu idade de 2172.2 ± 12.7 Ma, interpretada como a idade do magmatismo intermediário. As rochas apresentam idades modelo Sm-Nd em torno de 2.2 Ga e valores positivos de ε_{Nd} inicial (+2.34 a +2.69). Portanto, essas rochas são correlacionadas com os folhelhos negros e grauvacas sin-orogênicas, como

parte um arco magmático riaciano. Além disso, os meta-andesitos e metadioritos do *greenstone belt* Crixás se somam a outras locais ocorrências de rochas magmáticas riacianas que vinham sendo reconhecidas na região do Domínio Crixás-Goiás nas últimas décadas (Jost et al., 1993; Queiroz, 2000; Bogossian, 2020).

Em síntese, o *greenstone belt* Crixás compreende duas assembleias de rochas formadas em períodos e contextos tectônicos distintos, e que se encontram imbricadas tectonicamente. A mais antiga compreende uma associação de komatiitos e toleítos de alto Mg arqueanos relacionados a uma pluma mantélica em um ambiente de platô oceânico. A outra associação compreende rochas magmáticas de composição intermediária associadas a rochas sedimentares depositadas em uma bacia proximal, formada em um arco intraoceânico de idade riaciana, que também está relacionado ao principal período de formação de depósitos de ouro na região.

Acredita-se que o modelo evolutivo apresentado neste trabalho pode ser corroborado e aperfeiçoado com base especialmente na determinação de idades robustas dos metakomatiitos e metabasaltos do *greenstone belt* Crixás. Além disso, o detalhamento geológico e o estudo geocronológico da Sequência Mina Inglesa, localizada em contatos tectônicos à noroeste do *greenstone belt* Crixás, também são de suma importância. Por fim, estudos futuros focados nas sequências metavulcânicas e metassedimentares dos outros *greenstones* que compõe a porção norte do Domínio Crixás-Goiás podem fornecer novas implicações e ajudar a elucidar questões como o posicionamento do Arco Crixás em relação ao continente paleoarqueano, os processos controladores da sedimentação em cada bacia específica, e o reconhecimento de mais registros magmáticos do arco paleoproterozoico e suas relações com os diferentes tipos de depósitos na região.

2. Referências Bibliográficas

Arndt, N.T., Lesher, C.M., Barnes, S.-J., 2008. Komatiite. Cambridge University Press, 465 p.

Arndt, N.T., Teixeira, N.A., White, W.M., 1989. Bizarre geochemistry of komatiites from the Crixás Greenstone belt, Brazil. Contr. Mineral. Petrol. 74, 549-564.

Bogossian, J., 2020. Gold systems in the Faina greenstone belt and crustal evolution of the southern Goiás Archean Block, central Brazil. PhD thesis, School of Earth Sciences, The University of Western Australia, 246 pp.

Cordeiro P.F.O., Oliveira. C.G., 2017. The Goiás Massif: Implications for a pre-Columbia 2.2–2.0 Ga continent-wide amalgamation cycle in central Brazil. Precambrian Res. 288, 403-420.

Dostal, J., 2008. Komatiites. Geoscience Canada 35, 21-31.

Ferreira, B.F., Marques, J.C., Frantz, J.C., de Souza, R.G., Campos, M.P., Figueiredo, F.L.A.R., Padilha, N.L., 2021. Stratigraphy and U–Pb detrital zircon provenance, Crixás Greenstone Belt, Goiás-Brasil: Gold-bearing vs barren siliciclastic rocks. J. S. Am. Earth Sci. 105, 102994. https://doi.org/10.1016/j.jsames.2020.102994.

Fortes, P.T.F.O., Pimentel, M.M., Santos, R.V., Junges, S., 2003. Sm-Nd study of the Crixás greenstone belt, Brazil: implications for the age of deposition of the upper sedimentary rocks and associated Au mineralization. J. S. Am. Earth Sci. 16, 503–512.

Jost, H., Apollo, J.F.H., Weber, W., Salles, R.R., Marques, J.C.M., Massucatto, A.J., Costa, D.A., Santos, B.A., 2019. Stratigraphic update, paleotectonic, paleogeographic, and depositional environments of the Crixás Greenstone Belt, Central Brazil. J. S. Am. Earth Sci. 96, 102329.

Jost, H., Chemale Jr., F., Dussin, I.A., Tassinari, C.C.G., Martins, R., 2010. A U–Pb zircon paleoproterozoic age for the metasedimentary host rocks and gold mineralization of the Crixás greenstone belt, Goiás, Central Brazil. Ore Geol. Rev. 37, 127–139.

Jost, H., Oliveira, A.M., 1991. Stratigraphy of the greenstone belts, Crixás region, Goiás, Central Brazil. J. S. Am. Earth Sci. 4, 201 -214.

Jost, H., Pimentel, M.M., Fuck, R.A., Danni, J.C., Heaman, L., 1993. Idade U-Pb do Diorito Posselândia, Hidrolina, Goiás. Rev. Brasil. Geociênc. 23, 352-355.

Kuyumjian, R.M., Jost, H., 2006. Low-and high-alumina komatiites of Goiás, Central Brazil. J. S. Am. Earth Sci. 20, 315–326.

Marques, J. C., Jost, H., Creaser, R. A., Frantz, J. C., Osorio, R. G., 2013. Age of arsenopyrite gold-bearing massive lenses of the Mina III and its implications on exploration, Crixás greenstone belt, Goiás, Brazil. In: III Simpósio Brasileiro de Metalogenia, Gramado, extended abstracts.

Queiroz, C.L., 2000. Evolução Tectono-Estrutural dos Terrenos Granito-Greenstone Belt de Crixás, Brasil Central. Tese de Doutorado, Instituto de Geociências, Universidade de Brasília, 209 pp.

Tassinari, C.C.G., Jost, H., Santos, J.C., Nutman, A.P., Bennell, M.R., 2006. Pb and Nd isotope signatures and SHRIMP U-Pb geochronological evidence of Paleoproterozoic age for Mina III gold mineralization. In: South American Symposium on Isotope Geology, 5, Pucon, Chile, Proceedings, pp. 615-617.